- DNA -

D-1

UCRL-52038
(WES TR-N-76-4)

FINAL REPORT ON A CALCULATIONAL PARAMETER STUDY OF SOILS TYPICAL OF SOME ESSEX I CRATERING SITES

Milton F. Goodrich
Jon B. Bryan
Jeffrey M. Thomsen
Charles M. Snell

March 15, 1976

Prepared for U.S. Energy Research & Development Administration under contract No. W-7405-Eng-48

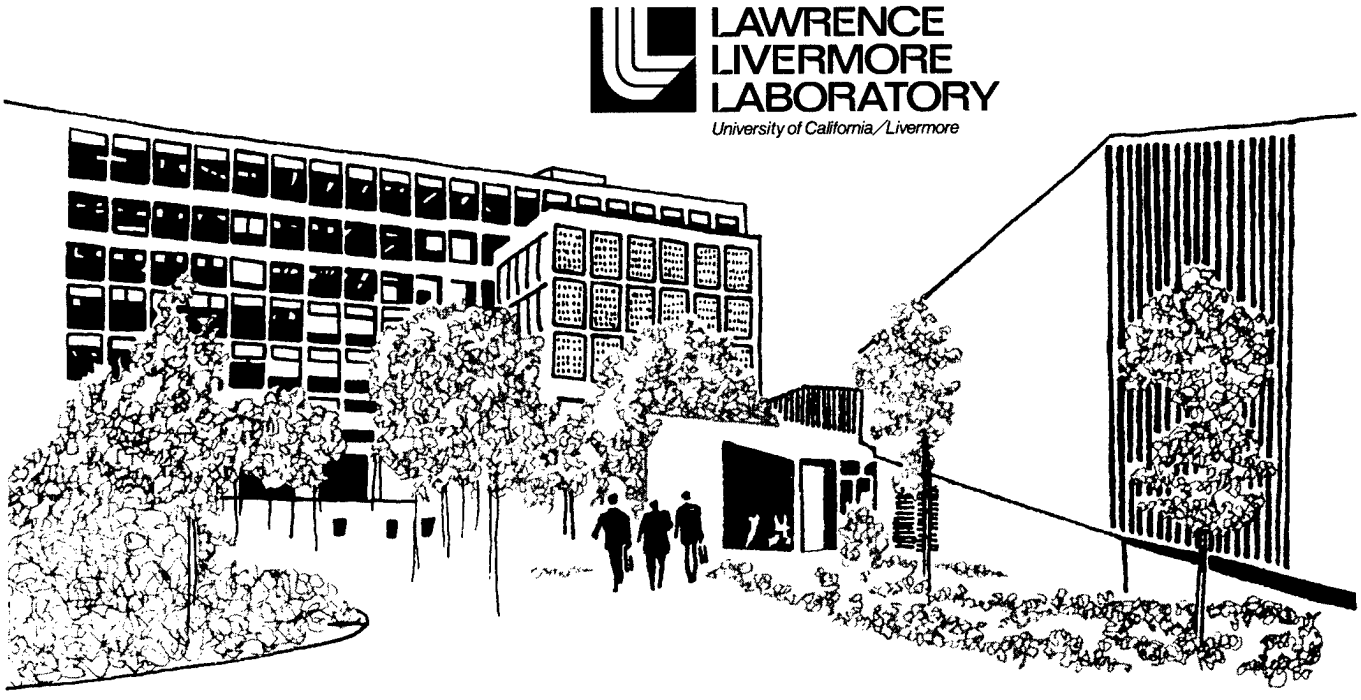

Printed in the United States of America
Available from
National Technical Information Service
U.S. Department of Commerce
5285 Port Royal Road
Springfield, VA 22161
Price: Printed Copy $; Microfiche $2.25

Page Range	Domestic Price	Page Range	Domestic Price
001–025	$ 3.50	326–350	10.00
026–050	4.00	351–375	10.50
051–075	4.50	376–400	10.75
076–100	5.00	401–425	11.00
101–125	5.50	426–450	11.75
126–150	6.00	451–475	12.00
151–175	6.75	476–500	12.50
176–200	7.50	501–525	12.75
201–225	7.75	526–550	13.00
226–250	8.00	551–575	13.50
251–275	9.00	576–600	13.75
276–300	9.25	601–up	*
301–325	9.75		

*Add $2.50 for each additional 100 page increment from 601 to 1,000 pages: add $4.50 for each additional 100 page increment over 1,000 pages.

Distribution Category
UC-11

LAWRENCE LIVERMORE LABORATORY
University of California/Livermore, California/94550

UCRL-52038 (WES TR-N-76-4)*

FINAL REPORT ON A CALCULATIONAL PARAMETER STUDY OF SOILS TYPICAL OF SOME ESSEX I CRATERING SITES

Milton F. Goodrich**
Jon B. Bryan
Jeffrey M. Thomsen
Charles M. Snell

MS. date: March 15, 1976

*Work sponsored by Office of Chief of Engineers under R & D Project 4A762719AT40, for the Explosive Excavation Division of the Weapons Effects Laboratory, U. S. Army Engineer Waterways Experiment Station, Vicksburg, Mississippi.

**Present address: Kaiser Engineers, Energy Sources Division, 300 Lakeside Drive, Oakland, CA.

Contents

FINAL REPORT ON A CALCULATIONAL PARAMETER STUDY OF SOILS TYPICAL OF SOME ESSEX I CRATERING SITES

Abstract

The one-dimensional computer calculations described in this report were performed to simulate stress-wave propagation and kinetic energy transfer associated with subsurface cratering detonations in soils. A hypothetical 20-ton-yield nuclear explosive was assumed as the energy source, surrounded by a single soil material. Various soil descriptions were selected in order to systematically study the range of soil response to the nuclear detonation. The soils were representative of the layered mixtures of sand and clay found at the ESSEX high-explosive cratering sites near Ft. Polk, Louisiana. Soil properties analyzed in this study include water saturation, bulk density, failure envelope, and low-pressure bulk modulus.

Introduction

The Earth Sciences (K) Division of the Lawrence Livermore Laboratory (LLL) has conducted a calculational parameter study for the Explosive Excavation Division* of the Weapons Effects Laboratory of the U.S. Army Engineer Waterways Experiment Station. The study began a systematic investigation into the influence of soil properties on nuclear cratering and ground motion.

Work performed during the study included investigating the static properties of soils, determining the relevant range of values of those properties to be used in the study, developing a constitutive relations model that could derive representative dynamic properties from given static properties for hypothetical soils spanning the ranges of interest in the study, and calculating the response of each hypothetical soil to a nuclear detonation in one dimension.

This report reviews the work performed, with emphasis on the results of the calculations. For some topics, more detailed information can be found in the two progress reports.[1,2]

Objective and Concept

OBJECTIVE

The calculational parameter study described here is part of a long-range parameter study proposed by the Explosive Excavation Division.[3] The overall objective of this study is to examine the phenomenology of nuclear cratering and to present the results in a form directly usable in an improved U.S. Army field handbook predicting various effects of

*Formerly known as the Explosive Excavation Research Laboratory (EERL) of the U.S. Army Engineer Waterways Experiment Station (WES); located at LLL, Livermore, California.

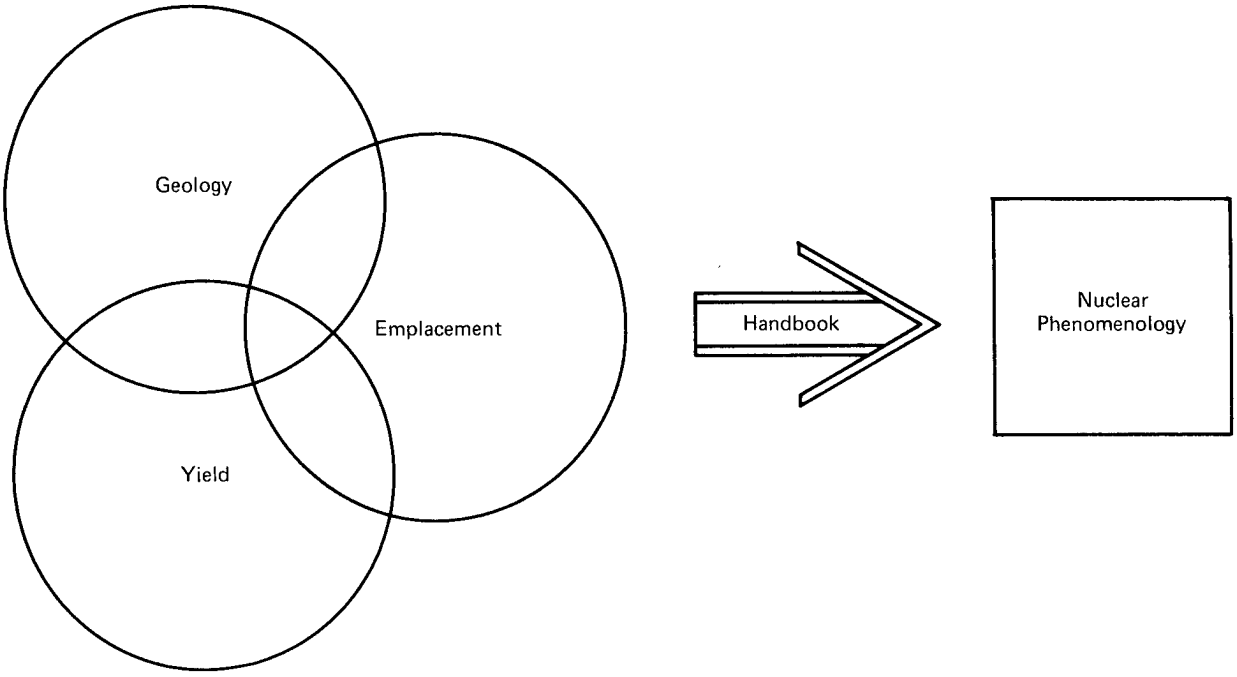

Fig. 1. Concept of total nuclear effects study. The study will produce information for a handbook that will predict nuclear phenomenology given the geology, yield, and emplacement.

nuclear weapons. Generally these effects are influenced by the site geology, the explosive yield, and the emplacement (i.e., both the configuration and the depth of burial). The effects of greatest interest are ground motion, crater size, and ancillary cratering-related effects. The concept of the total study is shown schematically in Fig. 1.

A complete investigation into the effects of site geology alone requires more work than is entailed in this year's calculational parameter study. Thus it is only a beginning step toward accomplishment of the long-range objectives of the study and is not expected to answer all questions about cratering effects. The primary goal of this year's study was to identify the material properties that have greatest influence on energy coupling and stress-wave propagation resulting from a buried nuclear detonation.

CONCEPT

The concept of the calculational parameter study is shown schematically in Fig. 2. Material properties were separated into two groups: bulk (or initial) properties and constitutive relations. Bulk properties relate to the undisturbed soil only, whereas constitutive relations describe the effects of pressure on the material. A comprehensive (although not exhaustive) list of bulk properties was compiled. Relationships between these properties were derived, and a set of independent variables was chosen.

Since this is a follow-on study designed to clarify and expand the results of the eight ESSEX I* cratering tests, conducted in the Peason Ridge area of Fort Polk,

*ESSEX is an acronym formed from effects of subsurface explosions.

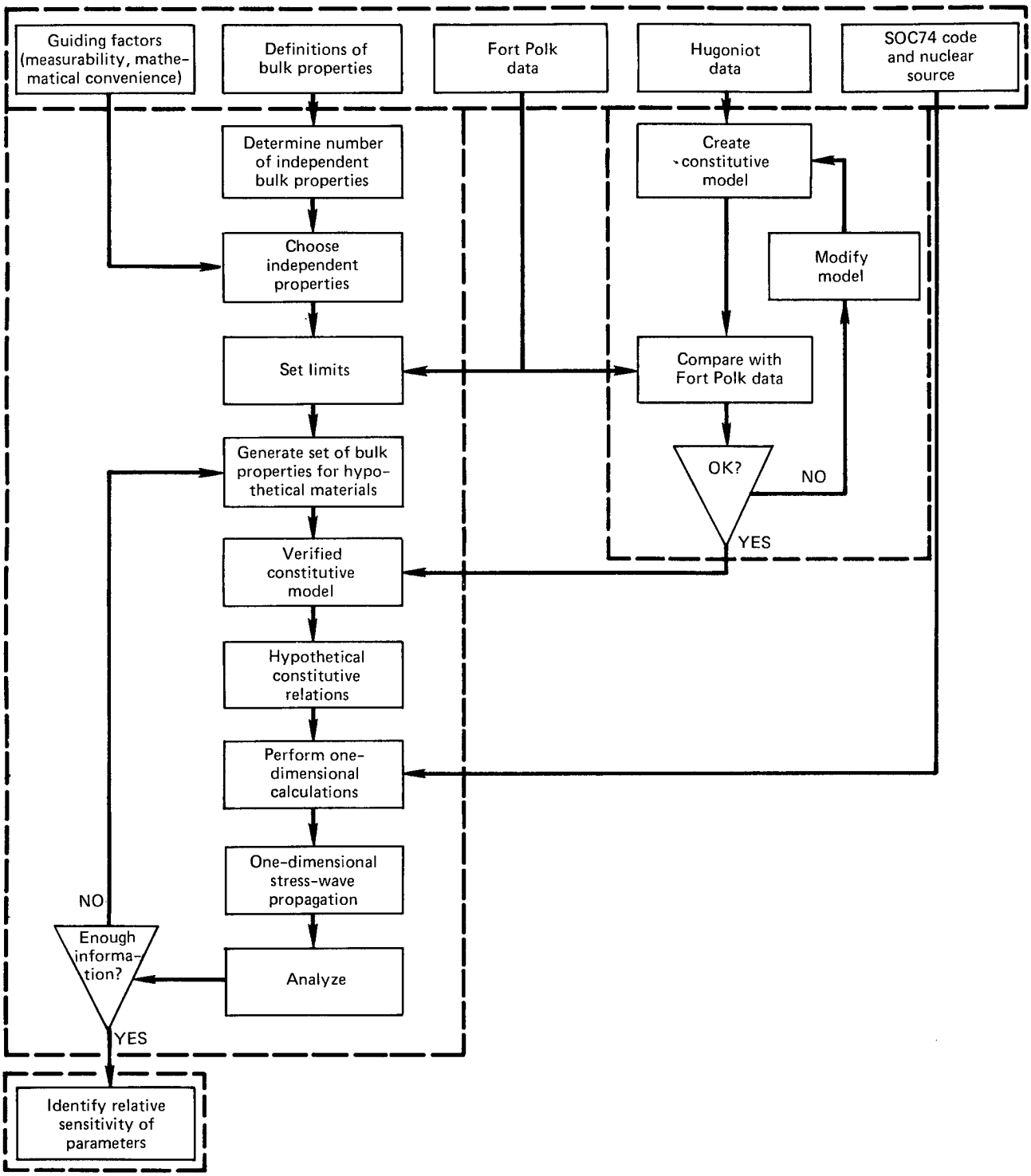

Fig. 2. The geologic parameter study concept.

Louisiana,[4,5] the study was limited to soils characteristic of that site. The Soils and Pavements Laboratory (S & PL) of WES conducted, for ESSEX, an extensive investigation of the soils at that test site. The investigation produced 13 idealized units with material properties typical of subsurface materials encountered at the eight locations studied.[6] These units were examined and used to infer appropriate limits for the study's independent variables.

Since a knowledge of the constitutive relations was needed in order to calculate the effect of a nuclear detonation in a given material, a model was developed to supply representative constitutive relations given the values of the independent bulk properties. The model's applicability was established by comparing model-generated constitutive relations for the 13 Fort Polk units with those recommended by S & PL (based on laboratory tests). The model was then used to develop constitutive relations for hypothetical soils with bulk properties spanning the ranges proposed for the study.

One-dimensional, spherical code calculations were performed for each hypothetical soil by means of the SOC74 code, which is a time-dependent, Lagrangian, finite-difference computer code[7-10] that can simulate stress-wave propagation through solid materials with generalized characteristics.

Stress wave propagation away from the nuclear source and energy coupling into the soil were calculated as a function of time. The results were plotted, analyzed, and compared with other calculational results. Sensitivity of the results to individual bulk properties could then be investigated systematically.

The general method became one of performing calculations on hypothetical materials, and varying the independent bulk parameters within the set limits. When the results proved sensitive to a particular parameter, more calculations were performed using additional values of that bulk property within the limiting range. This process was continued until adequate curves could be drawn showing the sensitivity of the calculational results to that bulk property.

Material Properties and Constitutive Model

GENERAL CONSIDERATIONS

In this study material properties have been considered under two categories: bulk properties and constitutive relations. Bulk properties are static characteristics of the material in its undisturbed state (initial condition) only, whereas constitutive relations define the effects of pressure on the materials.

BULK MATERIAL PROPERTIES

A review of bulk parameters, which quantitatively relate information about bulk properties, was performed for the purpose of defining independent parameters. A comprehensive but not exhaustive list of bulk parameters was compiled and is shown in Table 1. Mathematical relationships between these parameters were derived

Table 1. Definition of bulk material parameters.

Parameters	Symbol used in study	ASTM symbol	Description
		Composition parameters[a]	
Densities	ρ_0	γ_0	Bulk density (sample mass/sample volume)
	ρ_s	γ_d	Dry density (mass of solids/sample volume)
	ρ_w	γ_w	Mass of water per unit total volume (water mass/ sample volume)
	ρ_g	G_s	Grain density (mass of solids/volume of solids)
Volumes	e	e	Void ratio (volume of voids/volume of solids)
	e_w	--	Water ratio (volume of water/volume of solids)
	ϕ_0	--	Total porosity (volume of voids/sample volume)
	ϕ_a	V_a	Air-filled porosity (air volume/sample volume)
	ϕ_w	V_w	Water-filled porosity (water volume/sample volume)
	ϕ_s	V_s	Solid volume (volume of solids/sample volume)
Saturations	S_W	S	Water saturation (water volume/volume of voids)
	S_a	--	Air saturation (air volume/volume of voids)
Weights	W	W	Water content (weight of water/dry weight of sample)
	Z	--	Water content (weight of water/wet weight of sample)
		Elastic parameters[b]	
	K		Bulk modulus
	G		Shear modulus
	ν		Poisson's ratio
	λ		Lamé elastic parameter
	E		Young's modulus
	B		Constrained modulus
	k_0		Stress ratio in uniaxial strain

[a]Three independent parameters.

[b]Two independent parameters.

and are given in Table 2. These parameters fall naturally into two groups: composition parameters and elastic parameters. Examination of the relationships between each group's members indicates a total of five independent bulk parameters. Of these five independent parameters, three must be composition and two elastic. Composition parameters chosen as independent must include one density and one volume ratio,

Table 2. Mathematical relationships among parameters.

Composition parameters (using ρ_g, ρ_0, and S_W as a base)

$\rho_0 = \rho_g(1 - \phi_0) + \phi_0 S_W$ (Note: the density of water is unity)

$\phi_a = \phi_0(1 - S_W)$ (Note: $\phi_a + \phi_w + \phi_s \equiv 1$)

$\rho_s = \rho_g(1 - \phi_0)$

$\phi_w = \phi_0 S_W$

$\rho_w = \phi_0 S_W$

$\phi_s = 1 - \phi_0$

$\rho_g = \rho_g$

$S_W = S_W$

$e = \phi_0/(1 - \phi_0) = (\phi_0/\phi_s)$

$S_a = 1 - S_W$ (Note: $S_W + S_a \equiv 1$)

$e_w = \phi_w/\phi_s = \phi_0 S_w/(1 - \phi_0) = (\phi_0 - \phi_a)/(1 - \phi_0)$

$W = \phi_0 S_W/[\rho_g(1 - \phi_0)] = \rho_w/\rho_s$

$\phi_0 = (\rho_g - \rho_0)/(\rho_g - S_w)$

$Z = \phi_0 S_W/[\rho_g(1 - \phi_0) + \phi_0 S_W] = \rho_w/\rho_0$

Elastic parameters (using K and ν as a base)

$K = K$

$E = 3K(1 - 2\nu)$

$G = 3K(1 - 2\nu)/2(1 + \nu)$

$B = 3K(1 - \nu)/(1 + \nu)$

$\nu = \nu$

$k_0 = \nu/(1 - \nu)$

$\lambda = 3K\nu/(1 + \nu)$

or saturation. The remaining composition parameter and the two independent elastic parameters can then be selected from their respective groups, at the investigator's convenience.

Since the study was limited to materials typical of Fort Polk, the value of each bulk parameter was calculated for all 13 Fort Polk units. These are shown in Table 3; the ranges for each of these parameters will be discussed in the next section. Values of the elastic parameters, other than the bulk modulus K and the limiting value of Poisson's ratio ν, are not shown.

CHOOSING INDEPENDENT BULK PARAMETERS

The three composition parameters chosen as independent during the study were grain density ρ_g, bulk density ρ_0, and water saturation S_w. These were chosen primarily for practical reasons. Grain density can be assumed to be constant (ρ_g = 2.67 Mg/m^3), since it shows only a slight variation at Fort Polk (2.66 to 2.70 Mg/m^3, see Table 3). It was felt that bulk density would be more easily measured under field conditions than most other parameters. Water saturation S_w was used because previous experience on rocks indicates that this factor has a strong influence on both

Table 3. Material properties from the 13 Fort Polk units.

Unit	Clay (%)	Sand (%)	ρ_0 (Mg/m^3)	ρ_s (Mg/m^3)	ρ_w (Mg/m^3)	ρ_g (Mg/m^3)	e	e_w	ϕ_0	ϕ_a	ϕ_w	ϕ_s	S_w	S_a	W	Z	Initial K (GPa)	Initial ν
1	25	75	1.939	1.6160	0.3230	2.66	0.646	0.532	0.3925	0.0690	0.3230	0.6075	0.823	0.17	0.1999	0.167	0.172	0.30
2	35	65	1.843	1.4175	.4255	2.66	0.876	0.799	.4671	.0420	.4255	.5329	0.911	.08	.3002	.230	1.034	.33
3	35	65	1.795	1.3350	.4600	2.67	1.000	0.920	.5000	.0400	.4600	.5000	0.920	.08	.3446	.256	1.552	.33
4	40	60	1.763	1.2417	.5212	2.70	1.174	1.133	.5401	.0190	.5212	.4599	0.965	.03	.4197	.295	0.621	.33
5	5	95	1.987	1.6026	.3844	2.66	0.659	0.638	.3975	.0130	.3844	.6025	0.967	.03	.2399	.194	3.793	.28
6	5	95	1.997	1.5976	.3994	2.66	0.665	0.665	.3994	.0000	.3994	.6006	1.00	.00	.2500	.200	5.172	.48
7	5	95	1.955	1.5766	.3784	2.67	0.693	0.641	.4095	.0310	.3784	.5905	0.924	.07	.2400	.193	1.138	.30
8	35	65	1.859	1.3872	.4718	2.68	0.932	0.912	.4824	.0107	.4718	.5176	0.978	.02	.3401	.253	2.234	.33
9	35	65	2.019	1.6546	.3646	2.67	0.614	0.588	.3803	.0160	.3643	.6197	0.958	.04	.2204	.180	5.659	.20
10	40	60	1.843	1.3550	.4880	2.68	0.978	0.965	.4944	.0065	.4880	.5056	0.987	.01	.3601	.264	3.945	.38
11	40	60	1.796	1.2641	.5318	2.70	1.136	1.136	.5318	.0000	.5318	.4682	1.000	.00	.4207	.296	4.682	.48
12	35	65	1.923	1.4757	.4473	2.67	0.809	0.809	.4473	.0000	.4473	.5527	1.000	.00	.3031	.233	5.013	.48
13	35	65	1.865	1.3913	0.4736	2.67	0.919	0.909	0.4789	0.0053	0.4736	0.5211	0.989	0.01	0.3404	0.253	7.31	0.20

ground motion and cratering in the range of interest (0.9 to 1.0).[11,12]

Bulk modulus K and Poisson's ratio ν were chosen as the independent elastic parameters. Bulk modulus was chosen because it can be estimated from a measurement of the speed of sound if the initial shear modulus is small enough to be neglected. Poisson's ratio increases very rapidly with confining pressure at very low pressures (~.01 GPa) from its initial value, shown for each unit in Table 3, to a value of 0.46 to 0.48 (very close to the limiting value at high pressures of 0.5) for almost all Fort Polk units. Hence, instead of using the range of initial values of ν from the Fort Polk data, a constant value, 0.48, was used.

Therefore two of the five independent parameters were held constant, while three were varied. Limits of variation for these three variables were chosen so as to completely cover their ranges at Fort Polk. Table 4 lists the values of the two independent bulk parameters held constant and the ranges of values of the remaining three.

By using the values of the independent composition parameters (ρ_g, ρ_0, and S_w) shown in Table 4, the ranges of each dependent composition parameter exhibited by the 13 Fort Polk units are spanned more than adequately. This is shown in Table 5, which compares the ranges of the dependent composition parameters calculated from Table 4 with the ranges obtained directly from Table 3. Not only the limits but also the distribution of the Fort Polk data within those limits is important for the study. Figure 3 shows this distribution by plotting ρ_0 versus S_w for the 13 Fort Polk units. The data are randomly scattered within an envelope approximately

Table 4. Range of values of the five independent bulk parameters considered in the study

Independent bulk parameters held constant
Grain density ρ_g: 2.67 Mg/m^3
Poisson's ratio ν: 0.48
Independent bulk parameters varied
Bulk density ρ_0: 1.7 to 2.1 Mg/m^3
Water saturation S_w: 0.8 to 1.0
Initial bulk modulus K: 2.5 to 7.5 GPa

Table 5. Ranges for the dependent composition parameters.

Composition parameter	Range Calculated from Table 4	Range from 13 Fort Polk units (Table 3)
ρ_s (Mg/m^3)	1.12-1.86	1.2417-1.6546
ρ_w (Mg/m^3)	0.24-0.58	0.3230-0.5318
e	--	0.6137-1.1744
ϕ_0	0.30-0.58	0.3803-0.5401
ϕ_a	0.0-0.12	0.0-0.069
ϕ_w	0.24-0.58	0.3230-0.5318
e_w		0.5317-1.136
ϕ_s	0.42-0.70	0.4599-0.6197
S_a	0.0-0.20	0.0-0.17
W	--	0.1999-0.4207
Z	0.11-0.34	0.167-0.296

limited by a ρ_0 range from 1.75 to 2.05 and an S_w range of 0.9 to 1.0, excluding only unit 1. The parameter study covers a somewhat larger area, with ρ_0 ranging from 1.7 to 2.1 and S_w ranging from 0.8 to 1.0. This was done to ensure complete coverage of the dependent variables over their respective ranges at Fort Polk and account for the possibility that the composition of all materials at the site might exhibit a wider variation than that determined from the 13 idealized units.

For the elastic parameters, the range of values of initial bulk modulus (2.5 to 7.5 GPa) does not span the entire range of values found in the Fort Polk data (0.172 to 7.31 GPa), as seen from Table 3. Experience has shown that the effect of the elastic parameters on nuclear cratering and close-in ground motion (3 to 15 m for an 84-GJ nuclear detonation) was minuscule. A few calculations were performed at different values of K to prove this point, and no further analysis of the remainder of the elastic parameters shown in Table 1 was performed.

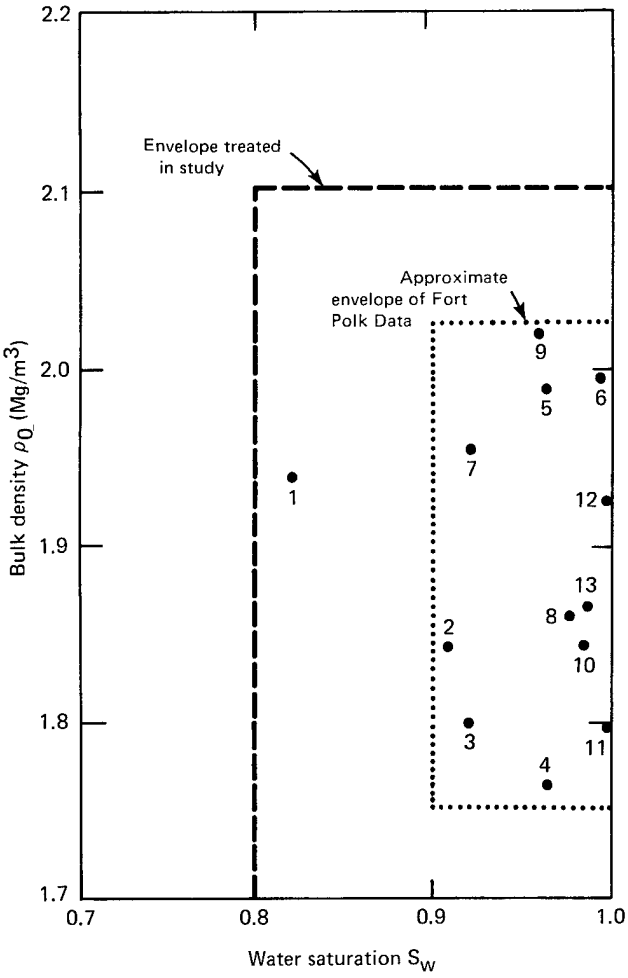

Fig. 3. Distribution of Fort Polk units in ρ_0-S_w space. The number beside each data point is the Fort Polk unit number.

CONSTITUTIVE MODEL FOR SOILS

A constitutive model was developed to provide constitutive relations for hypothetical soils having bulk properties in the ranges discussed in the preceding section. This model consists of two parts: a computer model that predicts compressibility and an empirical model that gives failure information. This section discusses briefly each of these models. More detailed information is presented in a previous progress report.[2]

Since the SOC74 computer code was used for the calculations, the model was constructed so as to output constitutive relations compatible with that code. The SOC74 code provides for a great deal of flexibility in the modeling of material behavior. Regimes of response that can be modeled include linear elastic or incrementally elastic compression hysteretic compaction, brittle failure, ductile flow (elastic-plastic failure) tensile failure, liquefaction or vaporization of a solid, vaporization of only the water component in a solid, and gaseous behavior. Techniques are available to simulate certain types of rate-dependent

behavior. Since insufficient data are available to characterize rate-dependent effects in the soils being considered, the constitutive relations for all hypothetical soils used in the study were assumed to be rate-independent. The models used in the SOC74 code also assume that materials are isotropic and homogeneous.

The SOC74 code uses tabular stress-strain relationships to specify the response of solid media under hydrostatic compression. The user enters the tables, which give the pressure P as a function of the excess compression μ ($\mu = \rho/\rho_0 - 1$, where ρ_0 is the initial density of the material and ρ is its density at the pressure P). The general form of the relation expected by the code is shown in Fig. 4. Two curves are required for each material: a "virgin loading" curve and a "completely crushed" unloading (and reloading) curve. The virgin loading curve is assumed to be reversibly elastic until the transition pressure P_t is exceeded; once exceeded, irreversible compaction (hysteretic behavior) is allowed. The loading and unloading curves are assumed to merge into a single curve at and above a specified merge pressure P_m. All air void space is assumed to be irreversibly removed on loading between P_t and P_m. Partial compaction is allowed on loading to a maximum pressure between P_t and P_m. No further hysteretic compaction is allowed at pressures above P_m.

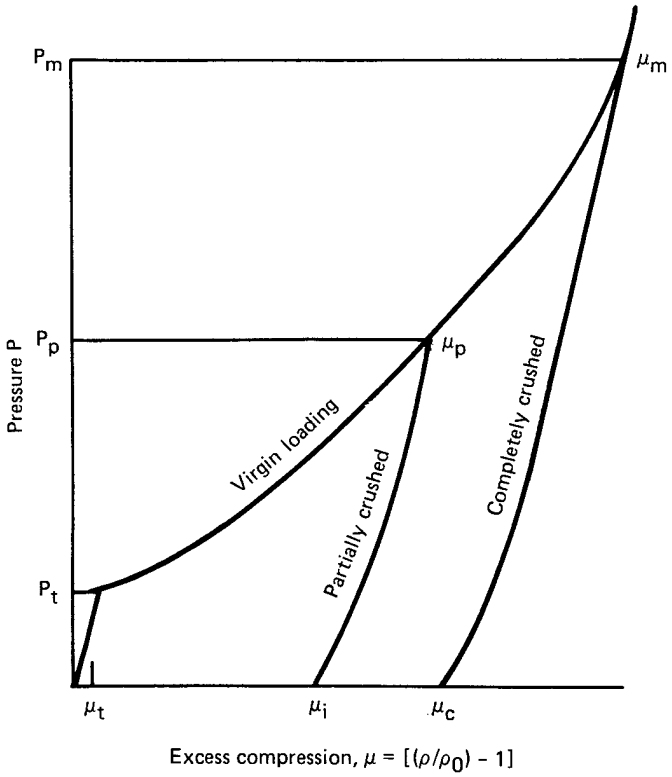

Fig. 4. General form of the compressibility curve for the SOC74 code.

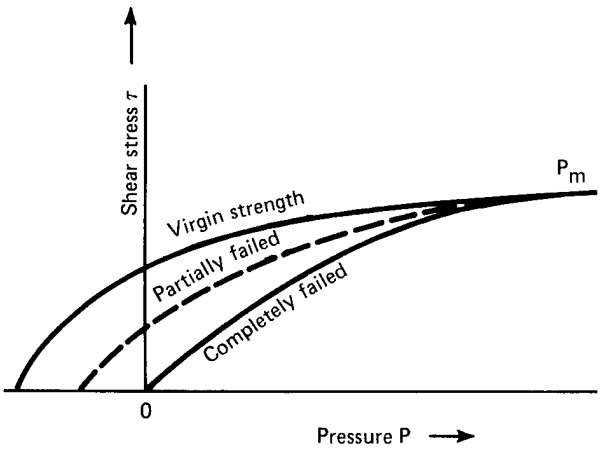

Fig. 5. General form of the failure curve for the SOC74 code.

The failure criterion in SOC74 is represented by a table giving permissible shear stress τ versus confining pressure P. This specification limits the deviatoric stress (shear stress) that a material can support. Brittle failure and strength reduction may be simulated by specifying two strength curves for a material: a "virgin" curve and a "completely failed" curve. The material strength is gradually reduced from the virgin curve to the completely failed curve as damage to the

material increases. The general form of the relation expected by SOC74 is shown in Fig. 5.

Compressibility Model

The soil-compressibility model is an extension of the model developed by Butkovich[13] for certain rock types. Input numbers for the computer model are shown in Table 6. Three of the first four input numbers, ρ_0, S_w, and K, will be recognized as the independent bulk parameters chosen for variation in the study (see Table 4).

Values for P_T and P_m are dependent somewhat on the failure model used; input for these quantities is discussed in the section that follows. Finally, the weight fractions of clay and sand must be provided so that proper weighting of the loading Hugoniots of sand and clay can be computed, as discussed in Ref. 2. These weight fractions were held constant (ZCLA = 0.25 and ZSIL = 0.75) in the study.

The model appears to be quite adequate for predicting compressibility for soils typical of Fort Polk. In a recent progress report,[2] compressibility curves generated using the bulk properties of the 13 Fort Polk units (see Table 3) were compared to the WES-recommended curves (S & PL), which were based on laboratory tests. For almost all units, adequate agreement was observed. Figure 6 shows this comparison at low pressures (0 to 0.04 GPa) for unit 5. This unit layer was recommended at or near shot depth on several of the ESSEX I high-explosive experiments.[6]

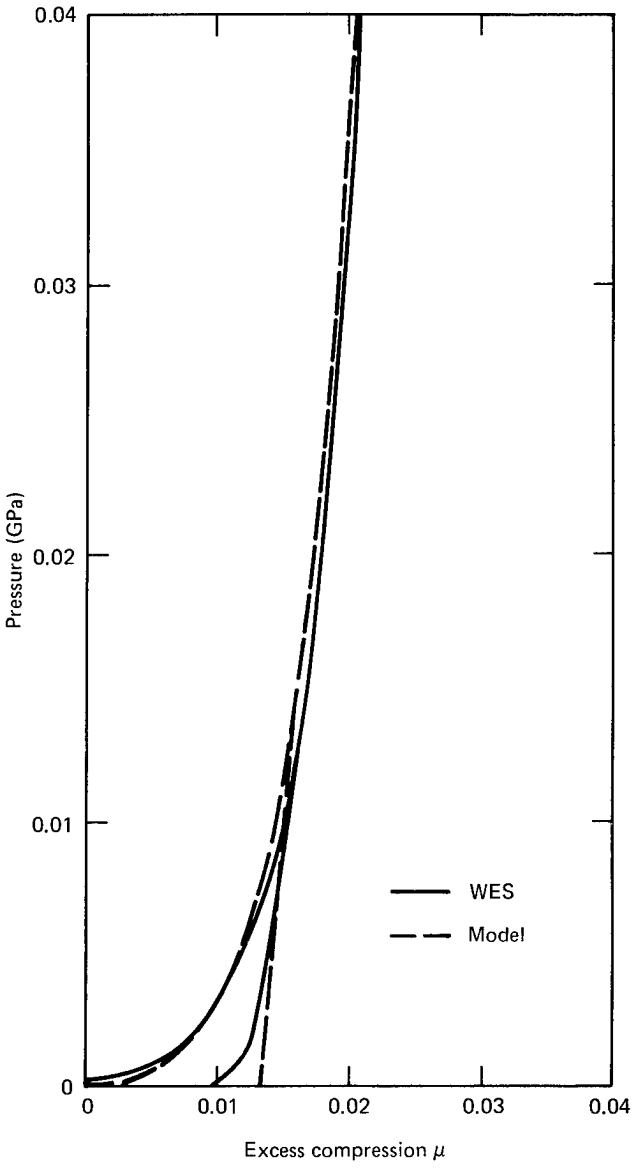

Fig. 6. Comparison of the model-generated compressibility curve using the bulk properties of Fort Polk unit 5 soil with the WES-recommended curve.

Table 6. Input required for soil-compressibility model

Symbol	
ρ_0	Initial bulk density (Mg/m^3)
ρ_g	Grain density (2.67 Mg/m^3)
S_w	Water saturation
K	Initial bulk modulus [GPa × 100 (Mbar)
P_T	Transition pressure [GPa × 100 (Mbar)]
P_M	Merge pressure [GPa × 100 (Mbar)]
ZCLA	Weight fraction of clay (0.25)
ZSIL	Weight fraction of sand (0.75)

Failure Model and Strength Parameters

As discussed earlier in this section, SOC74 requires a failure curve of the form shown in Fig. 5. Moreover, the compressibility model requires the input of two strength parameters, P_M and P_T. So far three independent bulk parameters have been chosen for variation. If in addition the failure curve and P_M and P_T were also independently varied, the number of independent variables in the study would become prohibitively large. This section discusses how the failure curves for the hypothetical soils were chosen and how P_M and P_T were tied to those curves, thereby reducing the number of independent variables from six to four.

In the progress report[2] an attempt was made to correlate the measured maximum shear strengths of the Fort Polk soils with their bulk properties, in particular, water content. Such a correlation was found by Butkovich[13] to exist for some rock types. However, the results found for Fort Polk soils were inconclusive.

In order to establish approximate failure criteria for the hypothetical soils, then, an empirical model was developed. This was based on the WES-recommended failure curves for the 13 Fort Polk units[6] and for an additional unit, unit 14.[14] This latter was identified by S & PL as a "weak rock," having strength characteristics exceeding those of the other 13 units. These units were divided into four groups: uncemented-saturated (units 6, 11, and 12), uncemented-unsaturated (units 1, 2, 4, 5, 7, 8, and 10), cemented-unsaturated (units 9 and 13), and weak rock (unit 14). Maximum and minimum typical (or fitted) curves were then drawn for each of the four groups. These sets of typical curves were then used as another independent variable.

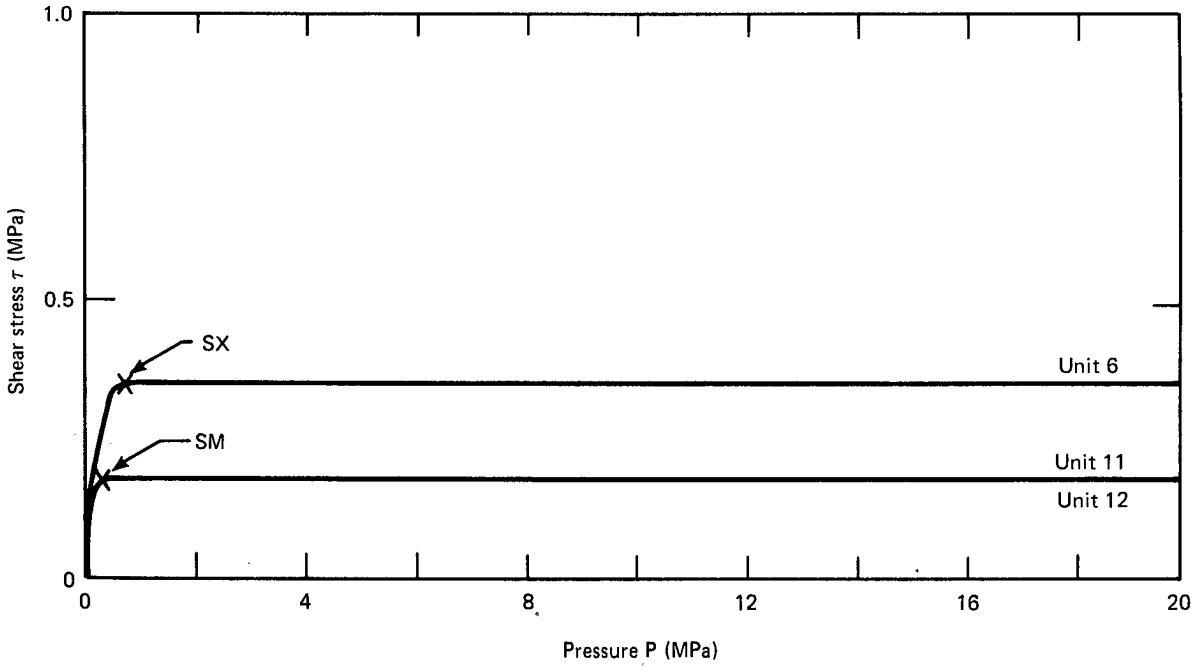

Fig. 7. Failure curves for uncemented-saturated soils (SM and SX).

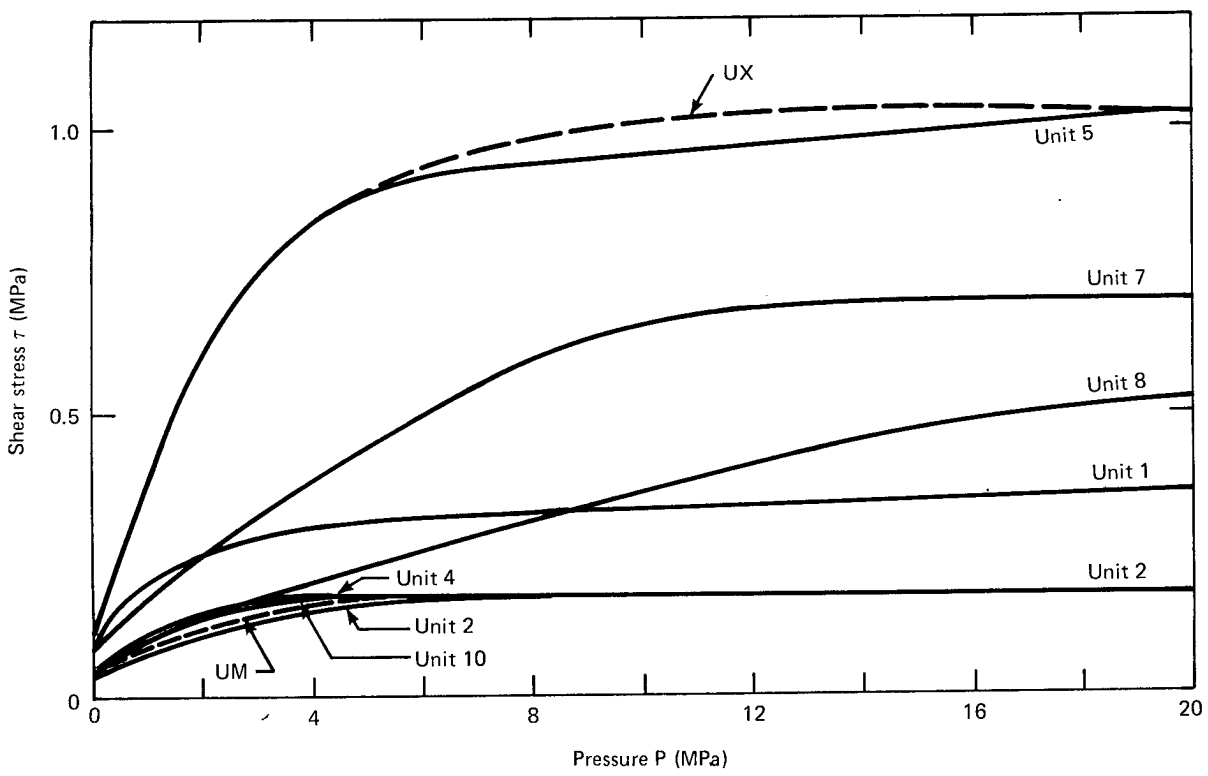

Fig. 8. Failure curves for uncemented-unsaturated soils (UM and UX).

Typical curves for the uncemented-saturated group (SM and SX) are shown in Fig. 7. In this case they correspond to the actual maximum and minimum curves recommended by WES. Fig. 8 shows typical curves for the uncemented-unsaturated group (UM and UX). They also correspond closely with the maximum and minimum curves recommended by WES. The unsaturated-cemented (CM and CX) curves, as Fig. 9 shows, do not follow the data as closely. In particular, the plateau or step that appears in the data for unit 9 was not included in the CX curve. This was because this region is not reached on initial loading. (Use of a constant Poisson's ratio does not allow failure to occur below P_M). Since the step behavior is thought to be associated with pore collapse, it should not be present during unloading after loading to higher pressures. Thus the same curve, CX, was used for both loading and unloading. Finally, Figure 10 shows the typical curves for weak rock (RM and RX). The RX curve follows the unit 14 curve closely. The RM curve was chosen so as to have a maximum shear strength τ_x exactly half that of the RX curve, 10 MPa.

For the study, the merge pressure P_M was chosen to be a function of the maximum shear strength τ_x. Figure 11 shows P_M versus τ_x for the unsaturated Fort Polk units. The values show considerable scatter. Hence, somewhat arbitrarily, P_M (in megapascals) was related linearly to τ_x:

$$P_M \equiv 5\tau_x + 9.5.$$

This line falls in the middle of the data shown in Fig. 11 and hence is representative of Fort Polk soils.

The transition pressures P_T were the

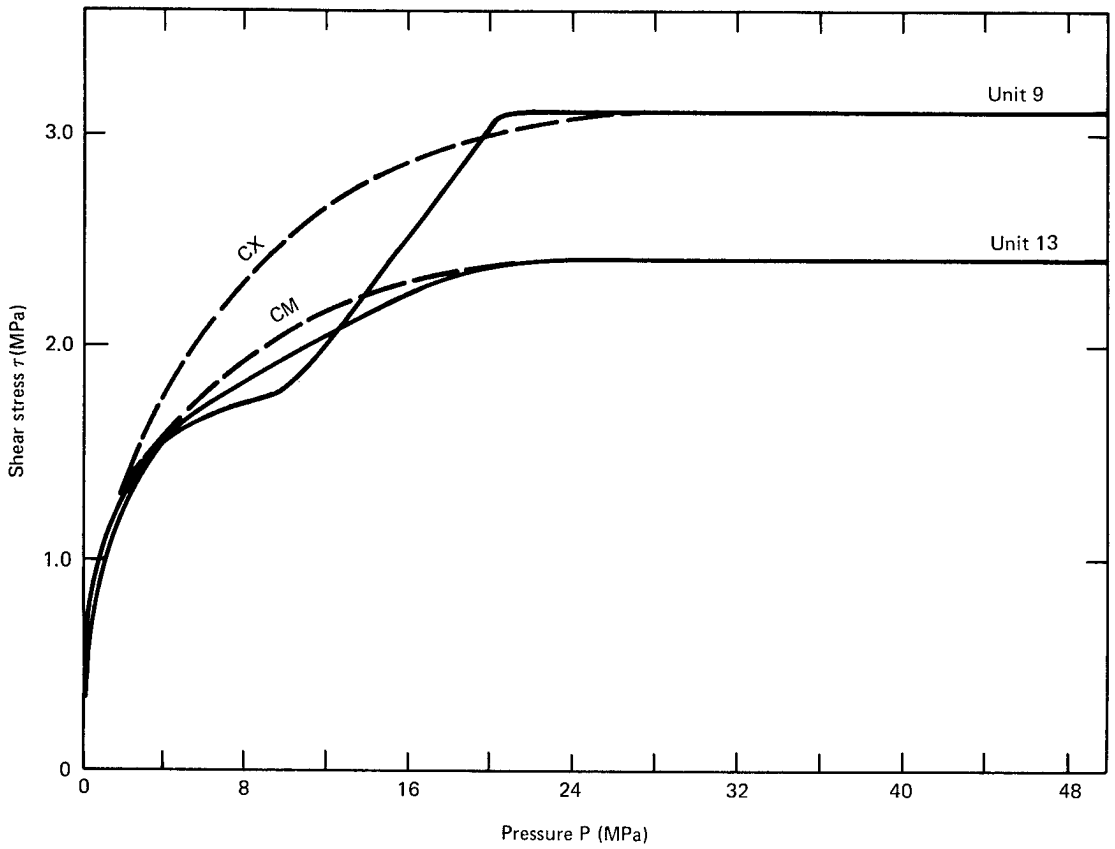

Fig. 9. Failure curves for unsaturated-cemented soils (CM and CX).

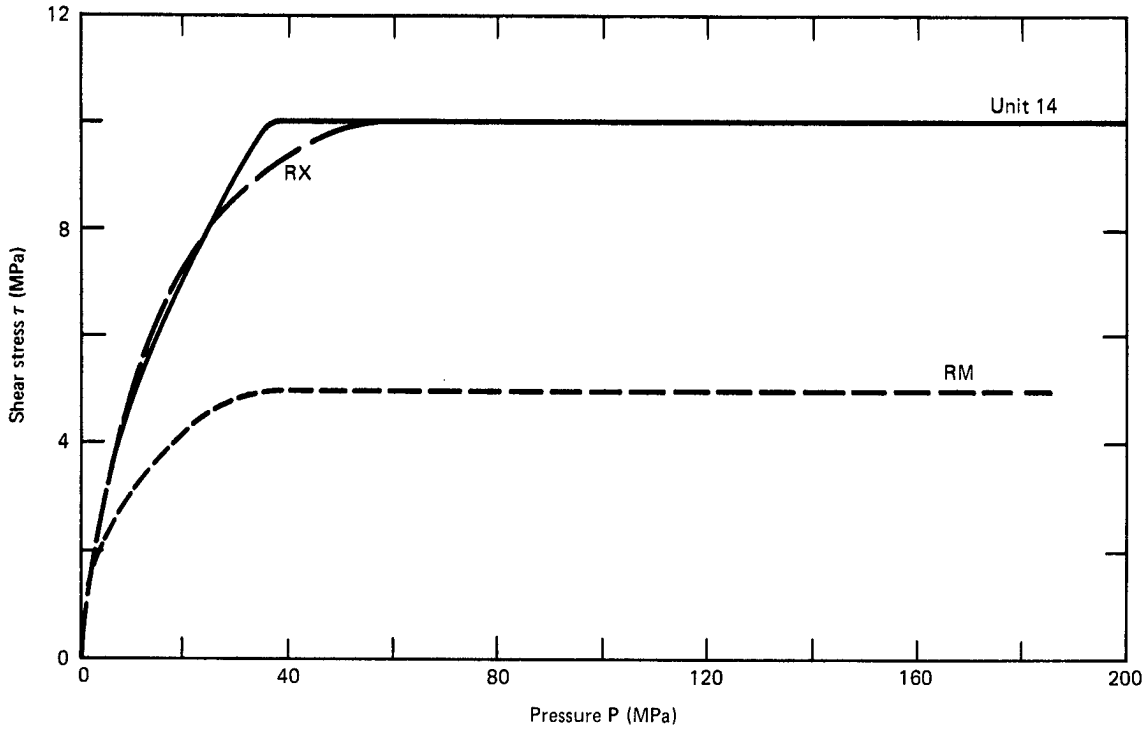

Fig. 10. Failure curves for weak rock (RM and RX).

Table 7. P_T, P_M, and τ_x used for hypothetical soils of the Fort Polk type.

Failure Model	Curve	τ_x (MPa)	P_M (MPa)	P_T (MPa)
Uncemented, saturated	SM	0.17	0.31	0.01
	SX	0.23	0.50	0.01
Uncemented, unsaturated	UM	0.17	10.4	0.1
	UX	1.03	14.7	0.1
Cemented, unsaturated	CM	2.40	21.5	5.0
	CX	3.10	25.1	5.0
Weak rock	RM	5.0	34.5	8.0
	RX	10.0	60.0	8.0

same for each set of curves for all four failure models. Their values were derived by averaging the values given for each group of Fort Polk units.

Table 7 summarizes τ_x, P_M, and P_T for each of the eight failure curves.

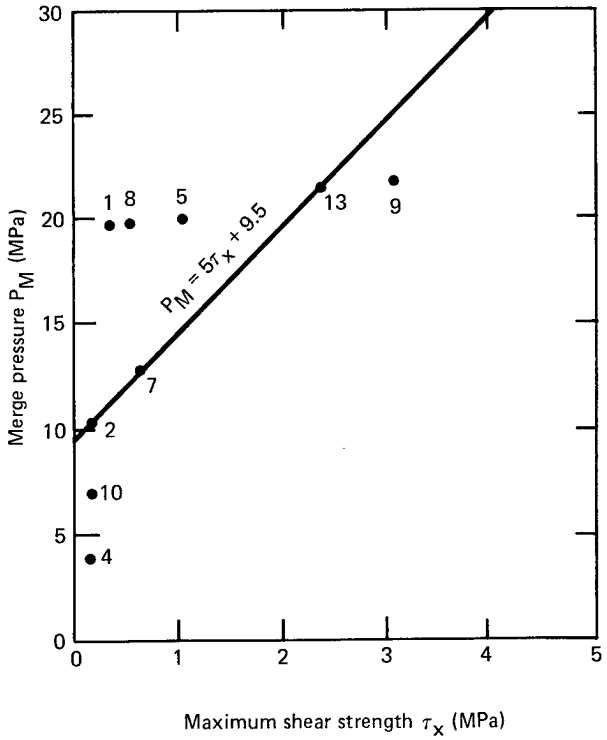

Fig. 11. Merge pressure P_M vs maximum shear strength τ_x for Fort Polk units.

Calculations Performed

ZONING, MATERIAL BOUNDARIES AND INITIAL CONDITIONS

A hypothetical nuclear source with an energy yield of 84 GJ (0.02 kt) was used for all calculations. It was represented by a sphere of iron gas initially having a 0.27-m radius, a 370-GPa pressure, and a 1.5-Mg/m^3 density. The equation of state of the iron gas used in SOC74 was developed by Chapin and Butkovich.[15]

The nuclear source was surrounded by a spherical shell of hypothetical soil extending from the source radius to a radius of 200 m, which is effectively infinite for these problems. Thus there were no reflections from the outer boundary during the 20-msec simulation.

Both source and soil were divided into zones consisting of concentric spherical shells. The source contained 20 zones of equal thickness, while the soil contained 505 zones varying in thickness according to a geometrical progression from 0.0136 m at the edge of the source to about 2 m at the outer edge of the problem (200 m). The initial state of the problems, including zoning and initial source conditions, is shown diagrammatically in Fig. 12.

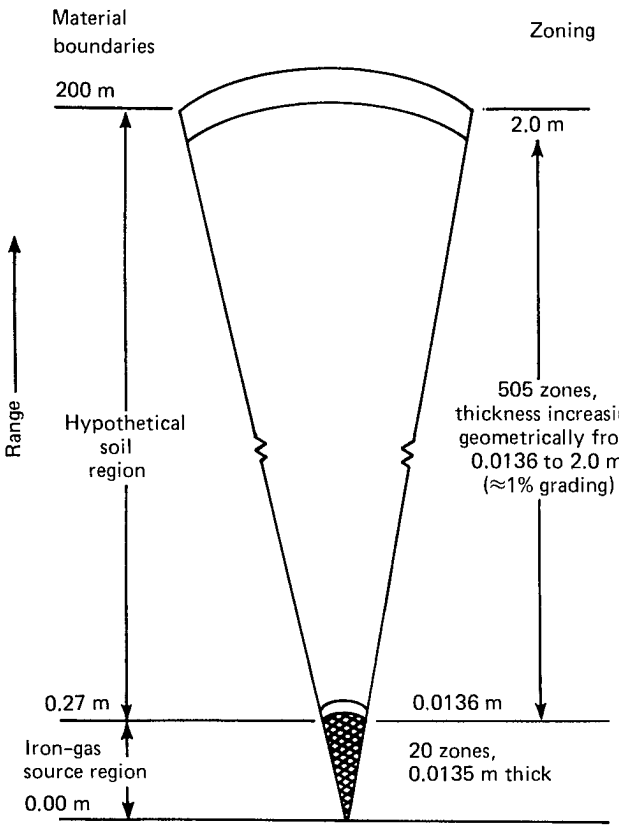

Fig. 12. Diagram of zoning and material boundaries for SOC74 hypothetical nuclear problems.

BULK PROPERTY AND CONSTITUTIVE-RELATION INPUT FOR INDIVIDUAL CALCULATIONS

Results from 25 SOC74 calculations are included in this report. For convenience in referring to individual calculations, mnemonics were developed. The mnemonic is of the following form:

$$F - \rho_0/S_w,$$

where F gives the letter designation of the failure model used (e.g., UM or CX). The middle part, ρ_0/S_w, gives the initial values of ρ_0 (Mg/m^3) and S_w used. There were only two calculations with values of K that differed from 5.0 GPa. For these two calculations the value of K is included in parentheses to the right of the mnemonic. (See Table 8, p. 18.)

The compressibility curves on loading and unloading, for each of the 25 calculations, are included in Appendix A. This

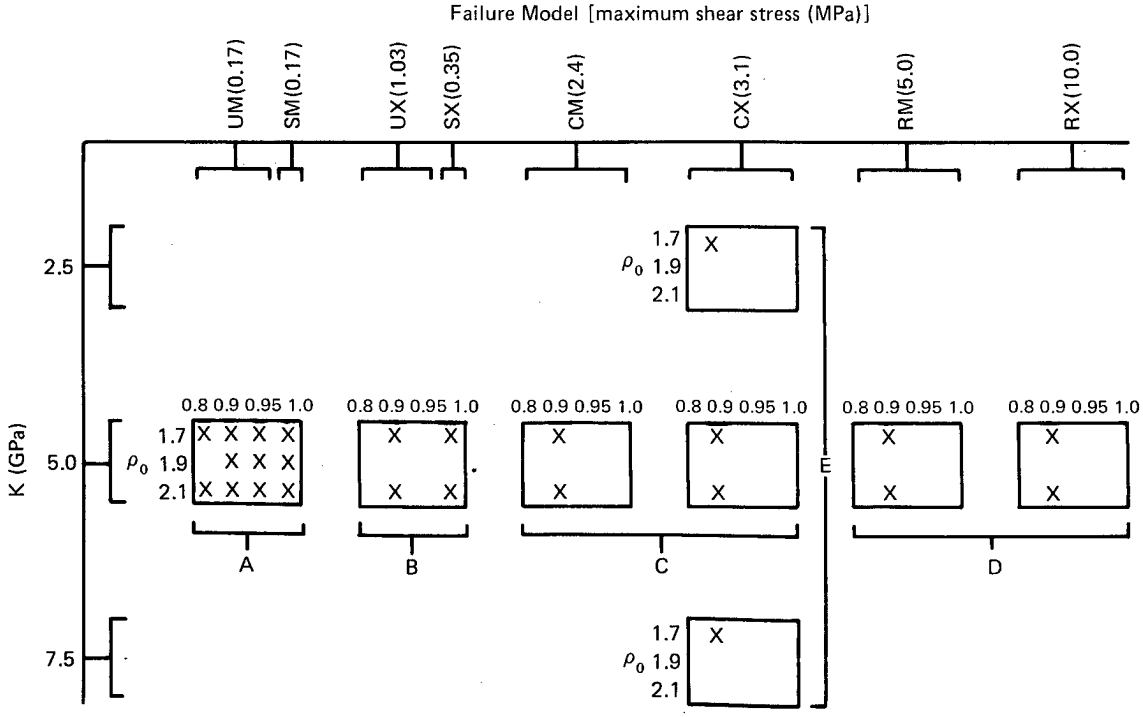

Fig. 13. Summary of calculations performed in the parameter study.

information, together with the appropriate failure curve (Figs. 7, 8, 9, or 10) describes completely the input for each calculation.

ORGANIZATION OF THE CALCULATIONS

Figure 13 shows the organization of the calculations. The values of all four independent variables (ρ_0, S_w, K, and failure model) are shown for each calculation. This was accomplished by constructing a series of small two-dimensional grids (in ρ_0 and S_w) and then overlaying a large two-dimensional grid in K and failure model. The small grids within the large grids are positioned so as to reflect the correct value of K and the correct failure model. The locations of the X's within each small grid give the values of ρ_0 and S_w. Thus the calculations needed to investigate the effect of a particular independent variable can be readily identified. For example, the effect of density can be determined with the calculations performed for K = 5.0 GPa and for all failure models at S_w = 0.9. In addition, it can be determined for the UM-SM failure curves for S_w = 0.9, 0.95, and 1.0.

Figure 14 shows the calculations performed in (ρ_0, S_w) space, overlaid on Fig. 3. This shows that the limits of the

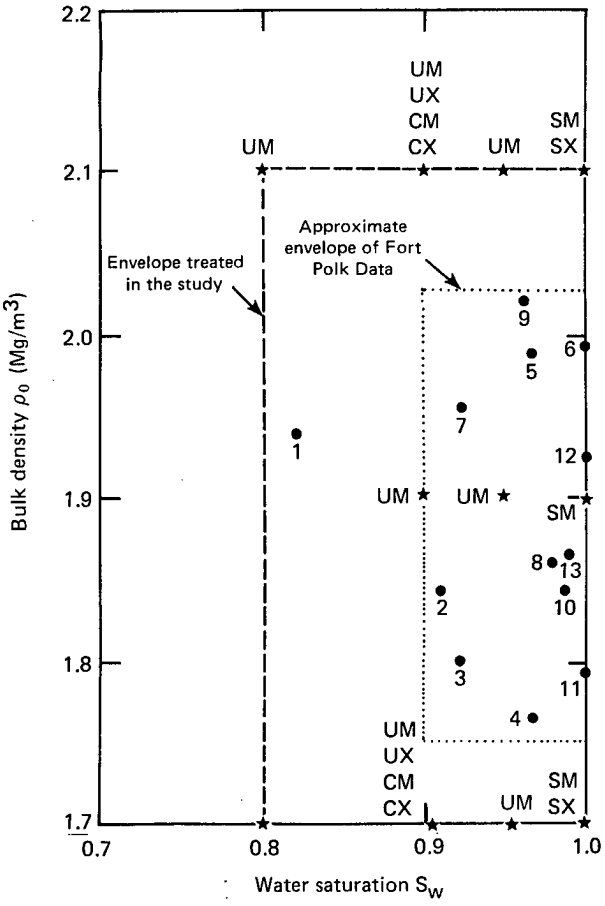

Fig. 14. Plot of calculations performed in ρ_0-S_w space.

study are covered sufficiently in that space, for all failure curves typical of the 13 Fort Polk units. It can also be seen that most of the calculations performed were at $S_w \geq 0.9$. Thus the study was biased toward the region where most of the Fort Polk data is concentrated.

Calculational Results

PHENOMENOLOGY OF THE NUCLEAR DETONATION

The total yield, 84 GJ (20 tons), resides initially in the sphere of iron gas representing the nuclear device. The high initial pressure in the iron gas causes it to expand rapidly, compressing the surrounding soil. For a short time after energy release (~19 μsec) the shock wave generated in the soil by the iron-gas expansion is strong enough to vaporize the soil (pressures exceeding 110 GPa). The shock wave

attenuates very rapidly, and by the time it has reached a range of approximately 0.55 m, it is unable to cause further soil vaporization. Since this radius is roughly twice the initial radius of the iron-gas region (0.27 m), the total mass of vaporized soil is considerably greater (roughly by a factor of 10) than the mass of the nuclear source. The combined mass of iron gas and vaporized soil, then, comprises the nuclear cavity, which continues to expand into the surrounding soil.

Spherical divergence and inelastic effects continue to attenuate the peak pressures as the shock wave travels beyond the soil-vaporization radius. In the pressure regions between 10 and 100 GPa, the shock wave can vaporize the free

Table 8. Figures giving plots of kinetic energy vs time and peak stress and particle velocity vs range for the 25 SOC74 calculations.

	Calculation	Kinetic energy	Peak stress	Peak particle velocity
A-	UM-1.7/0.8	55	56	57
	UM-1.7/0.9	26, 45, 55	27, 46, 56	28, 47, 57
	UM-1.7/0.95	48, 55	49, 56	50, 57
	SM-1.7/1.0	20, 51, 55	21, 52, 56	22, 53, 57
	UM-1.9/0.9	45, 58	56, 59	47, 60
	UM-1.9/0.95	48, 58	49, 59	50, 60
	SM-1.9/1.0	51, 58	52, 59	53, 60
	UM-2.1/0.8	61	62	63
	UM-2.1/0.9	29, 45, 61	30, 46, 62	31, 47, 63
	UM-2.1/0.95	48, 61	49, 62	50, 63
	SM-2.1/1.0	23, 51, 61	24, 52, 62	25, 53, 63
B-	UX-1.7/0.9	26	27	28
	UX-2.1/0.9	29	30	31
	SX-1.7/1.0	20	21	22
	SX-2.1/1.0	23	24	25
C-	CM-1.7/0.9	16, 32	17, 33	18, 34
	CX-1.7/0.9	32	33	34
	CM-2.1/0.9	35	36	37
	CX-2.1/0.9	35	36	37
D-	RM-1.7/0.9	38	39	40
	RX-1.7/0.9	38	39	40
	RM-2.1/0.9	41	42	43
	RX-2.1/0.9	41	42	43
E-	CX-1.7/0.9(2.5)	16	17	18
	CX-1.7/0.9(7.5)	16	17	18

water contained in the soil (but not the solid material). As cavity expansion continues, the gas pressure drops and radial expansion decelerates. A typical plot of cavity pressure versus time is shown in Fig. 15. By the time the pressure at the front drops below 10 GPa, it has separated from the cavity and has started to propagate in a manner similar to a shock wave driven by high explosive in the same soil.

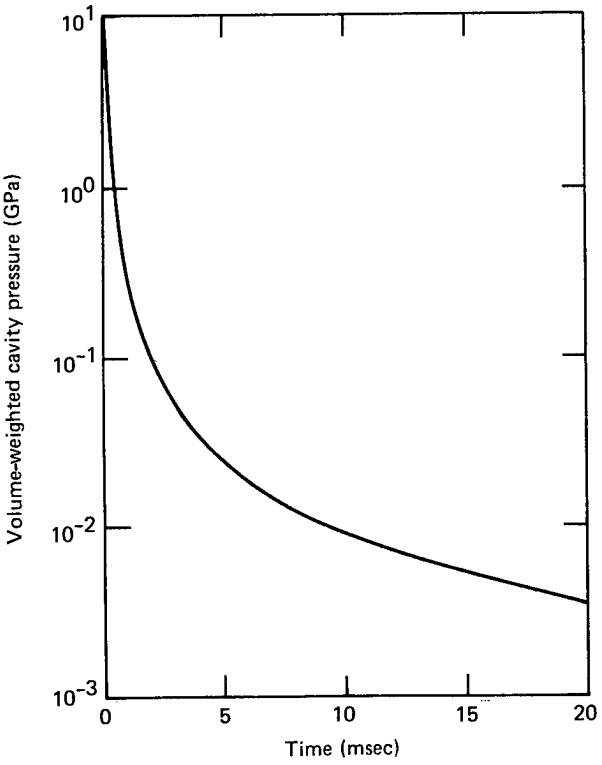

Fig. 15. Typical curve of cavity pressure vs time for an 84-GJ (20-ton) nuclear detonation, Z = 20%.

EFFECT OF INDEPENDENT VARIABLES ON GROUND MOTION AND ENERGY COUPLING

This section reviews the direct results obtained from 25 SOC74 calculations. Many quantities can be obtained from SOC74, as a function either of range or of time. The results presented in this section are limited mainly to kinetic energy coupled to the soil and to peak stress and particle velocity versus range in the soil. The calculational results are compared in order to show the effect of each of the four independent variables: K, failure envelope, ρ_0, and S_w.

Location of Plots for Individual Calculations

In order to allow for comparisons other than those presented in this section, Table 8 lists, for each of the 25 SOC74 calculations, the figures that can be consulted to obtain the kinetic energy versus time and peak stress and particle velocity versus range. They are grouped according to the letter designations "A" through "E", as shown in Fig. 13.

Effect of Initial Bulk Modulus

As already mentioned, the effect of the initial bulk modulus K on ground motion was felt to be minimal. Therefore only two calculations were performed with values that differed from 5.0 GPa: CX-1.7/0.9 (2.5) and CX-1.7/0.9 (7.5), where K was equal to 2.5 and 7.5 GPa, respectively. Unsaturated, cemented hypothetical soils were chosen for the variation of K in order to maximize the effect for soils typical of Fort Polk. Figure 16 shows the kinetic energy coupled to the soil for the two calculations referred to above and CX-1.7/0.9 (this calculation according to the convention used in this report, has K = 5.0 GPa). The three curves are nearly the same, indicating that varying K does not affect the coupling of kinetic energy. Cratering is directly related to the coupled kinetic energy, and hence K also does not affect cratering. Figures 17 and 18 show, for the same three calculations, the

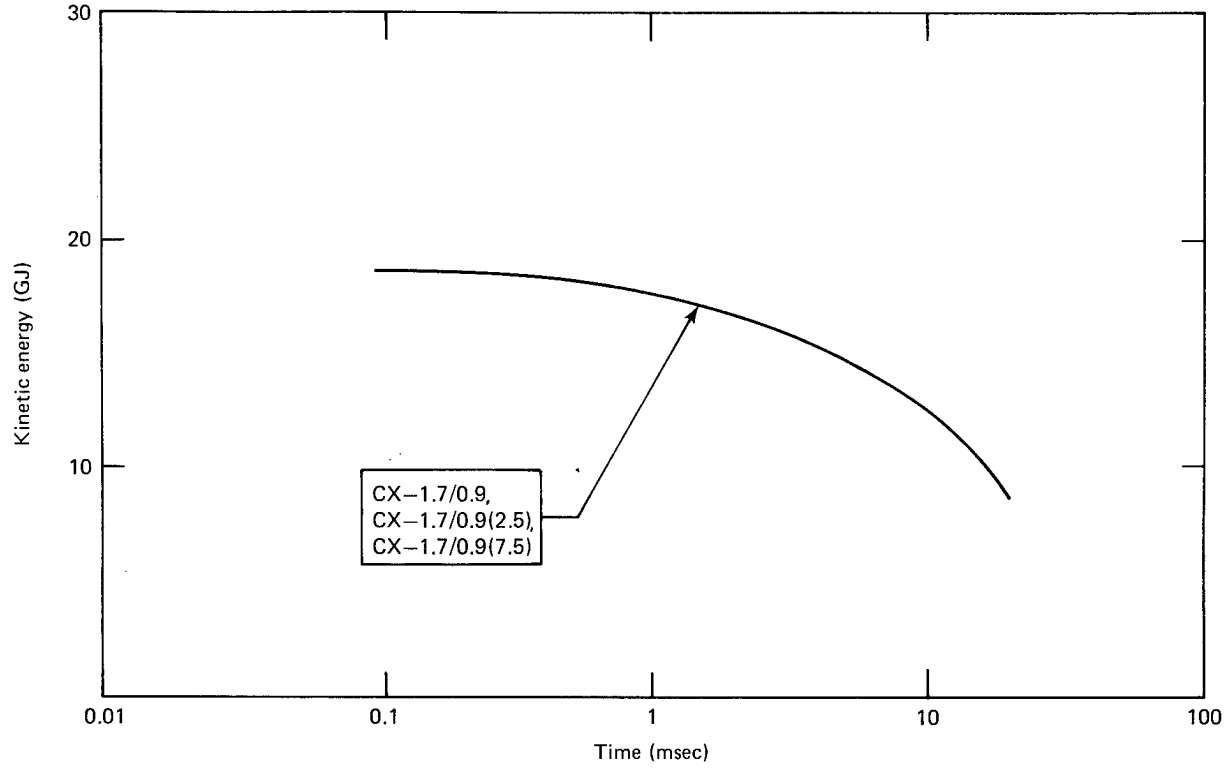

Fig. 16. Effect of K on kinetic energy vs time.

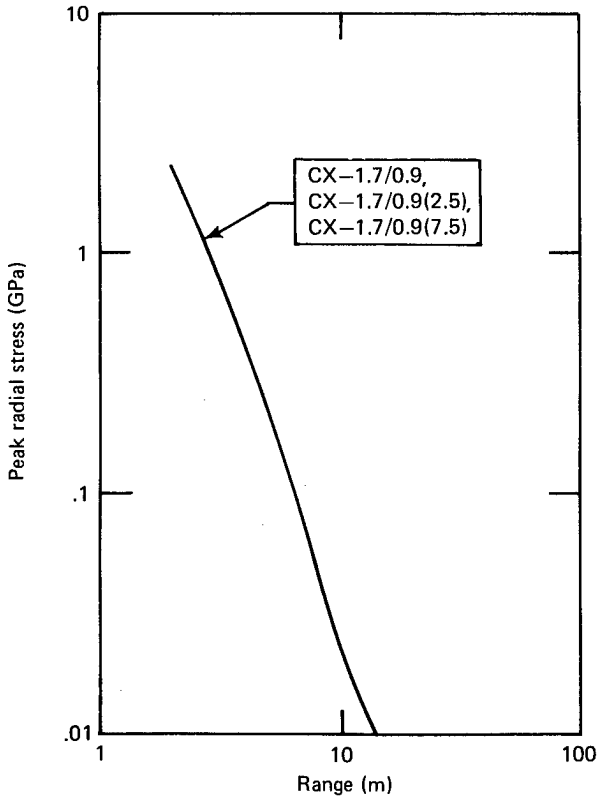

Fig. 17. Effect of K on peak stress vs range.

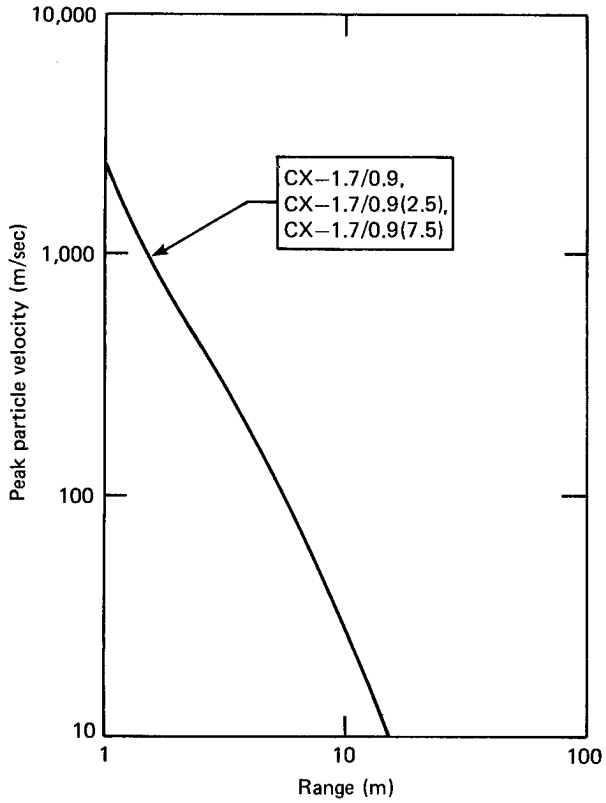

Fig. 18. Effect of K on peak particle velocity vs range

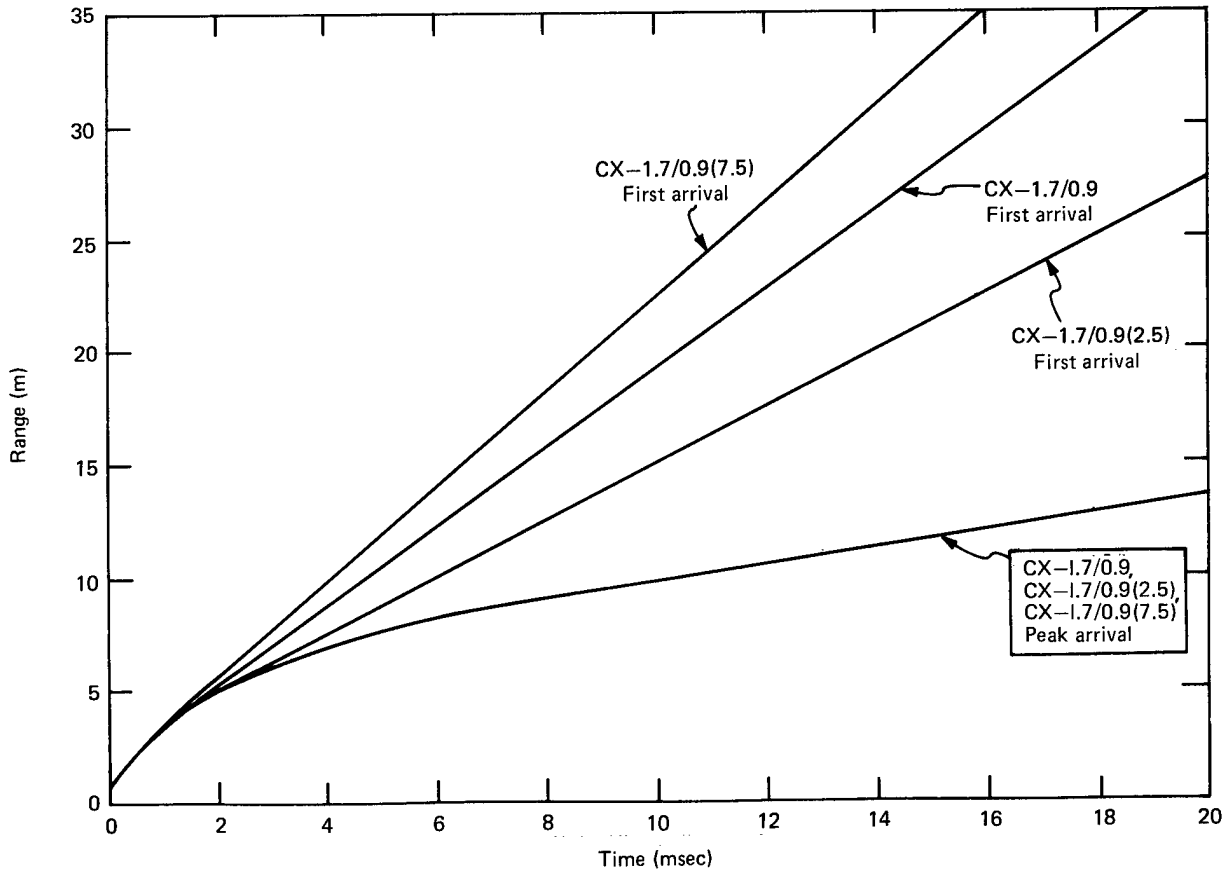

Fig. 19. Effect of K on first arrival and peak arrival times.

peak stress versus range and peak particle velocity versus range, respectively. Again, varying K has no effect on the calculated results. Figure 19 shows that varying K also does not affect the peak arrival time. First arrival, however, is affected because K determines the velocity of the acoustic wave. Very little kinetic energy is associated with this "precursor," however, and consequently it has very little effect on cratering or close-in ground motion.

To summarize, for soils of the Fort Polk type, K has only a minor effect on the close-in ground motion and dynamic crater formation resulting from a nuclear detonation.

Effect of Failure

In this section we analyze in two ways the effect of failure on energy coupling and ground motion. First, we compare the relative effect of the maximum and minimum failure curves (Figs. 7 through 10) for each category (e.g., uncemented, saturated soils). Second, we attempt to give the total, qualitative effect of failure by summarizing results from all of the calculations.

Figures 20, 21, and 22 show the effect of the maximum and minimum failure curves on coupled kinetic energy versus time, and peak stress and peak particle velocity versus range, respectively, for the uncemented, saturated soils (SM and SX) with

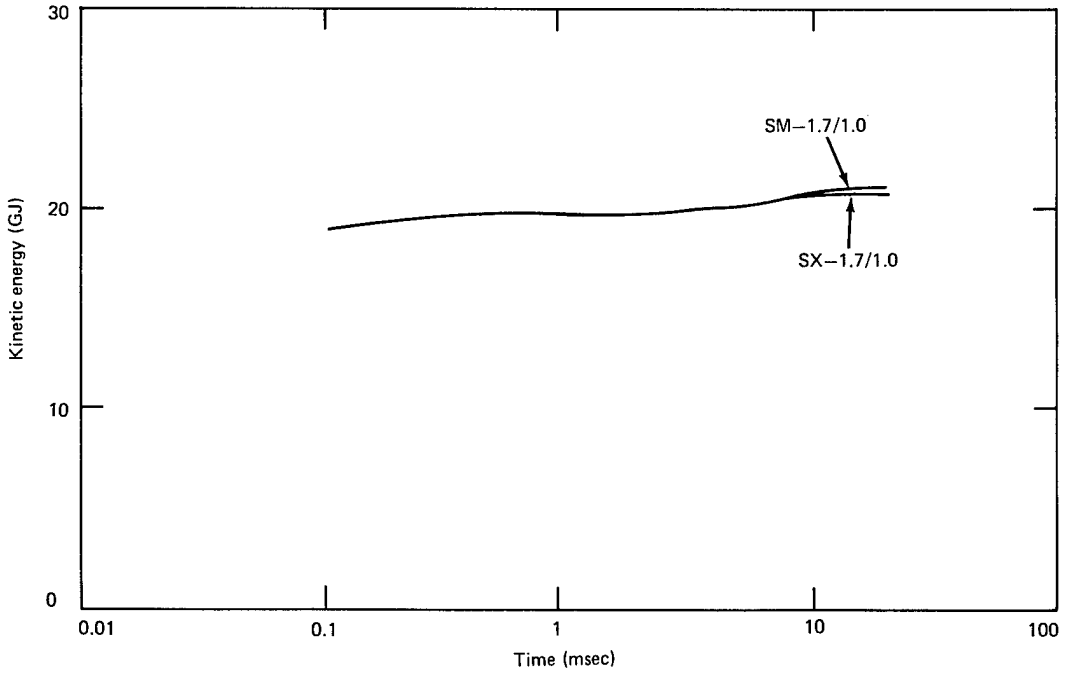

Fig. 20. Effect of failure on coupled kinetic energy for uncemented, saturated soils (ρ_0 = 1.7 Mg/m^3).

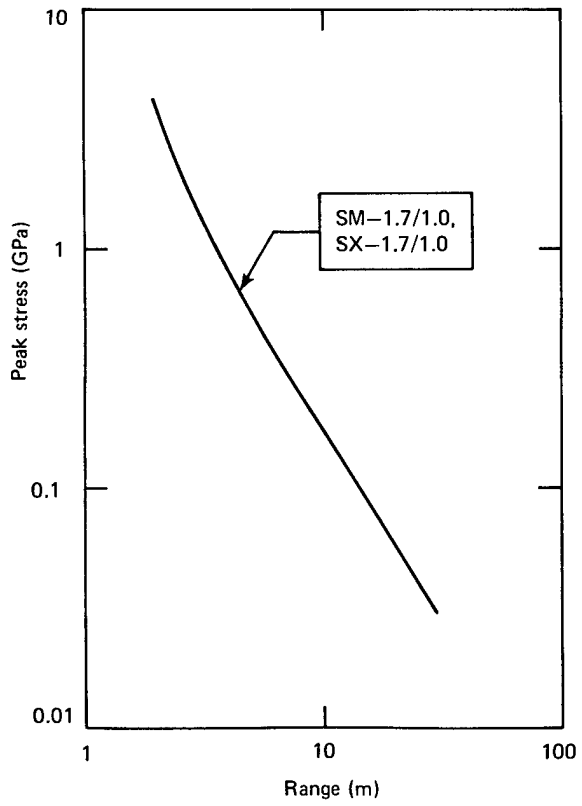

Fig. 21. Effect of failure on peak stress vs range for uncemented, saturated soils (ρ_0 = 1.7 Mg/m^3).

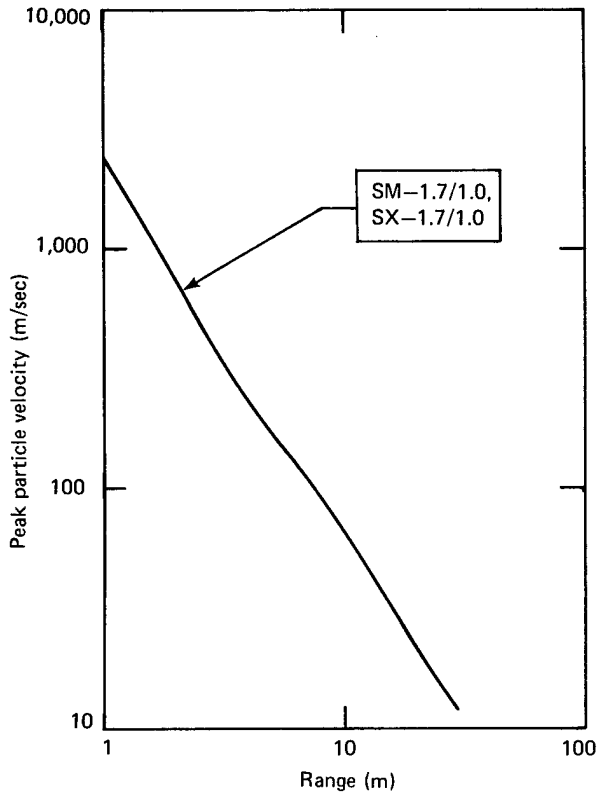

Fig. 22. Effect of failure on peak particle velocity vs range for uncemented, saturated soils (ρ_0 = 1.7 Mg/m^3).

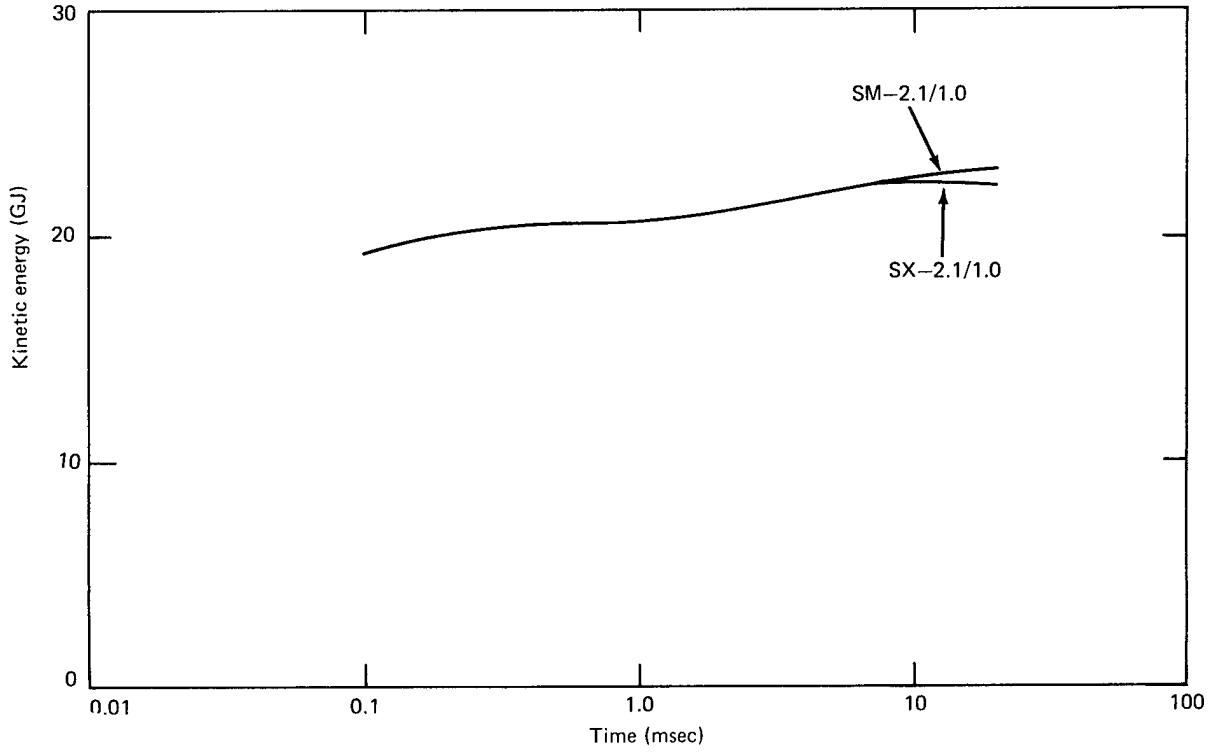

Fig. 23. Effect of failure on coupled kinetic energy for uncemented, saturated soils (ρ_0 = 2.1 Mg/m^3).

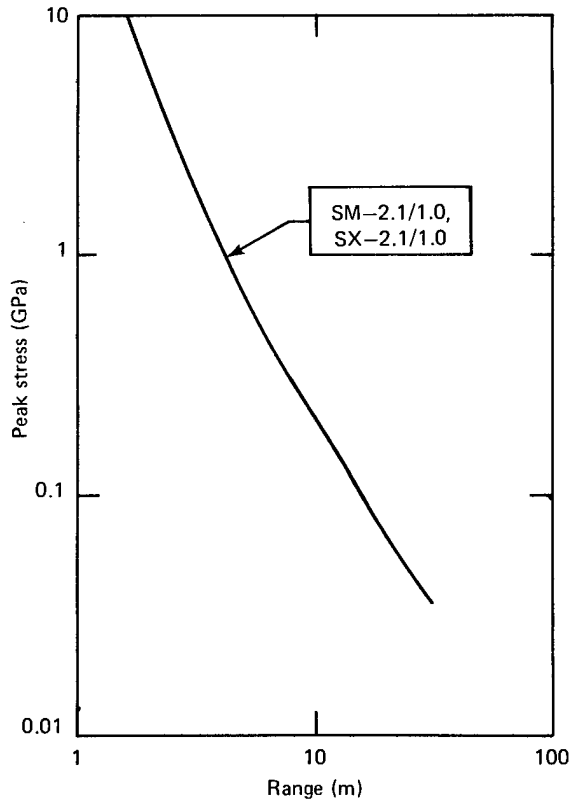

an initial bulk density ρ_0 = 1.7 Mg/m^3. Figures 23, 24, and 25 give the same comparison for soils with ρ_0 = 2.1 Mg/m^3. In all cases there are only very minimal differences between the curves, indicating that, for the saturated soils, either failure curve (or any drawn between the SM and SX curves in Fig. 7) will adequately represent the entire category.

The same comparison is shown in Figs. 26, 27, and 28 for ρ_0 = 1.7 Mg/m^3 and in Figs. 29, 30, and 31 for ρ_0 = 2.1 Mg/m^3 for the uncemented, unsaturated (UM and UX) category. These calculational results show that, although the differences

Fig. 24. Effect of failure on peak stress vs range for uncemented, saturated soils (ρ_0 = 2.1 Mg/m^3).

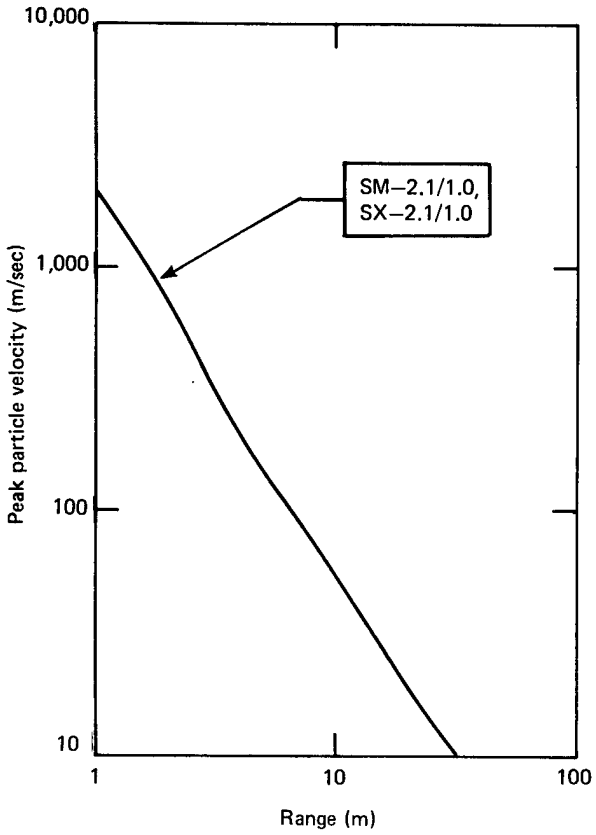

Fig. 25. Effect of failure on peak particle velocity vs range for uncemented, saturated soils (ρ_0 = 2.1 Mg/m^3).

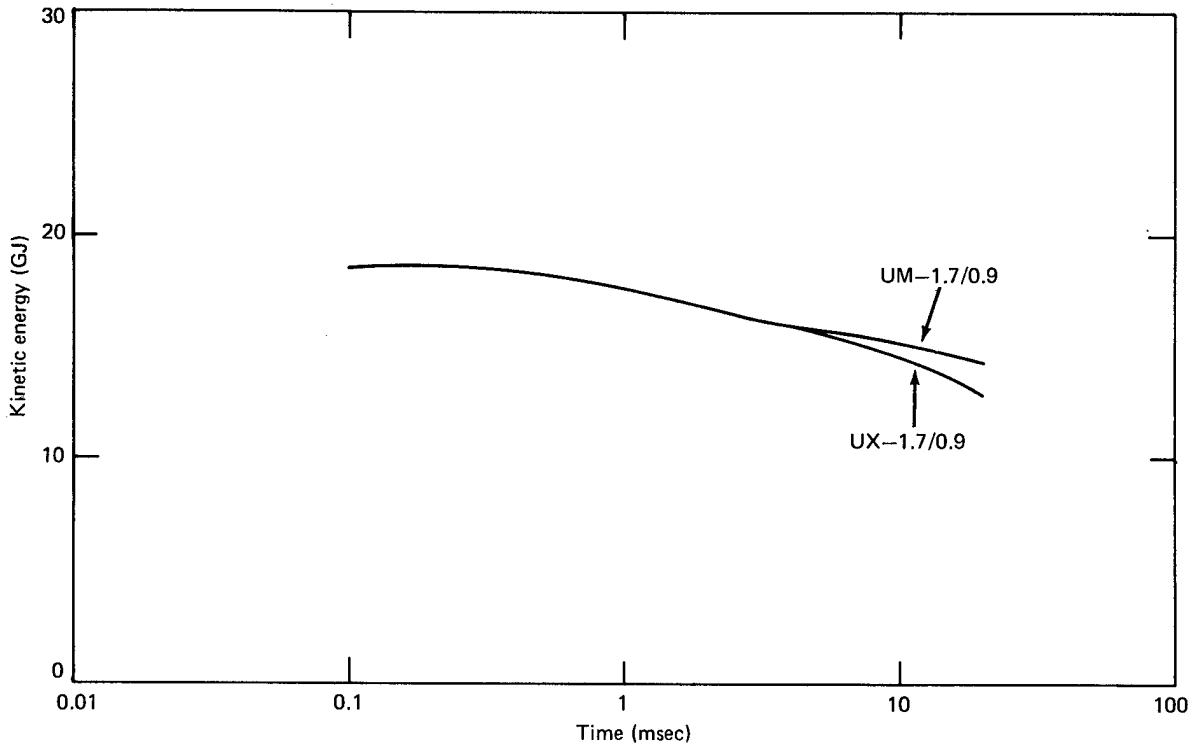

Fig. 26. Effect of failure on kinetic energy coupling for uncemented, saturated soils (S_w = 0.9, ρ_0 = 1.7 Mg/m^3).

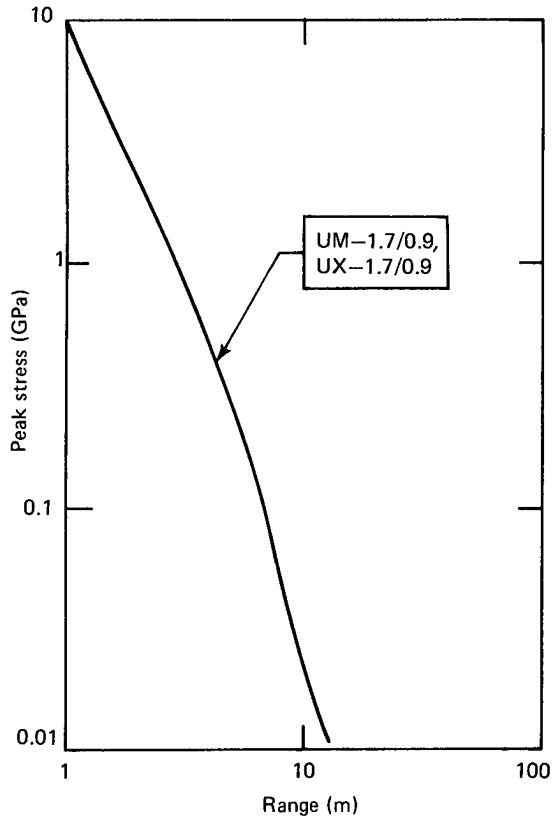

Fig. 27. Effect of failure on peak stress vs range for uncemented, unsaturated soils (S_w = 0.9, ρ_0 = 1.7 Mg/m^3).

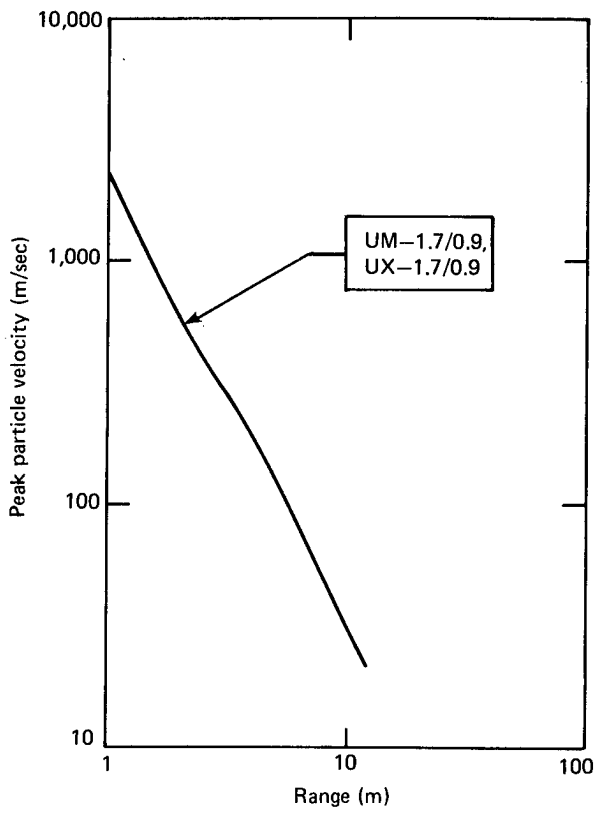

Fig. 28. Effect of failure on peak particle velocity vs range for uncemented, unsaturated soils (S_w = 0.9, ρ_0 = 1.7 Mg/m^3).

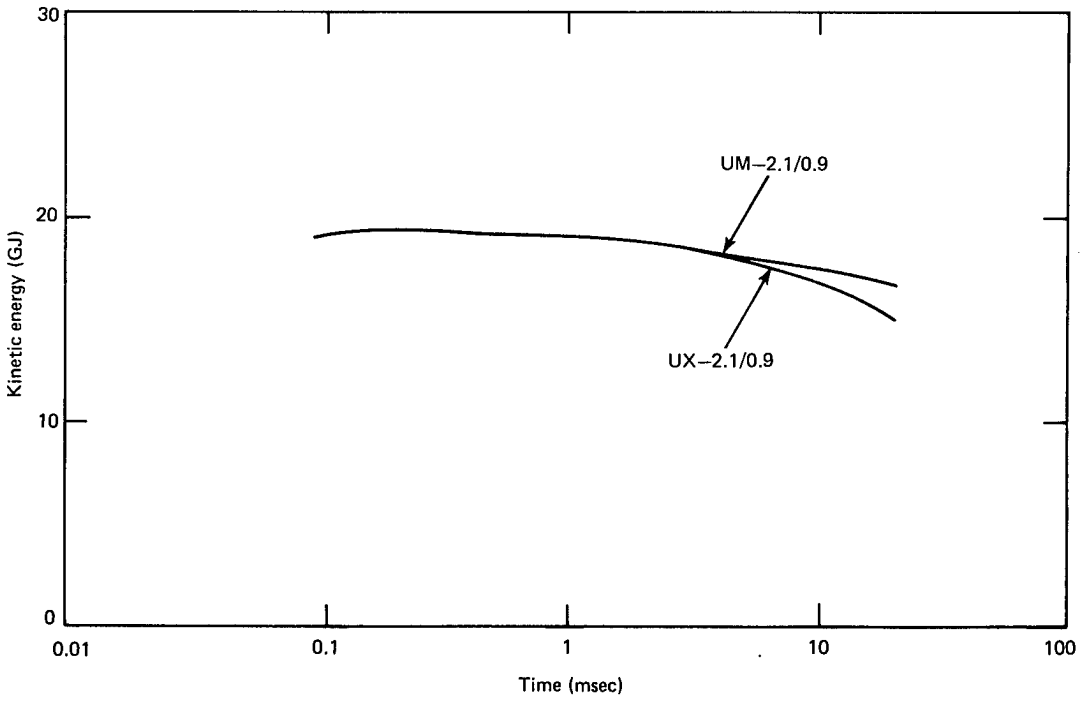

Fig. 29. Effect of failure on coupled kinetic energy for uncemented, unsaturated soils (S_w = 0.9, ρ_0 = 2.1 Mg/m^3).

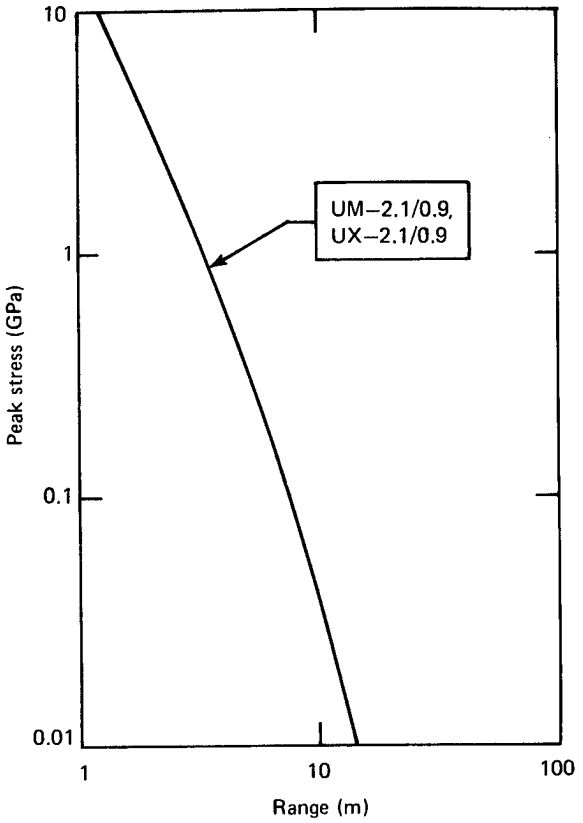

Fig. 30. Effect of failure on peak stress vs range for uncemented, unsaturated soils (S_w = 0.9, ρ_0 = 2.1 Mg/m^3).

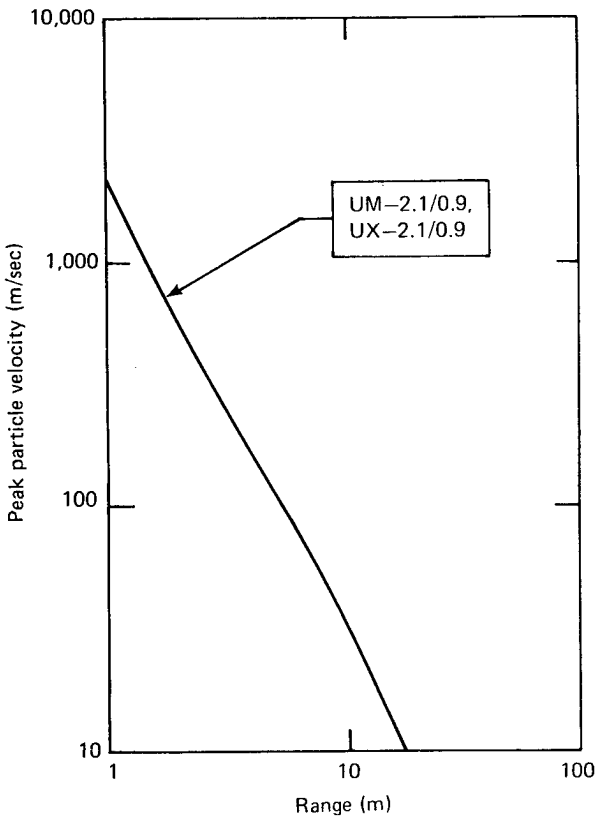

Fig. 31. Effect of failure on peak particle velocity vs range for uncemented, unsaturated soils (S_w = 0.9, ρ_0 = 2.1 Mg/m^3).

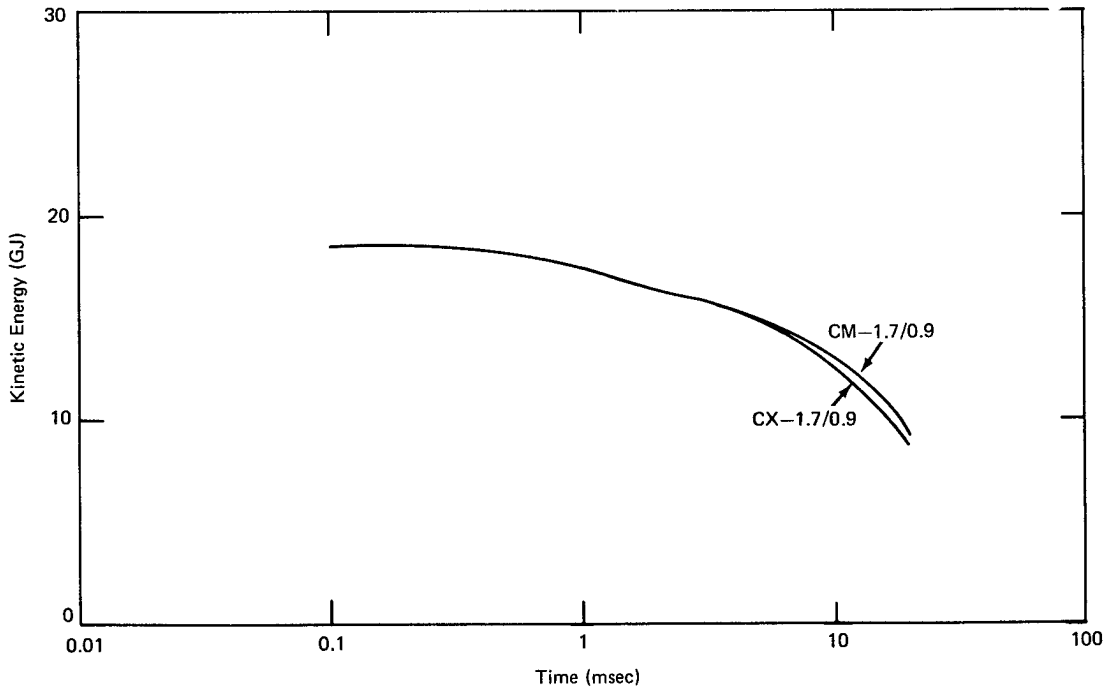

Fig. 32. Effect of failure on kinetic energy coupling for unsaturated, cemented soils (S_w = 0.9, ρ_0 = 1.7 Mg/m^3).

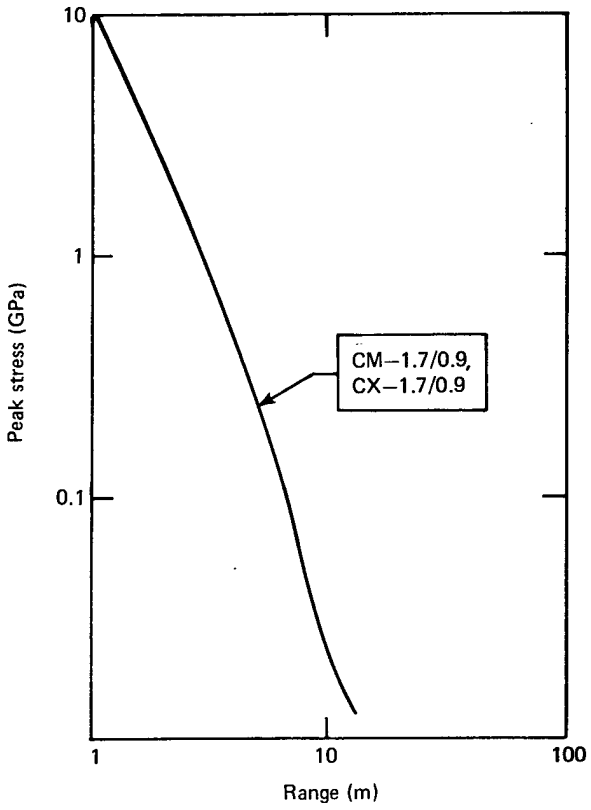

Fig. 33. Effect of failure on peak stress vs range for unsaturated, cemented soils (S_w = 0.9, ρ_0 = 1.7 Mg/m^3).

between the peak-stress and peak-particle-velocity curves are very small at both densities, the UX failure curve gives a lower coupled kinetic energy than does the UM curve at late times (>10 msec).

The above is seen to be true also for the cemented, unsaturated soils, as shown in Figs. 32, 33, and 34 for ρ_0 = 1.7 Mg/m^3 and in Figs. 35, 36, and 37 for ρ_0 = 2.1 Mg/m^3. Again, for both densities, the calculated peak stresses and particle velocities are not significantly affected by the difference in shear strength between the CM and CX curves (Fig. 9).

For the weak rocks there is a large difference between the maximum shear strengths of the RM and RX curves (Fig. 10). This difference, about 5 MPa, leads to a more substantial effect on kinetic

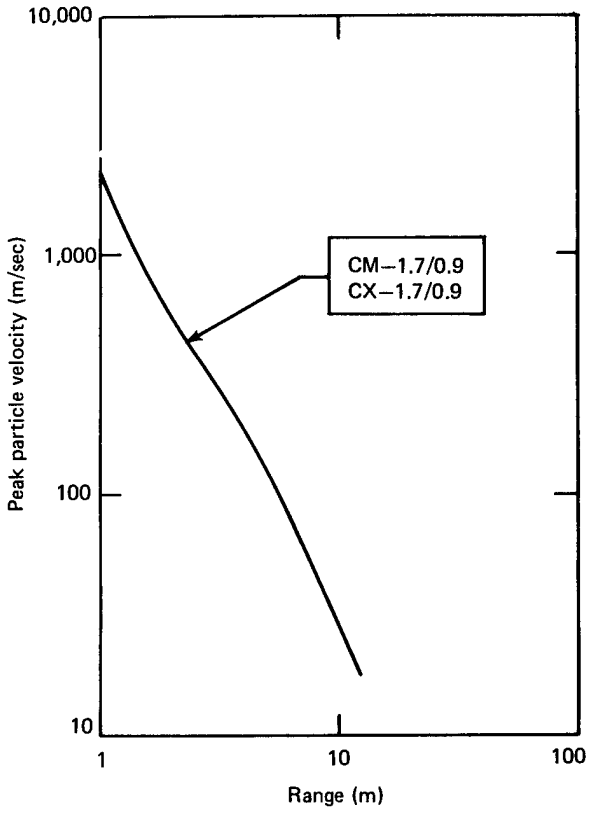

Fig. 34. Effect of failure on peak particle velocity vs range for unsaturated, cemented soils (S_w = 0.9, ρ_0 = 1.7 Mg/m^3).

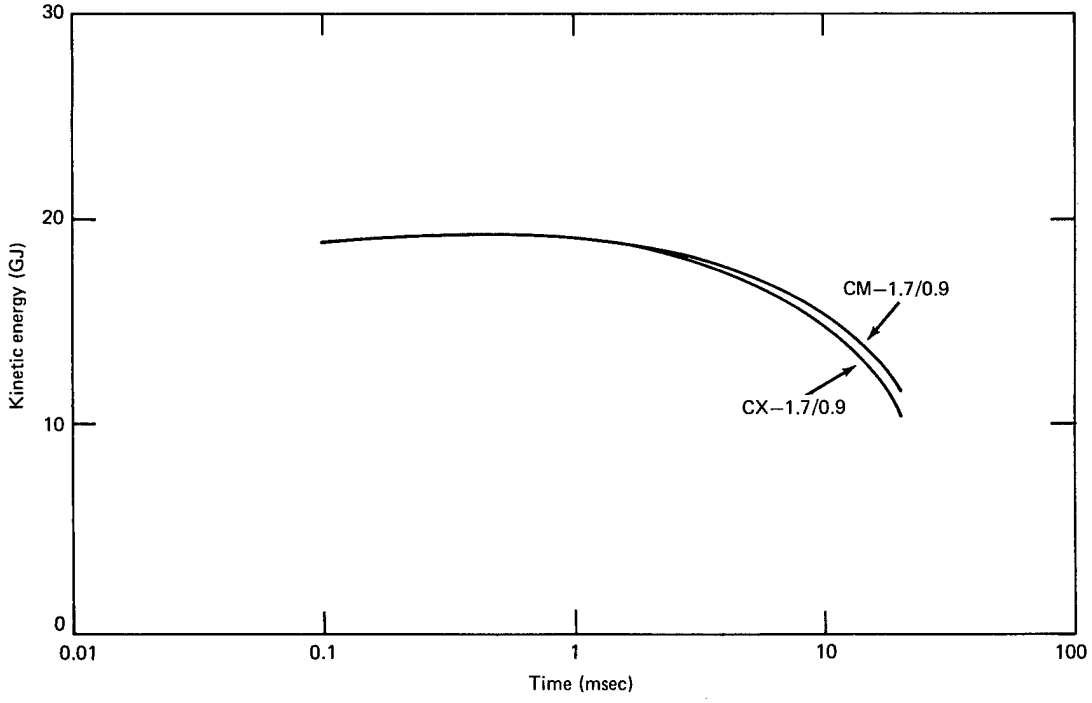

Fig. 35. Effect of failure on kinetic energy coupling for unsaturated, cemented soils (S_w = 0.9, ρ_0 = 2.1 Mg/m^3).

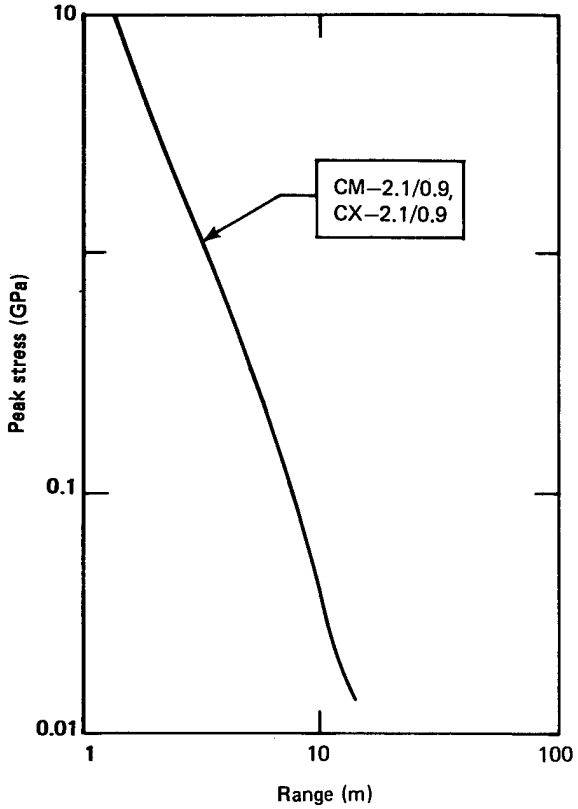

Fig. 36. Effect of failure on peak stress vs range for unsaturated, uncemented soils (S_w = 0.9, ρ_0 = 2.1 Mg/m^3).

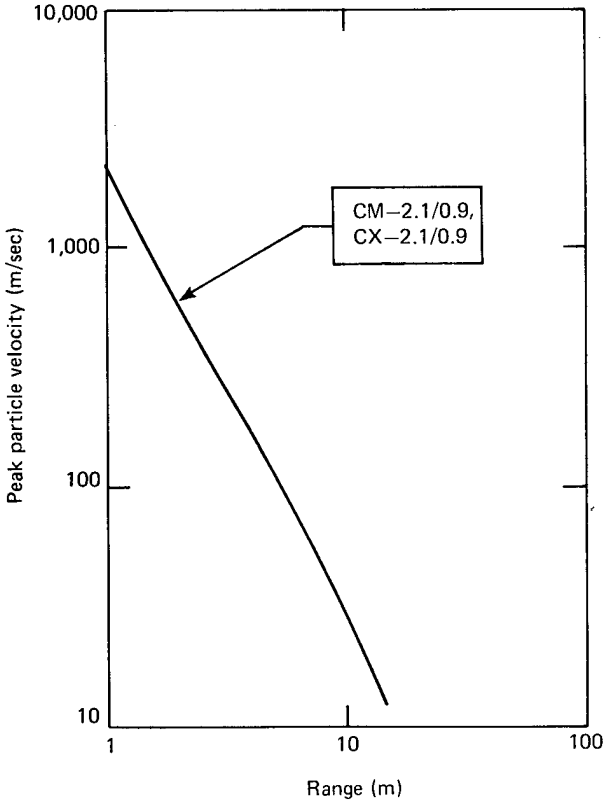

Fig. 37. Effect of failure on peak particle velocity vs range for unsaturated, cemented soils (S_w = 0.9, ρ_0 = 2.1 Mg/m^3).

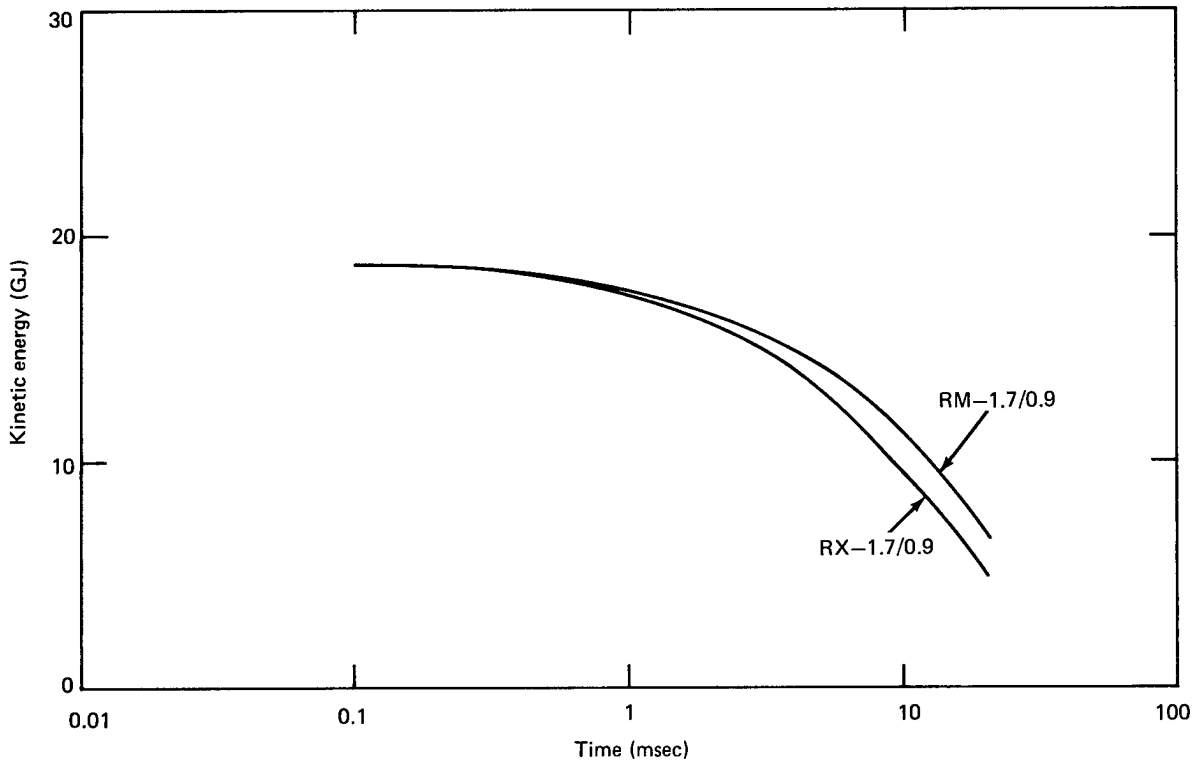

Fig. 38. Effect of failure on kinetic energy coupling for weak rocks (S_w = 0.9, ρ_0 = 1.7 Mg/m^3).

energy coupling and to a slight, but noticeable, effect on the peak particle velocity versus range. These effects are shown in Figs. 38, 39, and 40 for ρ_0 = 1.7 Mg/m^3 and in Figs. 41, 42, and 43 for ρ_0 = 2.1 Mg/m^3.

Thus increasing the strength τ_x within any one category lowers the kinetic energy coupled to the material at late times (>10 msec) and also lowers the peak particle velocities in the intermediate range (~10 m). The peak stress, however, is not affected.

It is more interesting to look at the total effect of failure, using all of the calculations. In order to do this, the

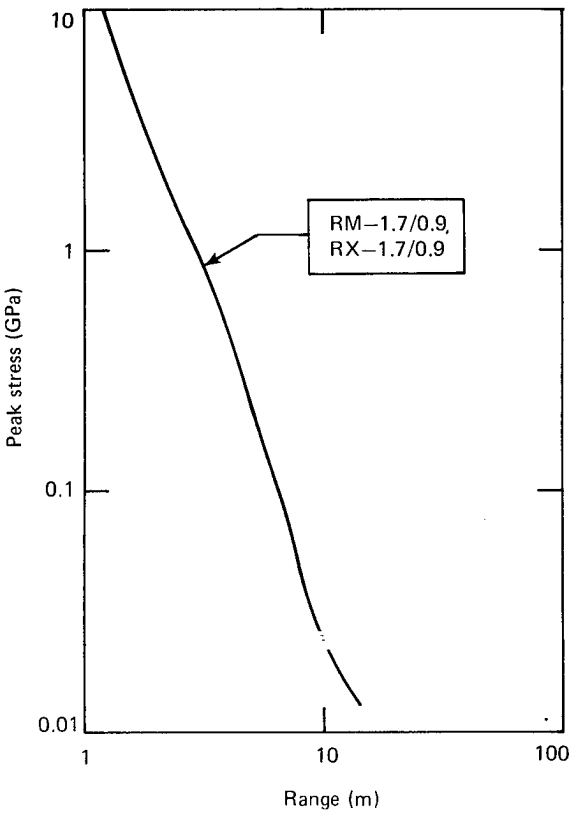

Fig. 39. Effect of failure on peak stress vs range for weak rocks (S_w = 0.9, ρ_0 = 1.7 Mg/m^3).

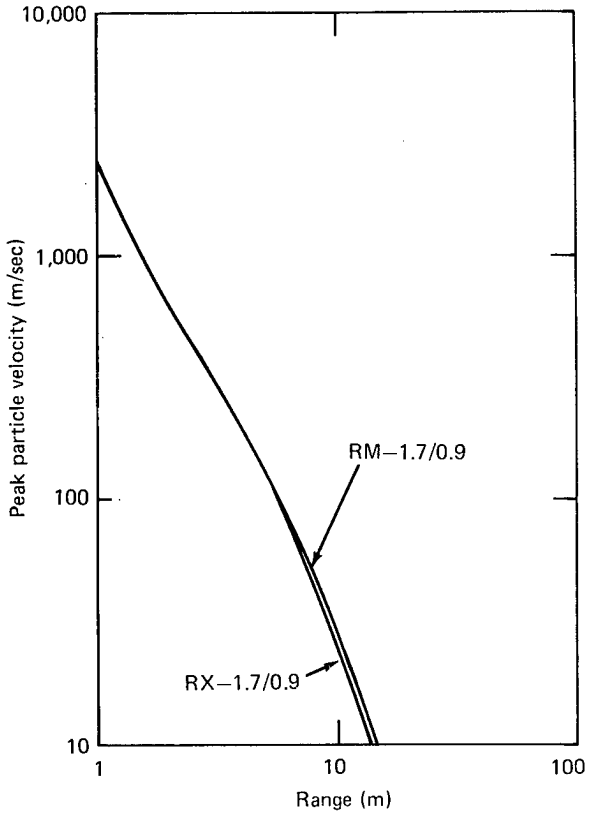

Fig. 40. Effect of failure on peak particle velocity vs range for weak rocks (S_w = 0.9, ρ_0 = 1.7 Mg/m^3).

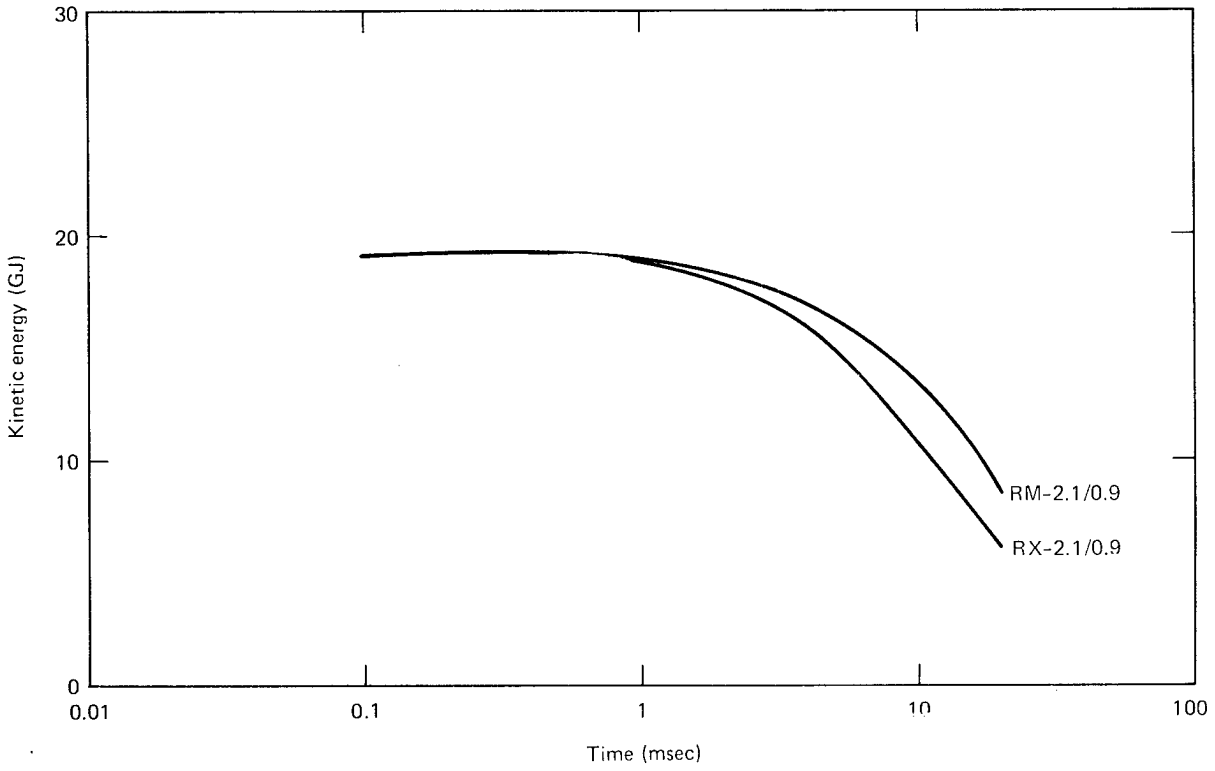

Fig. 41. Effect of failure on kinetic energy coupling for weak rocks (S_w = 0.9, ρ_0 = 2.1 Mg/m^3).

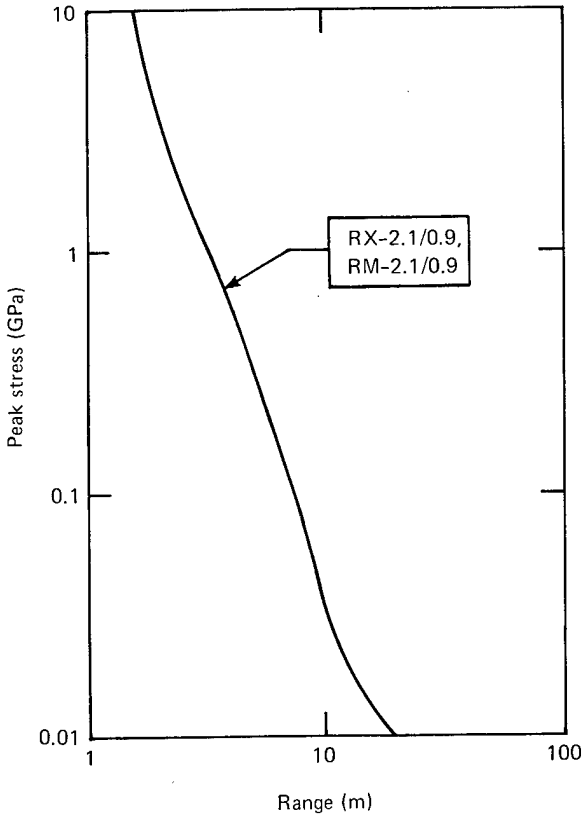

Fig. 42. Effect of failure on peak stress vs range for weak rocks (S_w = 0.9, ρ_0 = 2.1 Mg/m^3).

kinetic energies were plotted at a constant time (15 msec) and the peak particle velocities and stresses at a constant range (12 m). This time and range were chosen because they are very important to low-yield nuclear cratering at the optimum depth of burial for soils. Figure 44a plots the coupled kinetic energy at 15 msec versus τ_x. For both sets of calculations (ρ_0 = 1.7 and ρ_0 = 2.1 Mg/m^3) the coupled kinetic energy decreases with increasing τ_x. Also, the difference between the two curves is roughly constant. Figures 44b and c plot the peak stress and particle velocity at the 12-m range versus τ_x. Although the peak particle velocity decreases slowly with increasing τ_x, no clear correlation exists for the two different densities, as was seen for the kinetic energies in Fig. 44a. The peak stress seems to increase with τ_x,

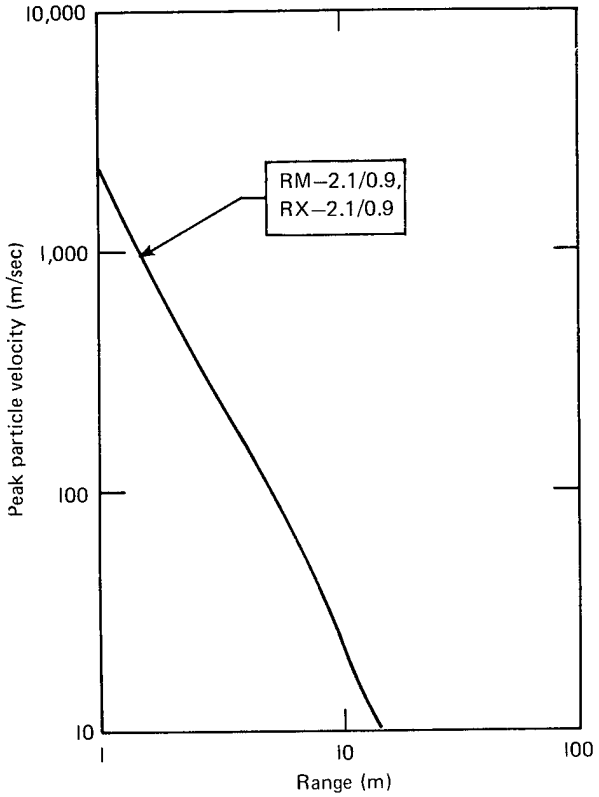

Fig. 43. Effect of failure on peak particle velocity vs range for weak rocks (S_w = 0.9, ρ_0 = 2.1 Mg/m^3).

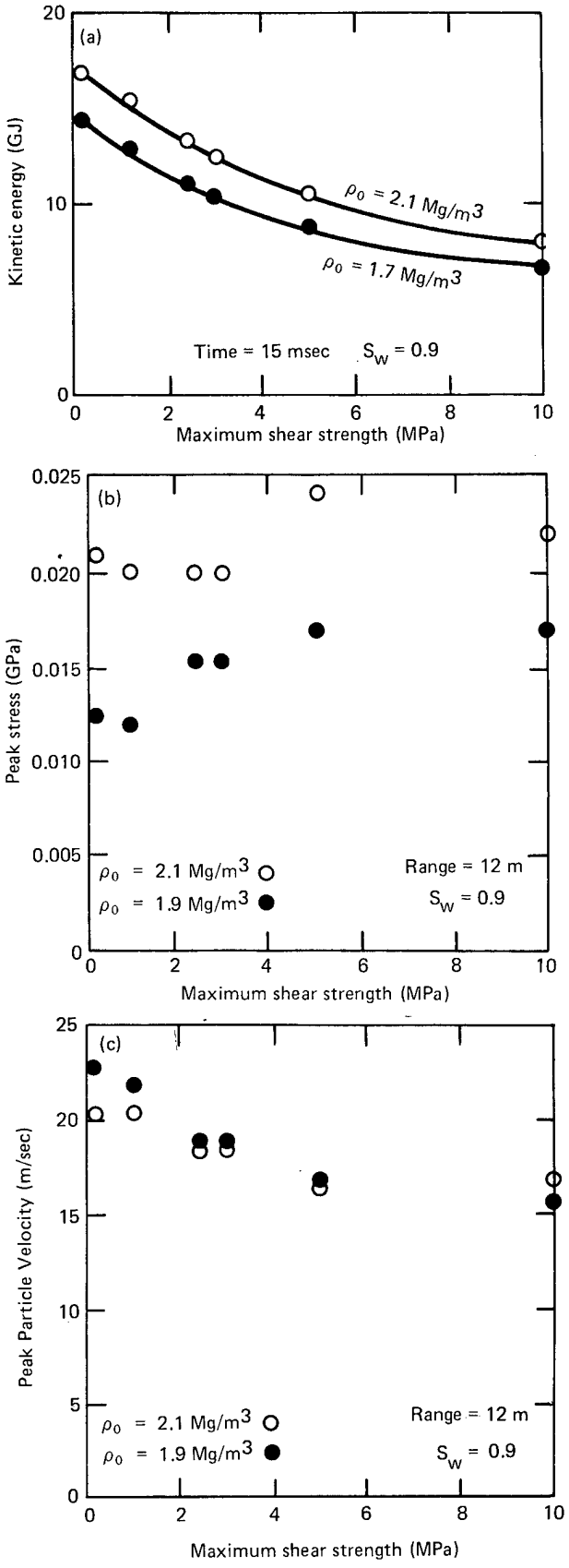

Fig. 44. Total effect of τ_x on kinetic energy coupling and ground motion.

but this may not be true in light of the artificial viscosity Q used in the SOC74 code. The effect of this term in the finite-difference equations is to spread the shock front out in both time and space. In order for the total impulse to be correct, then, the peak value must be reduced somewhat from its "true" value. As Q is increased, the effect increases. Since higher values of Q are required for the lower strength soils than for the weak rocks (τ_x > 5.0 MPa), the calculated peak-stress values at the lower values of τ_x on both the ρ_0 = 1.7 and ρ_0 = 2.1 Mg/m^3 curves are actually slightly higher. This indicates, then, that there is essentially no variation of peak stress with τ_x.

Effect of Density

As can be seen from Fig. 13, calculations were performed for hypothetical soils having initial bulk densities of 1.7, 1.9, and 2.1 Mg/m^3. In the preceding section it was found that both peak stress and peak particle velocity were not affected strongly by the maximum shear strength. The kinetic energy was affected, but the effect was similar for both of the densities (ρ_0 = 1.7 and ρ_0 = 2.1 Mg/m^3) used. In order to study the effect of density, then, the failure curve, as well as K, could be held constant. For the unsaturated soils, the UM curve (Fig. 8) was used; for the saturated soils, the SM curve (Fig. 7) was used. By using the results given in the preceding section, the effect of density can be found for all failure models within the scope of the study.

Figure 45 shows the effect of ρ_0 on kinetic energy coupling versus time for

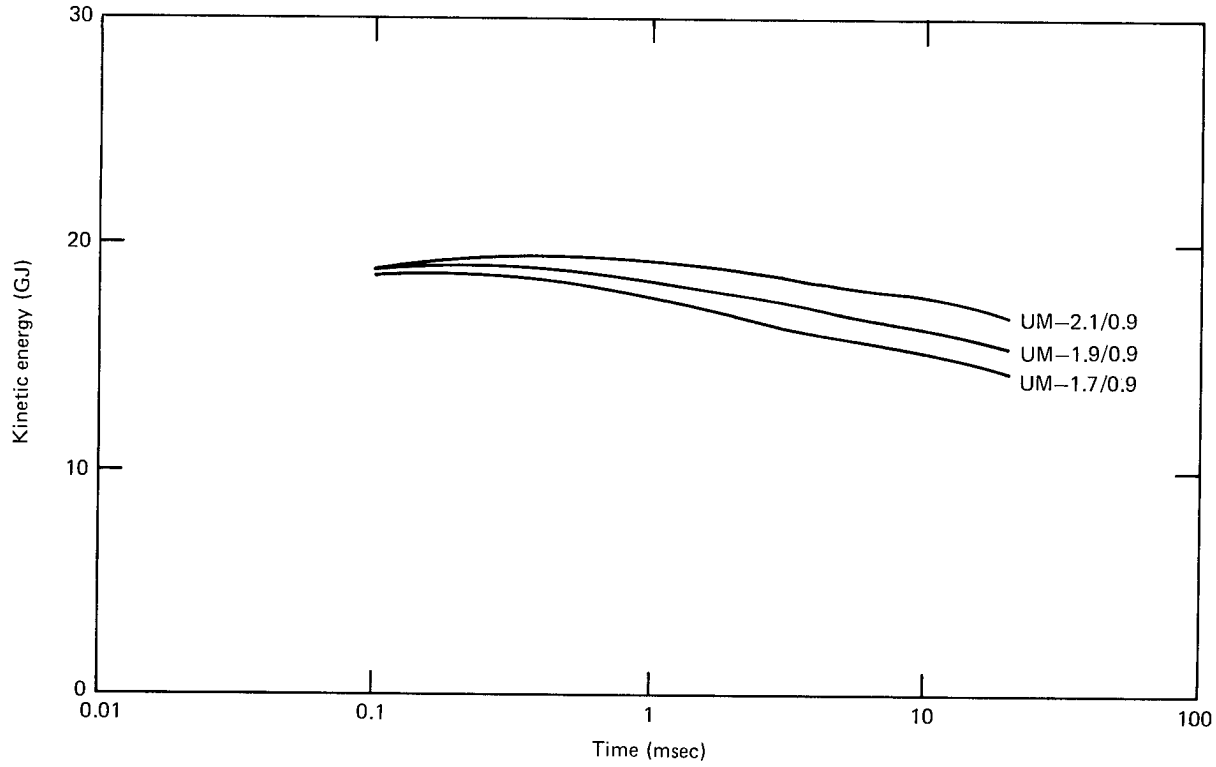

Fig. 45. Effect of density on kinetic energy coupling (uncemented soils, S_w = 0.9).

S_w = 0.9. Generally, increasing ρ_0 increases the kinetic energy coupled to the soil. Figures 46 and 47 show the effect of ρ_0 on peak stress and peak particle velocity versus range, respectively (also for S_w = 0.9). When ρ_0 is increased, the peak stress also increases, but the peak particle velocity decreases slightly.

Figures 48, 49, and 50 show the same comparison for S_w = 0.95 and Figs. 51, 52, and 53 for S_w = 1.0. The general effect is the same at all three saturations: increasing ρ_0 increases the coupled kinetic energy and peak stress, and decreases slightly the peak particle velocity.

In order to examine the total effect of density, Fig. 54a shows the coupled kinetic

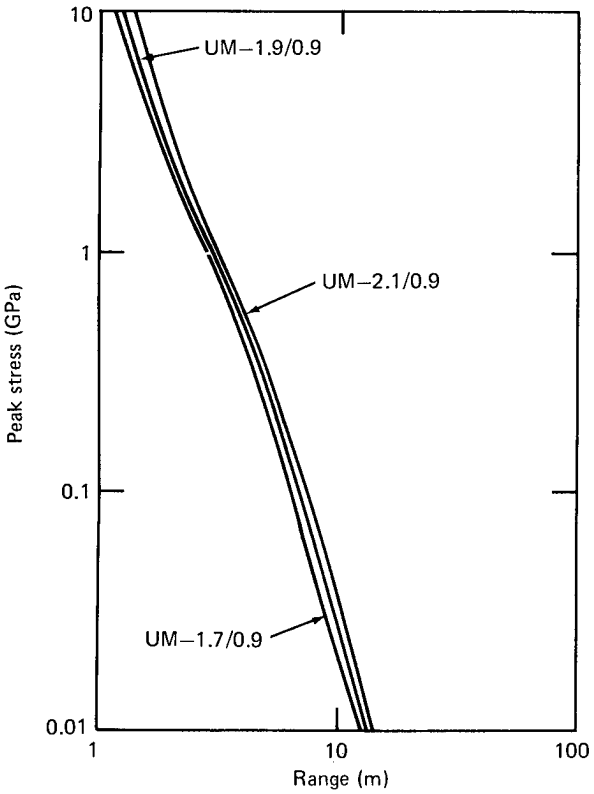

Fig. 46. Effect of density on peak stress vs range (uncemented soils, S_w = 0.9).

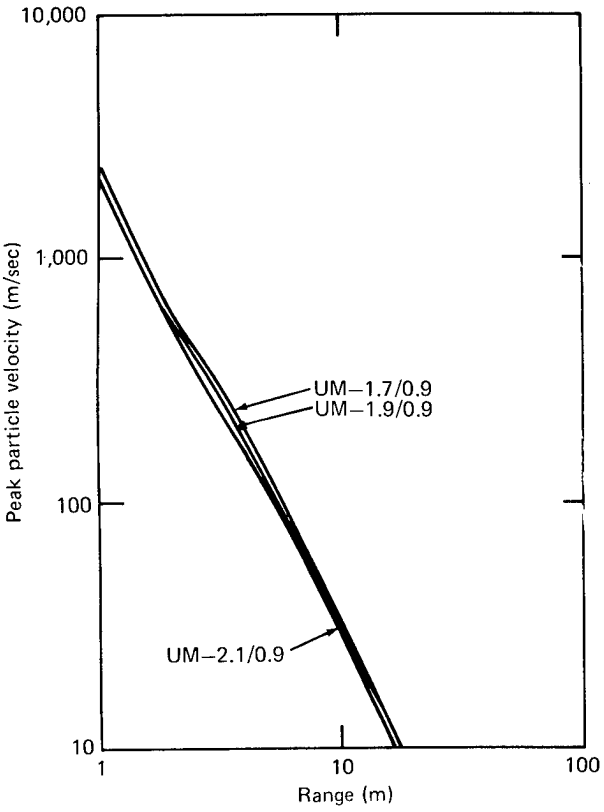

Fig. 47. Effect of density on peak particle velocity vs range (uncemented soils, S_w = 0.9).

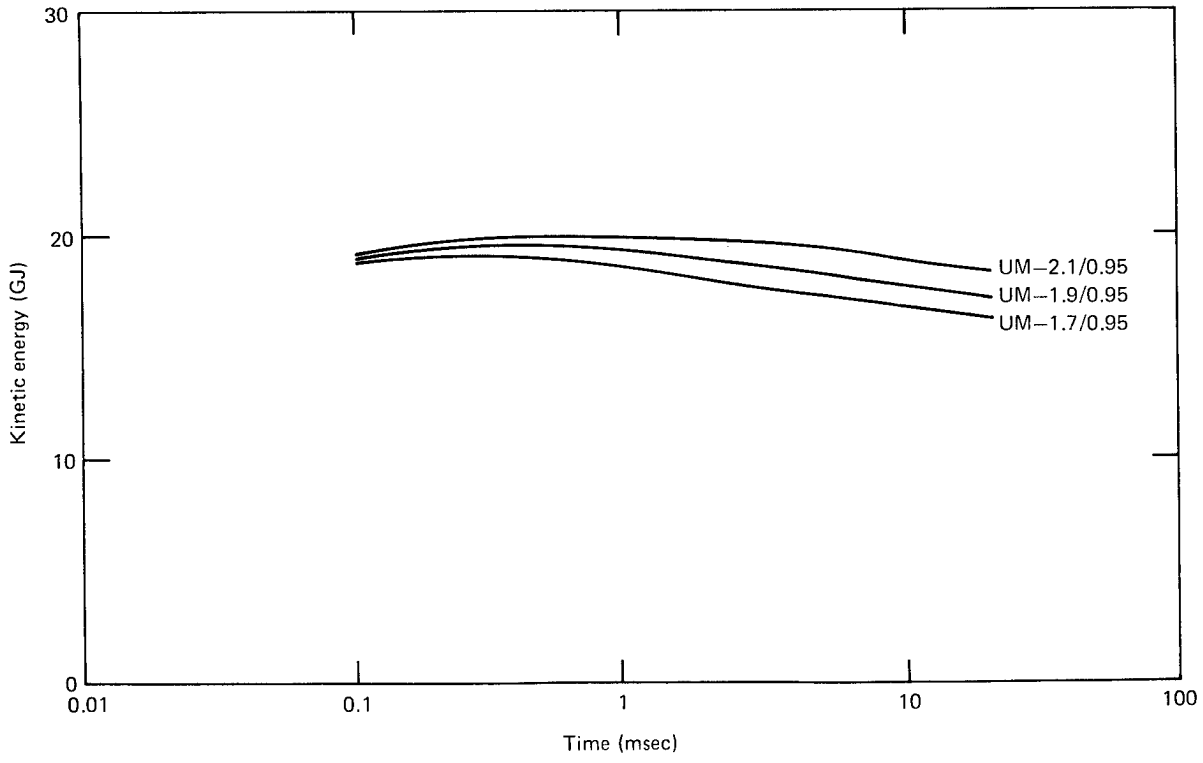

Fig. 48. Effect of density in kinetic energy coupling (uncemented soils, S_w = 0.95).

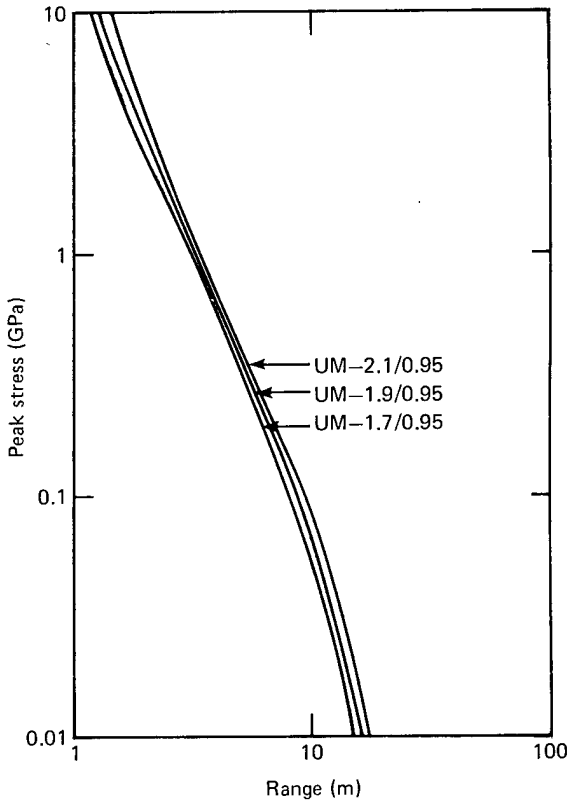

Fig. 49. Effect of density on peak stress vs range (uncemented soils, S_w = 0.95).

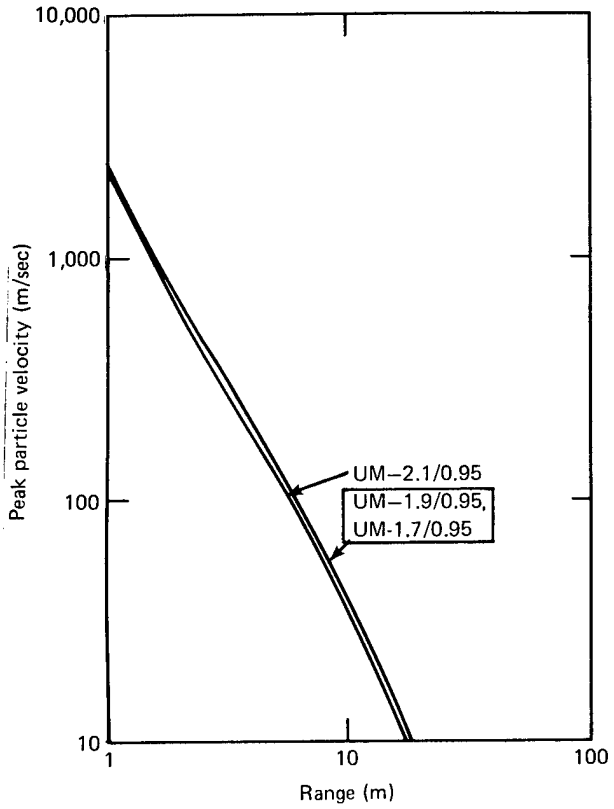

Fig. 50. Effect of density on peak particle velocity vs range (uncemented soils, S_w = 0.95).

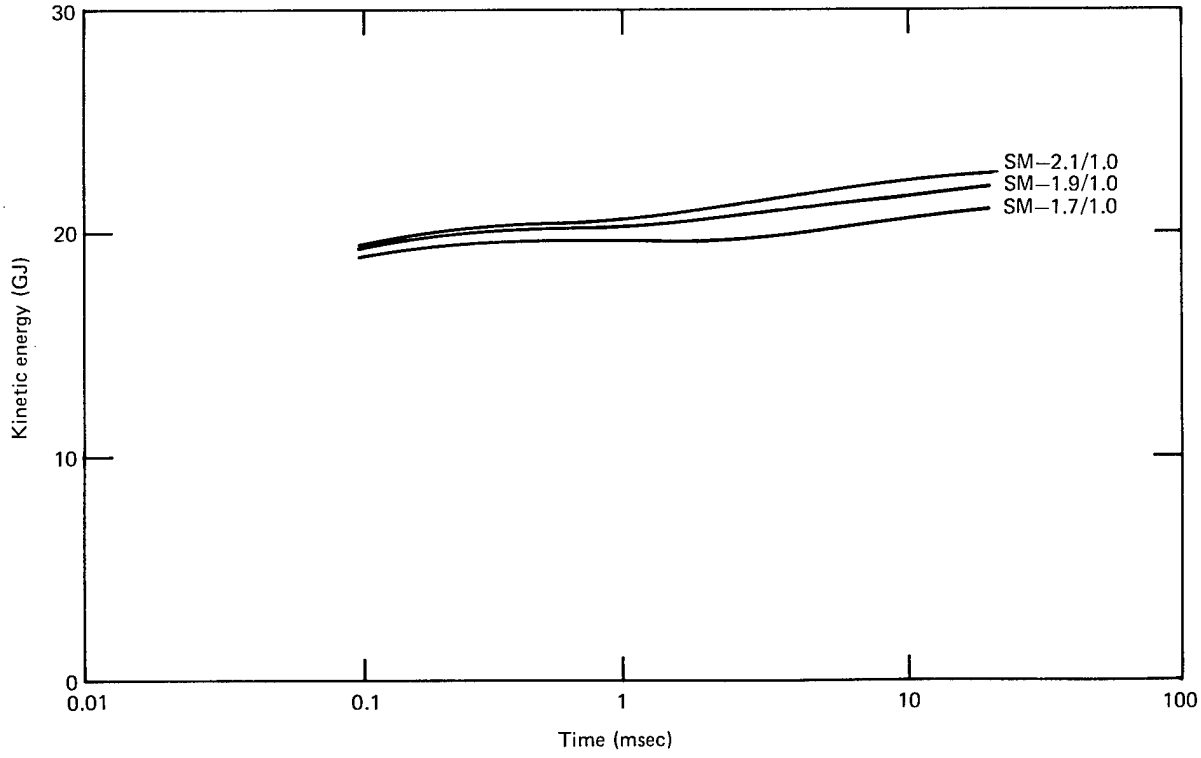

Fig. 51. Effect of density on kinetic energy coupling (uncemented soils, S_w = 1.0).

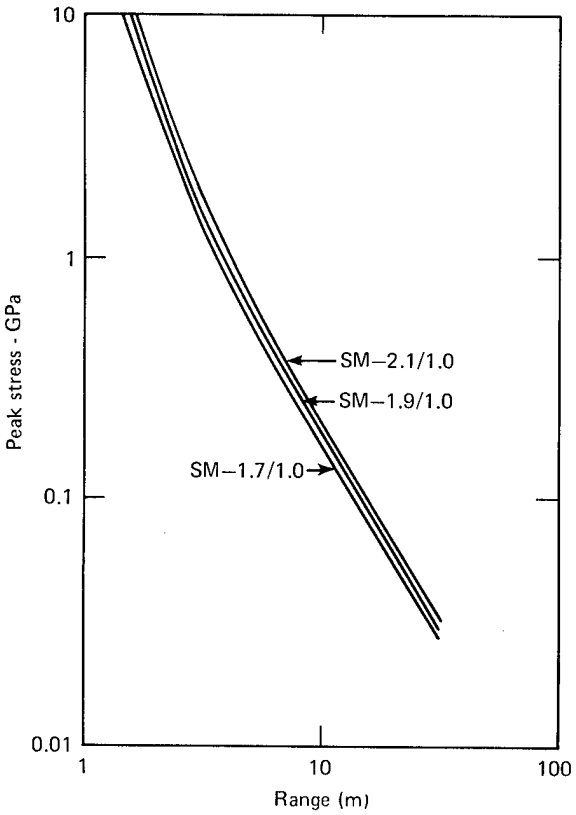

Fig. 52. Effect of density on peak stress vs range (uncemented soils, S_w = 1.0).

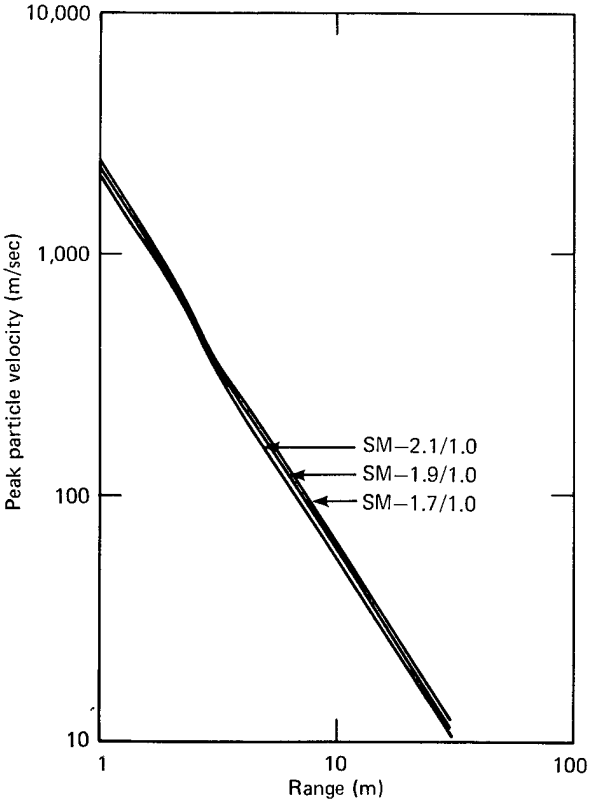

Fig. 53. Effect of density on peak particle velocity vs range (uncemented soils, S_w = 1.0).

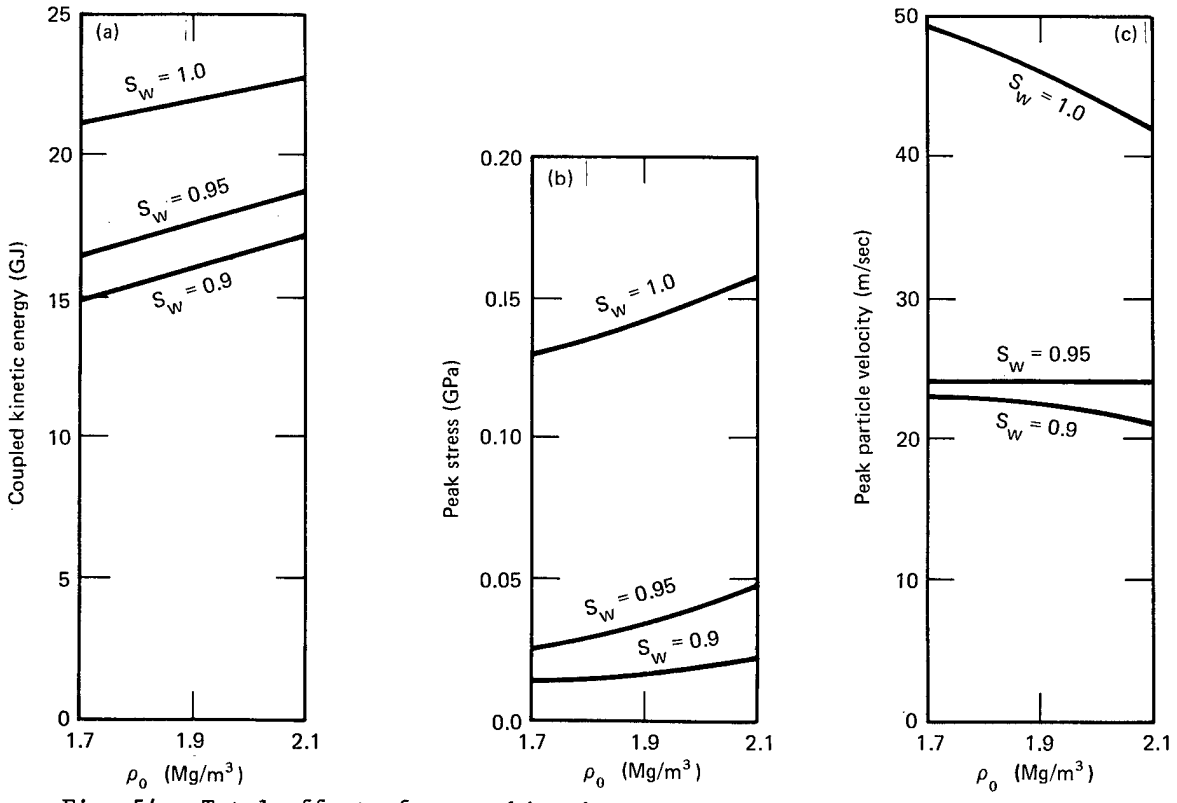

Fig. 54. Total effect of ρ_0 on kinetic energy coupling and ground motion.

energy at 15 msec versus ρ_0, and Figs. 54b and c show the peak stress and peak particle velocity, respectively, at a range of 12 m. At all three values of S_w, the kinetic energy increases linearly with ρ_0. The coupled kinetic energy at any time is the integral over all space of the density ρ times the square of the particle velocity. By increasing ρ_0, the quantity directly affected is ρ; hence one might expect a linear increase in the coupled kinetic energy with increasing ρ_0. Figure 54b shows that the peak stress is also almost linearly proportional to ρ_0, especially for $S_w = 1.0$. The peak-particle-velocity plot (Fig. 54c) shows that the effect of ρ_0 is strong only for $S_w \simeq 1.0$.

In conclusion, knowledge of the initial bulk density ρ_0 is shown calculationally to be important; it is a convenient variable because all three calculational quantities examined are roughly linearly proportional to it.

Effect of Saturation

The effects of three of the four independent variables have been discussed so far in this section. They have been discussed in their order of increasing importance to ground motion and cratering: K, failure, and density. This section reviews the effect of saturation at three different initial bulk densities: ρ_0 = 1.7, 1.9, and 2.1 Mg/m^3. As in the preceding section, the comparison is made for the UM and SM failure models and for K = 5.0 GPa.

Figure 55 shows the effect of varying S_w from 0.8 to 1.0 on kinetic energy coupling for ρ_0 = 1.7 Mg/m^3. The overall effect is substantial, especially at late time (15 to 20 msec), with the kinetic

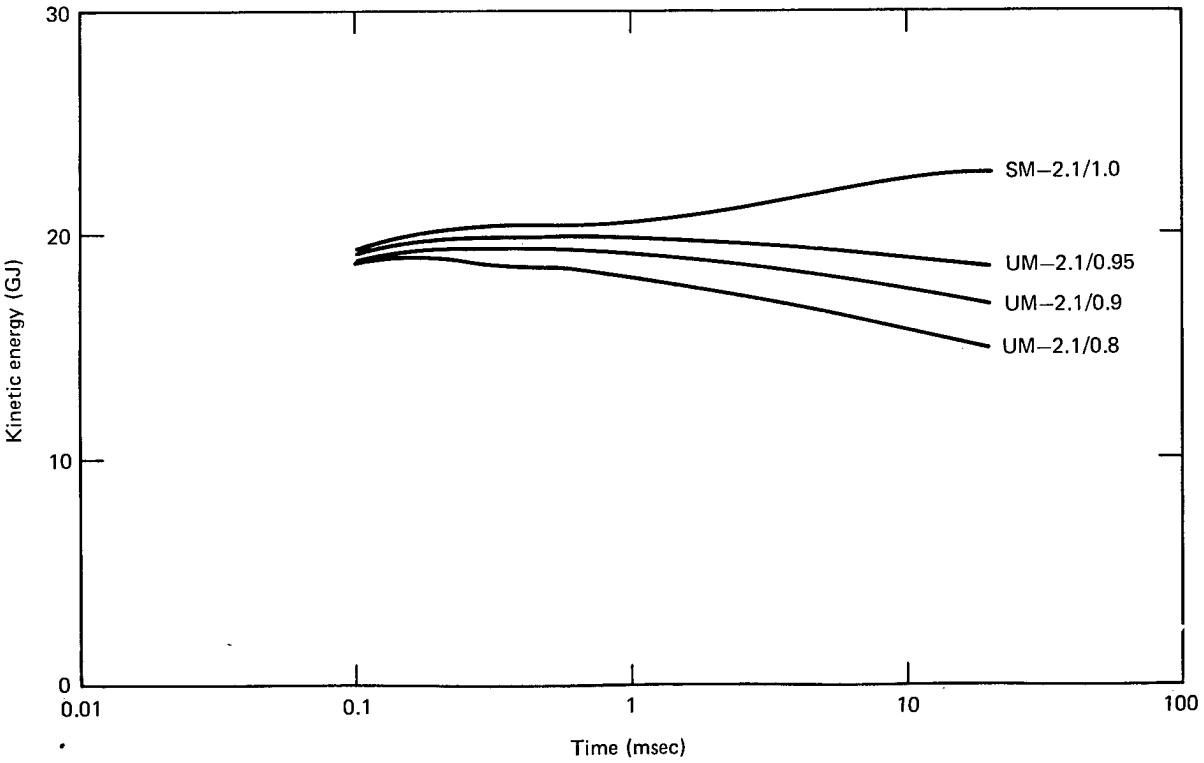

Fig. 55. Effect of saturation on kinetic energy coupling (uncemented soils, ρ_0 = 1.7 Mg/m^3).

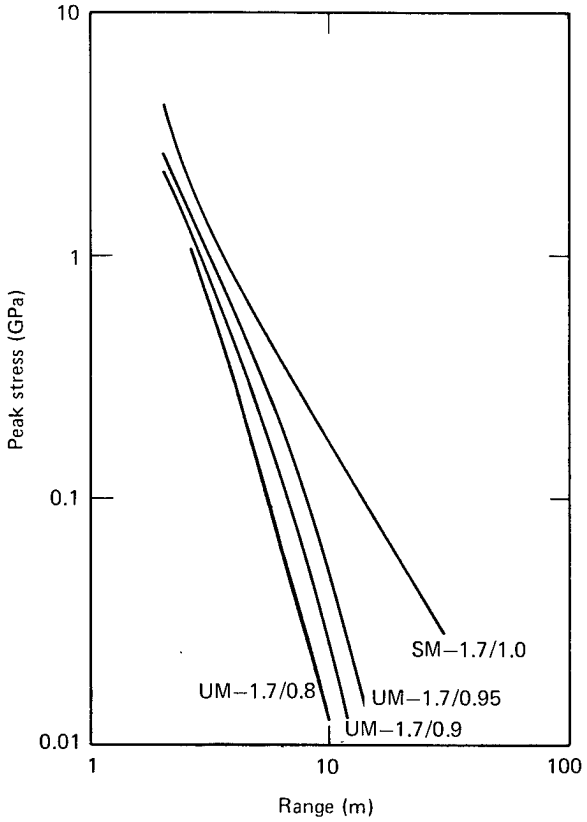

Fig. 56. Effect of saturation on peak stress vs range (uncemented soils ρ_0 = 1.7 Mg/m^3).

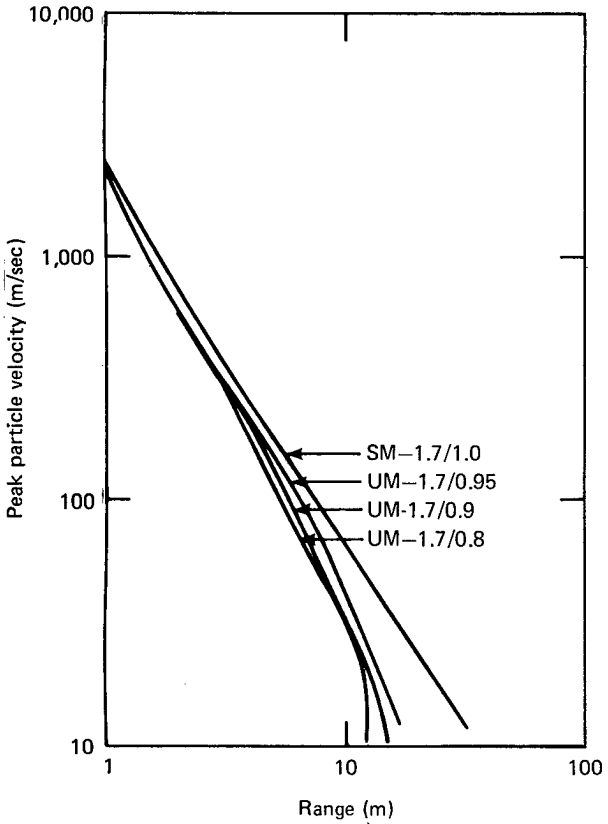

Fig. 57. Effect of saturation on peak particle velocity vs range (uncemented soils, ρ_0 = 1.7 Mg/m^3).

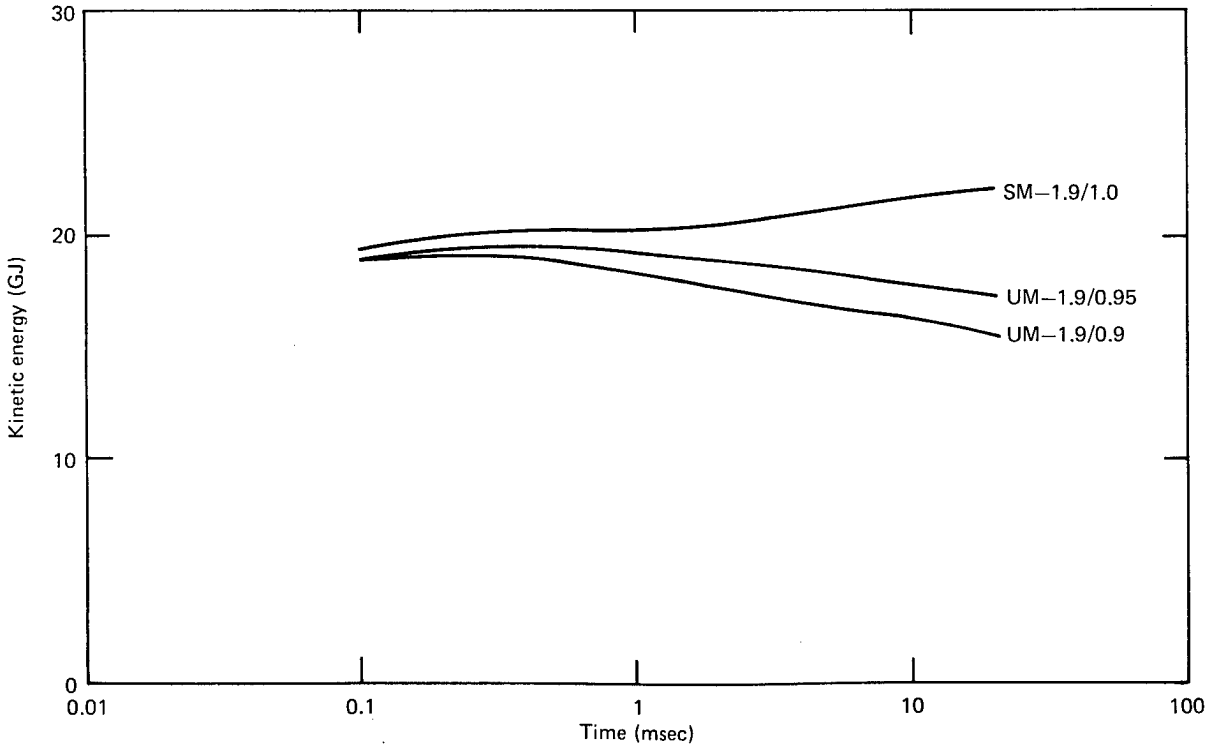

Fig. 58. Effect of saturation on kinetic energy coupling (uncemented soils, ρ_0 = 1.9 Mg/m^3).

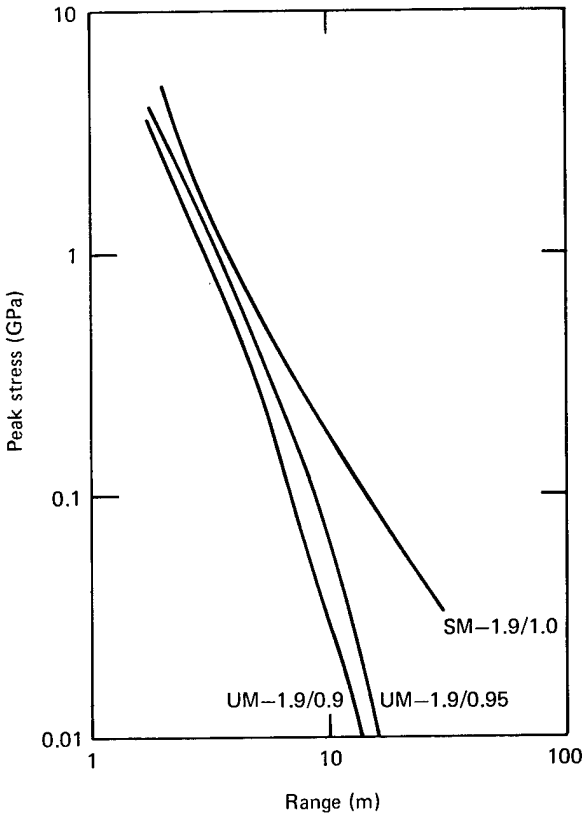

Fig. 59. Effect of saturation on peak stress vs range (uncemented soils, ρ_0 = 1.9 Mg/m^3).

energy coupled increasing almost twofold as S_w goes from 0.8 to 1.0. Furthermore, the effect of S_w increases as S_w approaches 1.0: the effect as S_w goes from 0.95 to 1.0 is roughly the same as the effect as S_w goes from 0.8 to 0.95. Thus increasing S_w increases the coupled kinetic energy substantially, and it becomes particularly important to know the value of S_w if it is in the range from 0.95 to 1.0.

Figures 56 and 57 show the effect of S_w on peak stress versus range and peak particle velocity versus range, respectively, also for ρ_0 = 1.7 Mg/m^3. The peak stress, like the kinetic energy, is affected very strongly by S_w, especially as S_w goes from 0.95 to 1.0. For example, at a range of 10 m, the peak stress goes from 0.012 GPa at S_w = 0.8 to 0.05 GPa at S_w = 0.95, a fourfold increase. At S_w = 1.0, the peak stress is 0.17 GPa, an increase of more than threefold over its value at S_w = 0.95. Beyond the 12- to 15-m range for the unsaturated soils, the peak stress attenuates very rapidly. This is because the Fort Polk soils are so compressible at low stresses. The peak-particle-velocity plot, Fig. 57, does not show as great a variation as is seen for the peak stress out to a range of about 11 m. Beyond that range, the unsaturated soils ($0.8 \leq S_w \leq 0.95$) attenuate the peak particle velocity very rapidly.

Figures 58, 59, and 60 show the kinetic energy coupling versus time and peak stress

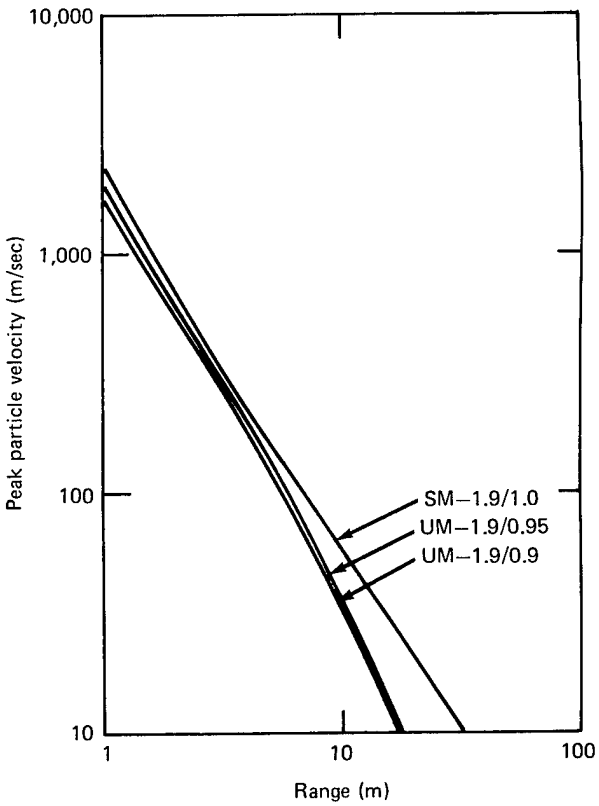

Fig. 60. Effect of saturation on peak particle velocity vs range (uncemented soils, ρ_0 = 1.9 Mg/m^3).

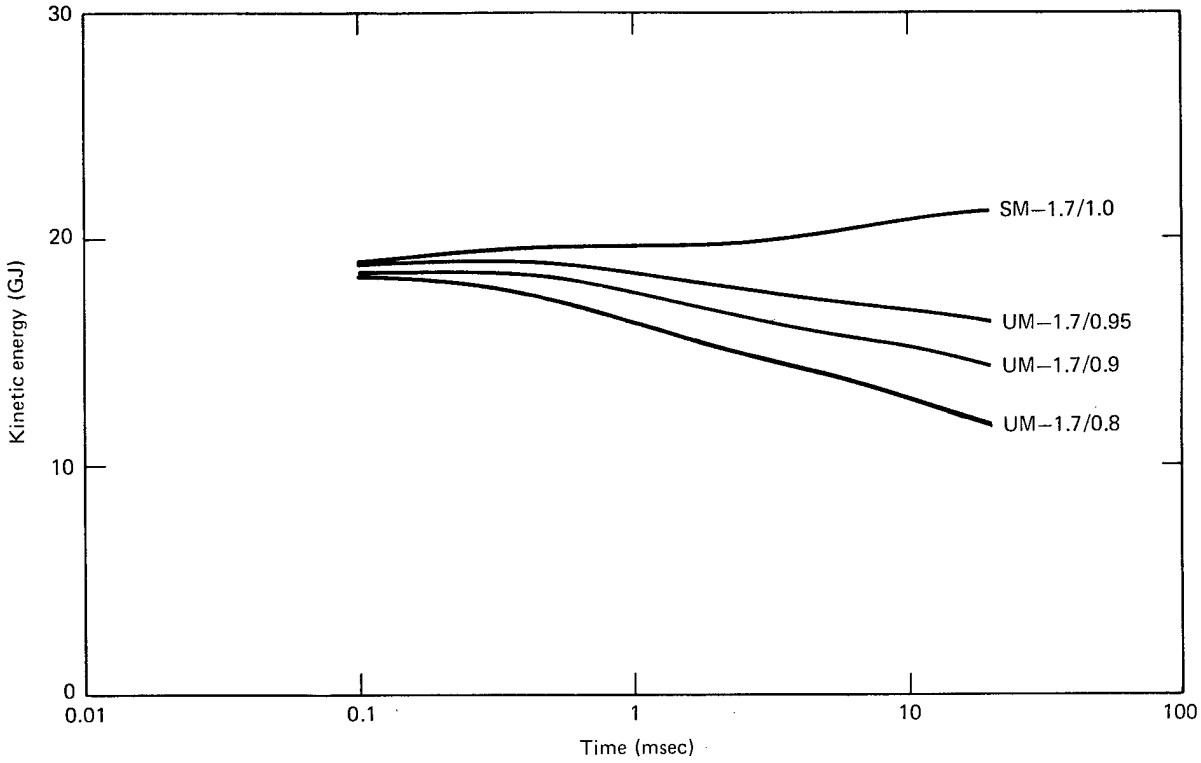

Fig. 61. Effect of saturation on kinetic energy coupling (uncemented soils, ρ_0 = 2.1 Mg/m^3).

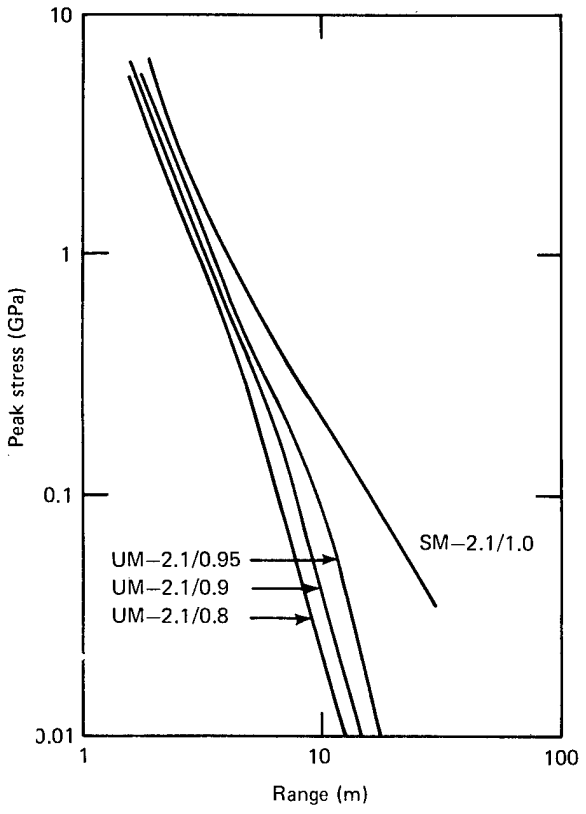

Fig. 62. Effect of saturation on peak stress vs range (uncemented soils, ρ_0 = 2.1 Mg/m^3).

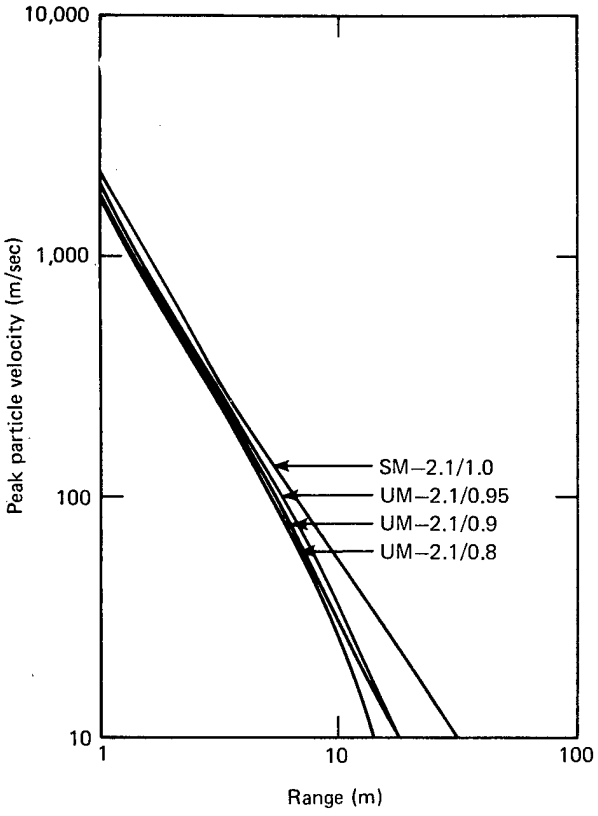

Fig. 63. Effect of saturation on peak particle velocity vs range (uncemented soils, ρ_0 = 2.1 Mg/m^3).

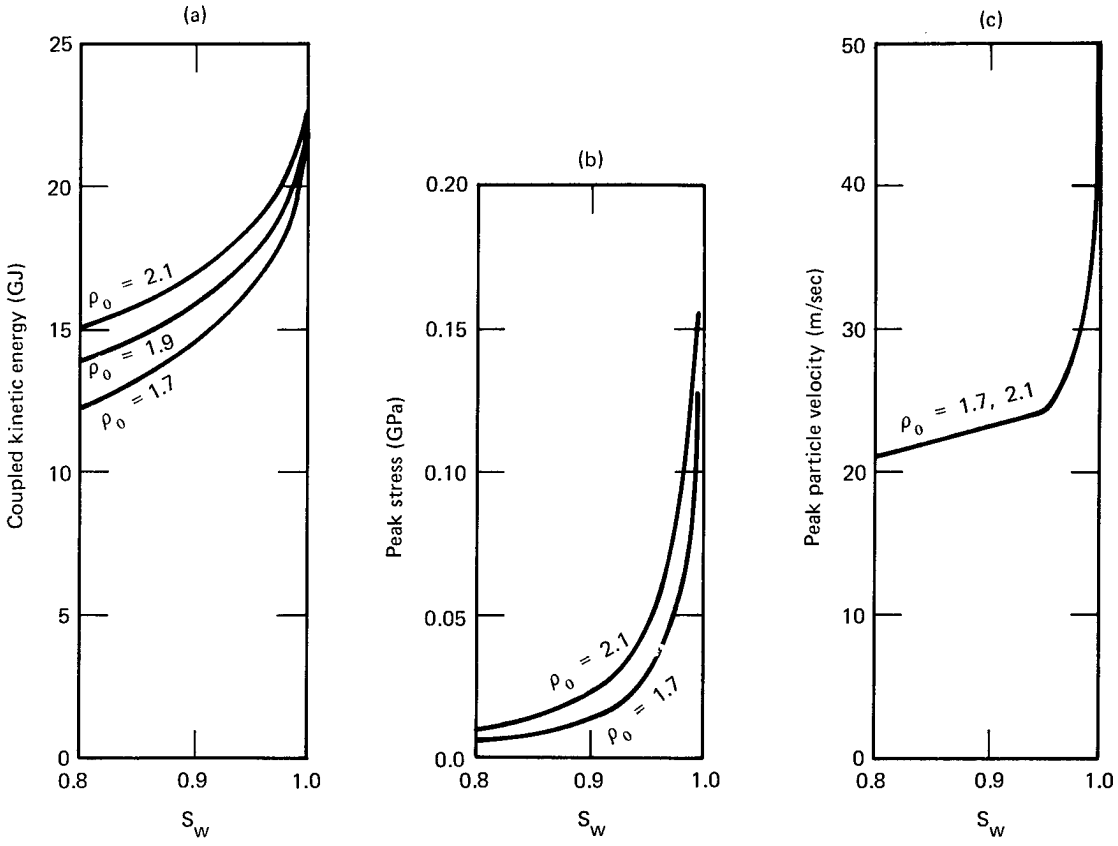

Fig. 64. Total effect of S_w on kinetic energy coupling and ground motion.

and particle velocity versus range, respectively, for ρ_0 = 1.9 Mg/m^3; likewise Figs. 61, 62, and 63 show the same calculational results for ρ_0 = 2.1 Mg/m^3. The general trends found for the low-density soils are followed also for those at higher densities.

Figure 64 reviews the total effect of S_w on kinetic energy coupling and ground motion for all three densities considered. Thus the relative effect of both ρ_0 and S_w can be seen in Fig. 64a for coupled kinetic energy. As S_w approaches 1.0, ρ_0 becomes relatively unimportant. Over the relevant Fort Polk range ($0.9 \leq S_w \leq 1.0$), S_w seems to be the most critical factor in the determination of the coupled kinetic energy. For $S_w < 0.9$, ρ_0 and S_w are equally important. Figure 64b shows the peak stress at the 12-m range versus S_w. Again, in the relevant Fort Polk range for S_w, the quantity S_w is clearly the critical factor in determining the peak stress. On the scale of the effect of S_w on peak particle velocity (Fig. 64c) the determining factor is only S_w, and it is critical to know its value if it lies between 0.95 and 1.0.

To summarize, then, S_w has been found to be the most important of the independent bulk parameters considered in the study. Increasing S_w increases both the strength of the ground motion and the kinetic energy coupling, especially as S_w approaches 1.0.

Summary and Conclusions

A calculational parameter study was performed to investigate the sensitivity of ground motion and energy coupling induced by a buried nuclear explosive to changes in the bulk properties of the emplacement medium. Of specific interest in the study were soils typical of the sites of the ESSEX I high-explosive-cratering experiments located at Fort Polk, Louisiana. The calculations were one-dimensional and utilized a hypothetical 84-GJ (20-ton) nuclear source. Constitutive relations based on the bulk properties that were varied in the study were generated using a constitutive model developed during the course of the study. Output from this model is used directly as input to SOC74, the computer code used in the study.

The bulk properties varied included the initial bulk density ρ_0, the initial bulk modulus K, and the initial water saturation S_w. An additional property, failure, took into account the shear strength of the soil. These properties, along with the grain density ρ_g and Poisson's ratio (held constant throughout the study), made up an independent set from which all other bulk properties could be calculated.

Results from 25 SOC74 calculations were plotted, and the relative effect of the four independent variables was examined. It was found that, in the order of increasing importance, K, failure, ρ_0, and S_w affected both the ground motion and the coupling of kinetic energy to the soil. Furthermore, it was found that, for values of S_w between 0.95 and 1.0, the calculational results varied considerably, with a slight increase in S_w leading to much stronger ground motions and much more efficient energy coupling.

In a study of the cratering efficiency of explosions in various rock types by Terhune et al.[16] it was concluded that the material properties in order of decreasing importance were water content, shear strength, porosity, and compressibility. Although the selection of independent parameters in our soil study varied somewhat from those chosen by Terhune et al., the results from our study provide similar conclusions for the prescribed range of Fort Polk soil parameters. Water saturation is the most sensitive parameter. Maximum shear strength, which ranged from about 0.2 to 10 MPa for the soils, is of less significance for soils than it is for rocks. For soils, bulk density (porosity for a given grain density) is a more important parameter to cratering than is shear strength. Finally, the initial or low-pressure bulk modulus is the least sensitive parameter studied.

Acknowledgements

The authors wish to acknowledge the advice and suggestions provided by B. K. Germain and J. S. Kahn of LLL during this investigation. Major C. H. Carmean, Maj.

L. C. Webster, Maj. A. E. Miller, and Dr. T. E. Ricketts of the Explosive Excavation Division of the U.S. Army Engineer Waterways Experiment Station provided technical guidance and direction. Mr. J. Q. Ehrgott and Dr. J. S. Zelasko of the Soils and Pavements Laboratory of the U.S. Army Engineer Waterways Experiment Station made valuable technical and editorial suggestions. In addition, the Explosive Excavation Division and the Soils and Pavements Laboratory fielded the high-explosive cratering tests and gathered much of the experimental data in Project ESSEX which served as a basis for this study.

A special thank-you goes to Linda Tripp, who prepared the initial manuscript as well as several revisions through the final draft, to Lydia Burrow, who helped prepare the final draft, and to Wallace Clements of the LLL Technical Information Department, who coordinated the production of the report.

References

1. M. F. Goodrich and J. M. Thomsen, Progress Report on the FY75 Geologic Parameter Study, Lawrence Livermore Laboratory, Rept. UCON 75-23 (March 1975).*

2. M. F. Goodrich, J. M. Thomsen, J. B. Bryan, and C. M. Snell, Second Progress Report on the FY75 Geologic Parameter Study, Lawrence Livermore Laboratory, Rept. UCON 75-40 (June 1975).*

3. A. Miller, Parameter Study--Long Range Program, U.S. Army Engineer Waterways Experiment Station, Explosive Excavation Research Laboratory, Livermore, Calif., Rept. WESEP-75-24 April 10, 1975).

4. W. T. Harvey, ESSEX-DIAMOND ORE Research Program, Preliminary Report--ESSEX-I, Phase 1, U.S. Army Engineer Waterways Experiment Station, Explosive Excavation Research Laboratory, Livermore, Calif., Rept. WES PR-E-74-1, Defense Nuclear Agency Rept. DNA PR 0002 (1974).

5. A. E. Miller, ESSEX-DIAMOND ORE Research Program, Preliminary Combined Results Report, ESSEX-I, Phase 2, Nuclear Cratering Device Simulation (Project ESSEX), U.S. Army Engineer Waterways Experiment Station, Explosive Excavation Research Laboratory, Livermore, Calif., Rept. EERL PR-E-75-1, Defense Nuclear Agency Rept. DNA PR 0016 (March 21, 1975).

6. J. Q. Ehrgott and R. L. Stanley, ESSEX-DIAMOND ORE Research Program, Material Property Investigation for the ESSEX-I Test Site at Fort Polk, Louisiana, U.S. Army Engineer Waterways Experiment Station, Vicksburg, Miss., Rept. WES-TR-S-75-3, Defense Nuclear Agency Rept. DNA PR 0014 (March 1975).

7. J. F. Schatz, The Physics of SOC and TENSOR, Lawrence Livermore Laboratory, Rept. UCRL-51532 (1973).

8. J. F. Schatz, SOC73, A One-Dimensional Wave Propagation Code for Rock Media, Lawrence Livermore Laboratory, Rept. UCRL-51689 (1974).

9. D. E. Burton and J. F. Schatz, Rock Modeling in TENSOR74, A Two-Dimensional Lagrangian Shock Propagation Code, Lawrence Livermore Laboratory, Rept. UCID-16719 (March 19, 1975).

10. C. M. Snell and G. D. Mendez, User Information for Revised SOC74 Codes, Lawrence Livermore Laboratory, Rept. UCID-16811 (March 10, 1975).

11. T. R. Butkovich, Effects of Water Saturation on Underground Nuclear Detonations, Lawrence Livermore Laboratory, Rept. UCRL-51110 (September 9, 1971).

12. B. K. Crowley, Effects of Porosity and Saturation on Shock-Wave Response in Tuffs, Lawrence Livermore Laboratory, Rept. UCRL-74207 (September 14, 1972).

13. T. R. Butkovich, A Technique for Generating Pressure-Volume Relationships for Rocks, Lawrence Livermore Laboratory, Rept. UCRL-51441 (1973).

14. J. Q. Ehrgott, Revised Profile for 12MU Location--ESSEX I, Phase 2, letter of transmittal to A. E. Miller, from J. Q. Ehrgott, of the U.S. Army Engineer Waterways Experiment Station, Soils and Pavements Laboratory (March 31, 1975).

*Internal document. Readers outside the Laboratory who desire further information on LLL internal documents should address their inquiries to the Technical Information Department, Lawrence Livermore Laboratory, Livermore, CA 94550.

15. C. E. Chapin and T. R. Butkovich, private communication, "Radiation Correction of Equation of State Tables Used in the SOC and TENSOR Computer Codes," UOPKA 69-34, memorandum, Lawrence Livermore Laboratory (June 1969).*

16. R. W. Terhune, T. F. Stubbs, and J. T. Cherry, "Nuclear Cratering from a Digital Computer," Peaceful Nuclear Explosions, 1970, 415-440.

Appendix

Compressibility of Hypothetical Materials

Compressibility was calculated for each hypothetical material using the model described under "Constitutive Model for Soils." The inputs for this model were the independent bulk properties plus the merge and transition pressures associated with the particular failure model used. Values for the independent bulk parameters and the failure model used can be obtained directly from the name listed at the top of each table, as discussed under "Bulk Property and Constitutive-Relation Input for Individual Calculations," while values of P_T and P_M are taken from Table 7. All compressibilities for hypothetical materials were derived assuming a mixture of 25 wt% clay and 75 wt% sand. The following tables list the P-μ data exactly as input to the SOC74 code, for all 25 hypothetical soils or weak rocks used in the study. Since the SOC74 program uses pressures (P) in megabar units and volumes (V) in cubic centimeter units, the actual tables are in those units. The quantities "EF" and "EV" are the calculated specific energies required to melt and vaporize the hypothetical soil, respectively.

Table A1. Coordinated failure model, UM - 1.7/0.80 (Fig. 8).

Input variables

ρ_0 = 1.7 Mg/m^3 S_w = 0.80 K = 5.0 GPa

P_T = 100 kPa P_M = 10.4 MPa

Output

Z = 0.2441 ϕ_0 = 0.5187 ϕ_a = 0.1037

e_w = 0.8622 EF = 5.471 kJ EV = 30.57 kJ

LOADING PATH

P	V	DP/DV	MU	DP/DMU
0.	0.588235	0.	0.	0.
0.000001	0.588224	-0.085002	0.000020	0.050000
0.000010	0.556184	-0.000281	0.057627	0.000156
0.000020	0.547119	-0.001103	0.075150	0.000571
0.000030	0.541900	-0.001916	0.085505	0.000966
0.000050	0.535373	-0.003064	0.098739	0.001511
0.000070	0.531076	-0.004654	0.107629	0.002250
0.000100	0.526491	-0.006543	0.117275	0.003110
0.000104	0.525983	-0.007879	0.118354	0.003709
0.000200	0.524887	-0.087576	0.120689	0.041103
0.000400	0.522706	-0.091679	0.125366	0.042761
0.000600	0.520649	-0.097266	0.129811	0.045000
0.001000	0.516861	-0.105597	0.138091	0.048308
0.002000	0.508853	-0.124872	0.156002	0.055832
0.004000	0.496828	-0.166312	0.183983	0.071478
0.006000	0.487883	-0.223601	0.205689	0.092139
0.009000	0.477658	-0.293382	0.231500	0.116229
0.009600	0.475921	-0.345538	0.235993	0.133536
0.010000	0.474808	-0.359367	0.238891	0.138051
0.015000	0.463149	-0.428046	0.270078	0.160321
0.020000	0.454212	-0.559479	0.295068	0.200084
0.024000	0.448244	-0.670264	0.312310	0.231989
0.030000	0.440582	-0.783088	0.335132	0.262906
0.040000	0.430029	-0.947550	0.367898	0.305194
0.060000	0.413532	-1.212379	0.422466	0.366517
0.100000	0.389116	-1.638264	0.511722	0.448148
0.150000	0.361429	-1.805893	0.627527	0.431761
0.200000	0.340137	-2.348303	0.729407	0.490772
0.300000	0.305304	-2.870815	0.926722	0.506804
0.400000	0.286622	-5.352870	1.052303	0.796301
0.500000	0.273572	-7.663022	1.150200	1.021483
0.600000	0.262846	-9.322365	1.237951	1.139588
0.800000	0.245790	-11.726750	1.393239	1.287930
1.000000	0.232432	-14.971973	1.530782	1.454083
1.500000	0.207777	-20.279757	1.831089	1.664967
2.000000	0.189889	-27.952328	2.097777	1.874845

UNLOADING PATH

0.	0.527210	0.115752	0.
0.000001	0.527198	0.115777	0.039392
0.000010	0.527090	0.116005	0.039448
0.000020	0.526971	0.116258	0.039556
0.000030	0.526852	0.116510	0.039669
0.000050	0.526615	0.117012	0.039839
0.000070	0.526380	0.117511	0.040066
0.000100	0.526030	0.118255	0.040348
0.000104	0.525983	0.118354	0.040541

Table A2. Coordinated failure model, UM - 1.7/0.90 (Fig. 8).

Input variables

ρ_0 = 1.70 Mg/m^3	S_w = 0.90	K = 5.0 GPa
P_T = 100 kPa	P_M = 10.4 MPa	

Output

Z = 0.2901	ϕ_0 = 0.5480	ϕ_a = 0.0548
e_w = 1.091	EF = 05.938 kJ/cm^3	EV = 31.773 kJ

LOADING PATH

P	V	DP/DV	MU	DP/DMU
0.	0.588235	0.	0.	0.
0.000001	0.588224	-0.085002	0.000020	0.050000
0.000010	0.571654	-0.000543	0.029006	0.000310
0.000020	0.566742	-0.002036	0.037924	0.001121
0.000030	0.563848	-0.003455	0.043251	0.001877
0.000050	0.560139	-0.005392	0.050160	0.002895
0.000070	0.557626	-0.007960	0.054891	0.004227
0.000100	0.554866	-0.010869	0.060139	0.005717
0.000104	0.554555	-0.012845	0.060734	0.006719
0.000200	0.553265	-0.074428	0.063207	0.038821
0.000400	0.550699	-0.077952	0.068160	0.040376
0.000600	0.548283	-0.082755	0.072869	0.042478
0.001000	0.543835	-0.089927	0.081644	0.045584
0.002000	0.534451	-0.106573	0.100634	0.052659
0.004000	0.520426	-0.142600	0.130295	0.067427
0.006000	0.510060	-0.192940	0.153266	0.087067
0.009000	0.498299	-0.255084	0.180486	0.110216
0.009600	0.496313	-0.302120	0.185209	0.127021
0.010000	0.495042	-0.314674	0.188253	0.131434
0.015000	0.481824	-0.378255	0.220852	0.153378
0.020000	0.471826	-0.500113	0.246721	0.193280
0.024000	0.465222	-0.605718	0.264418	0.226028
0.030000	0.456834	-0.715261	0.287636	0.258424
0.040000	0.445448	-0.878275	0.320548	0.303833
0.060000	0.428024	-1.147882	0.374303	0.372059
0.100000	0.402941	-1.594661	0.459856	0.467549
0.150000	0.374113	-1.734453	0.572346	0.444483
0.200000	0.352247	-2.286609	0.669953	0.512260
0.300000	0.316668	-2.810702	0.857575	0.532985
0.400000	0.296915	-5.062453	0.981156	0.809183
0.500000	0.282838	-7.103901	1.079758	1.014183
0.600000	0.271202	-8.593845	1.168992	1.120644
0.800000	0.252577	-10.738134	1.328936	1.250444
1.000000	0.237881	-13.609175	1.472814	1.390061
1.500000	0.210511	-18.268455	1.794316	1.555199
2.000000	0.190463	-24.940076	2.088445	1.699939

UNLOADING PATH

0.	0.565999	0.057980	0.
0.000001	0.565985	0.058007	0.037216
0.000010	0.565868	0.058248	0.037269
0.000020	0.565717	0.058516	0.037370
0.000030	0.565577	0.058782	0.037476
0.000050	0.565298	0.059314	0.037636
0.000070	0.565022	0.059842	0.037848
0.000100	0.564610	0.060629	0.038113
0.000104	0.564555	0.060734	0.038293

Table A3. Coordinated failure model, UM - 1.7/0.95 (Fig. 8).

Input variables

ρ_0 = 1.7 Mg/m^3	S_w = 0.95	K = 5.0 GPa
P_T = 100 kPa	P_M = 10.4 MPa	

Output

Z = 0.3152	ϕ_0 = 0.5640	ϕ_a = 0.0282
e_w = 1.2287	EF = 6.243 kJ	EV = 32.490 kJ

LOADING PATH

P	V	DP/DV	MU	DP/DMU
0.	0.588235	0.	0.	0.
0.000001	0.588224	-0.085002	0.000020	0.050000
0.000010	0.579739	-0.001061	0.014656	0.000615
0.000020	0.577121	-0.003820	0.019259	0.002173
0.000030	0.575536	-0.006312	0.022064	0.003564
0.000050	0.573441	-0.009543	0.025800	0.005354
0.000070	0.571966	-0.013564	0.028444	0.007563
0.000100	0.570282	-0.017809	0.031482	0.009875
0.000104	0.570087	-0.020526	0.031835	0.011345
0.000200	0.568692	-0.068812	0.034366	0.037925
0.000400	0.565917	-0.072084	0.039437	0.039438
0.000600	0.563304	-0.076546	0.044258	0.041483
0.001000	0.558497	-0.083214	0.053246	0.044505
0.002000	0.548367	-0.098710	0.072704	0.051393
0.004000	0.533255	-0.132343	0.103104	0.065789
0.006000	0.522116	-0.179556	0.126637	0.084987
0.009000	0.509520	-0.238181	0.154488	0.107717
0.009600	0.507399	-0.282803	0.159315	0.124292
0.010000	0.506042	-0.294747	0.162424	0.128657
0.015000	0.491975	-0.355459	0.195660	0.150442
0.020000	0.481401	-0.472838	0.221924	0.190376
0.024000	0.474452	-0.575587	0.239822	0.223490
0.030000	0.465668	-0.683098	0.263207	0.256567
0.040000	0.453830	-0.844704	0.296159	0.303475
0.060000	0.435902	-1.115620	0.349466	0.375187
0.100000	0.410456	-1.571918	0.433127	0.478117
0.150000	0.381008	-1.697939	0.543891	0.451411
0.200000	0.358830	-2.254413	0.639317	0.523968
0.300000	0.322846	-2.779069	0.822029	0.547309
0.400000	0.302510	-4.917424	0.944512	0.816437
0.500000	0.287875	-6.832886	1.043368	1.011575
0.600000	0.275745	-8.243643	1.133260	1.112448
0.800000	0.256266	-10.267588	1.295409	1.233433
1.000000	0.240843	-12.967533	1.442403	1.360602
1.500000	0.211998	-17.333922	1.774725	1.504564
2.000000	0.190775	-23.559914	2.083395	1.619853

UNLOADING PATH

0.	0.571648	0.029016	0.
0.000001	0.571633	0.029043	0.036365
0.000010	0.571496	0.029290	0.036416
0.000020	0.571344	0.029564	0.036514
0.000030	0.571192	0.029837	0.036618
0.000050	0.570891	0.030381	0.036773
0.000070	0.570591	0.030922	0.036979
0.000100	0.570146	0.031728	0.037237
0.000104	0.570087	0.031835	0.037413

Table A4. Coordinated failure model, SM - 1.7/1.0 (Fig. 7).

Input variables

ρ_0 = 1.7 Mg/m^3 S_w = 1.0 K = 5.0 GPa

P_T = 10 kPa $P_{M/}$ = 311 kPa

Output

Z = 0.3417 ϕ_0 = 0.5808 ϕ_a = 0.

e_w = 1.3857 EF = 6.612 kJ EV = 33.304 kJ

LOADING PATH

P	V	DP/DV	MU	DP/DMU
0.	0.588235	0.	0.	0.
0.000000	0.588234	-0.085000	0.000002	0.050000
0.000003	0.588184	-0.060052	0.000087	0.035322
0.000010	0.588071	-0.060727	0.000280	0.035709
0.000020	0.587906	-0.060900	0.000560	0.035794
0.000030	0.587743	-0.061106	0.000838	0.035894
0.000050	0.587417	-0.061414	0.001393	0.036046
0.000070	0.587094	-0.061826	0.001945	0.036247
0.000100	0.586612	-0.062340	0.002767	0.036498
0.000200	0.585042	-0.063675	0.005459	0.037150
0.000400	0.582046	-0.066758	0.010634	0.038646
0.000600	0.579225	-0.070908	0.015555	0.040640
0.001000	0.574038	-0.077113	0.024732	0.043588
0.002000	0.563115	-0.091550	0.044609	0.050309
0.004000	0.546851	-0.122969	0.075678	0.064374
0.006000	0.534893	-0.167259	0.099724	0.083171
0.009000	0.521413	-0.222552	0.128155	0.105519
0.009600	0.518140	-0.264854	0.133078	0.121879
0.010000	0.516200	-0.276209	0.136248	0.126199
0.015000	0.503535	-0.334118	0.170070	0.147831
0.020000	0.491547	-0.447001	0.196696	0.187786
0.025000	0.480434	-0.546760	0.214776	0.221242
0.030000	0.470031	-0.652025	0.238308	0.254970
0.040000	0.452713	-0.811816	0.271274	0.303348
0.050000	0.441252	-1.083348	0.324102	0.378581
0.100000	0.418421	-1.548510	0.405846	0.489335
0.150000	0.388316	-1.660881	0.514835	0.458761
0.200000	0.365807	-2.221264	0.608050	0.536397
0.300000	0.329894	-2.746310	0.785810	0.562556
0.400000	0.308441	-4.772514	0.907125	0.824297
0.500000	0.293214	-6.567338	1.006164	1.009706
0.600000	0.280559	-7.902338	1.096651	1.105132
0.800000	0.260176	-9.811885	1.260913	1.217569
1.000000	0.243982	-12.350373	1.410976	1.332767
1.500000	0.213573	-16.442434	1.754258	1.456531
2.000000	0.191106	-22.254618	2.078061	1.544150

UNLOADING PATH

0.	0.588235	0.000000	0.
0.000000	0.588234	0.000003	0.035643
0.000003	0.588184	0.000087	0.035659

Table A5. Coordinated failure model, UM - 1.9/0.90 (Fig. 8).

Input variables

ρ_0 = 1.90 Mg/m^3 S_w = 0.90 K = 5.0 GPa

P_T = 100 kPa P_M = 10.4 MPa

Output

Z = 0.2061 ϕ_0 = 0.4350 ϕ_a = .0435

e_w = 0.6930 EF = 7.297 kJ EV = 35.380 kJ

LOADING PATH

P	V	DP/DV	MU	DP/DMU
0.	0.526316	0.	0.	0.
0.000001	0.526305	-0.095002	0.000020	0.050000
0.000010	0.514605	-0.000769	0.022756	0.000396
0.000020	0.511108	-0.002860	0.029754	0.001429
0.000030	0.509041	-0.004838	0.033935	0.002392
0.000050	0.506385	-0.007530	0.039358	0.003688
0.000070	0.504582	-0.011090	0.043073	0.005384
0.000100	0.502597	-0.015111	0.047193	0.007281
0.000104	0.502372	-0.017836	0.047661	0.008556
0.000200	0.501436	-0.102546	0.049616	0.049081
0.000400	0.499572	-0.107294	0.053533	0.051067
0.000600	0.497814	-0.113750	0.057254	0.053749
0.001000	0.494571	-0.123361	0.064185	0.057707
0.002000	0.487700	-0.145520	0.079180	0.066689
0.004000	0.477326	-0.192806	0.102633	0.085279
0.006000	0.469557	-0.257403	0.120878	0.109615
0.009000	0.460600	-0.334940	0.142675	0.137636
0.009600	0.459069	-0.392105	0.146484	0.157528
0.010000	0.458087	-0.407155	0.148943	0.162682
0.015000	0.447717	-0.482135	0.175556	0.187877
0.020000	0.439656	-0.620330	0.197107	0.232003
0.024000	0.434214	-0.734986	0.212112	0.266593
0.030000	0.427152	-0.849671	0.232150	0.299427
0.040000	0.417287	-1.013618	0.261281	0.343278
0.060000	0.401556	-1.271413	0.310690	0.404782
0.100000	0.377692	-1.676137	0.393506	0.483000
0.150000	0.350947	-1.869527	0.499701	0.470831
0.200000	0.330130	-2.401855	0.594269	0.528721
0.300000	0.295912	-2.922465	0.778621	0.542439
0.400000	0.278116	-5.619257	0.892431	0.878662
0.500000	0.265915	-8.196100	0.979261	1.151677
0.600000	0.255940	-10.024623	1.056404	1.296292
0.800000	0.240182	-12.692395	1.191317	1.482437
1.000000	0.227930	-16.322694	1.309116	1.697803
1.500000	0.205518	-22.309494	1.560929	1.985605
2.000000	0.189415	-31.051538	1.778634	2.296681

UNLOADING PATH

0.	0.503420	0.045481	0.
0.000001	0.503409	0.045503	0.047030
0.000010	0.503317	0.045694	0.047098
0.000020	0.503215	0.045905	0.047227
0.000030	0.503114	0.046117	0.047363
0.000050	0.502912	0.046537	0.047566
0.000070	0.502711	0.046955	0.047838
0.000100	0.502412	0.047578	0.048177
0.000104	0.502372	0.047661	0.048407

Table A6. Coordinated failure model, UM - 1.9/0.95 (Fig. 8).

Input variables

ρ_0 = 1.9 Mg/m^3 S_w = 0.95 K = 5.0 GPa

P_T = 100 kPa P_M = 10.4 MPa

Output

Z = 0.2238 ϕ_0 = 0.4477 ϕ_a = 0.0224

e_w = 0.7700 EF = 7.485 kJ EV = 36.063 kJ

LOADING PATH

P	V	DP/DV	MU	DP/DMU
0.	0.526316	0.	0.	0.
0.000001	0.526305	-0.095002	0.000020	0.050000
0.000010	0.520297	-0.001498	0.011569	0.000779
0.000020	0.518434	-0.005368	0.015204	0.002751
0.000030	0.517304	-0.008853	0.017420	0.004511
0.000050	0.515807	-0.013358	0.020373	0.006772
0.000070	0.514752	-0.018951	0.022466	0.009560
0.000100	0.513544	-0.024838	0.024870	0.012475
0.000104	0.513404	-0.028598	0.025149	0.014326
0.000200	0.512393	-0.094962	0.027172	0.047464
0.000400	0.510381	-0.099385	0.031222	0.049382
0.000600	0.508483	-0.105404	0.035070	0.051974
0.001000	0.504986	-0.114371	0.042239	0.055799
0.002000	0.497583	-0.135084	0.057745	0.064491
0.004000	0.486438	-0.179450	0.081980	0.082526
0.006000	0.478119	-0.240422	0.100805	0.106241
0.009000	0.468569	-0.314149	0.123240	0.133721
0.009600	0.466943	-0.368878	0.127152	0.153347
0.010000	0.465899	-0.383338	0.129677	0.158450
0.015000	0.454927	-0.455679	0.156924	0.183504
0.020000	0.446457	-0.590332	0.178872	0.227809
0.024000	0.440769	-0.703258	0.194085	0.262941
0.030000	0.433427	-0.817207	0.214312	0.296628
0.040000	0.423240	-0.981639	0.243540	0.342144
0.060000	0.407152	-1.243131	0.292677	0.407018
0.100000	0.383038	-1.658226	0.374087	0.491344
0.150000	0.355844	-1.839247	0.479061	0.476306
0.200000	0.334885	-2.376533	0.572005	0.537960
0.300000	0.300300	-2.898103	0.752633	0.553625
0.400000	0.282090	-5.491570	0.865770	0.883881
0.500000	0.269493	-7.938094	0.952986	1.146583
0.600000	0.259166	-9.683792	1.030803	1.285065
0.800000	0.242803	-12.222165	1.167669	1.461281
1.000000	0.230833	-15.662501	1.287998	1.662106
1.500000	0.206573	-21.312847	1.547841	1.924243
2.000000	0.189637	-29.522196	1.775388	2.197349

UNLOADING PATH

0.	0.514635	0.022896	0.
0.000001	0.514624	0.022918	0.045484
0.000010	0.514624	0.023116	0.045549
0.000020	0.514614	0.023335	0.045674
0.000030	0.514605	0.023553	0.045805
0.000050	0.513986	0.023988	0.046002
0.000070	0.513769	0.024420	0.046264
0.000100	0.513447	0.025064	0.046591
0.000104	0.513404	0.025149	0.046813

Table A7. Coordinated failure model, SM - 1.9/1.0 (Fig. 7).

Input variables

ρ_0 = 1.9 Mg/m^3	S_w = 1.0	K = 5.0 GPa
P_T = 10 kPa	P_M = 311 kPa	

Output

Z = 0.2427	ϕ_0 = 0.4611	ϕ_a = 0.
e_w = 0.8556	EF = 7.706 kJ	EV = 36.832 kJ

LOADING PATH

P	V	DP/DV	MU	DP/DMU
0.	0.526316	0.	0.	0.
0.000000	0.526315	-0.095000	0.000002	0.050000
0.000003	0.526279	-0.083533	0.000070	0.043962
0.000010	0.526197	-0.083999	0.000226	0.044197
0.000020	0.526078	-0.084234	0.000452	0.044304
0.000030	0.525960	-0.084514	0.000677	0.044431
0.000050	0.525724	-0.084933	0.001125	0.044621
0.000070	0.525490	-0.085492	0.001571	0.044875
0.000100	0.525142	-0.086191	0.002235	0.045191
0.000200	0.524006	-0.088002	0.004408	0.046011
0.000400	0.521836	-0.092184	0.008584	0.047894
0.000600	0.519791	-0.097799	0.012552	0.050402
0.001000	0.516024	-0.106172	0.019945	0.054108
0.002000	0.508058	-0.125541	0.035936	0.062535
0.004000	0.496095	-0.167176	0.060918	0.080058
0.006000	0.487194	-0.224710	0.080299	0.103191
0.008000	0.477017	-0.294757	0.103349	0.130153
0.009600	0.475288	-0.347087	0.107362	0.149514
0.010000	0.474180	-0.360959	0.109950	0.154565
0.015000	0.462569	-0.430635	0.137811	0.179466
0.020000	0.453665	-0.561549	0.160142	0.223899
0.024000	0.447717	-0.672489	0.175555	0.259524
0.030000	0.440078	-0.785401	0.195962	0.294021
0.040000	0.429550	-0.949877	0.225273	0.341164
0.060000	0.413082	-1.214498	0.274119	0.409450
0.100000	0.388687	-1.639656	0.354087	0.500199
0.150000	0.361035	-1.808206	0.457797	0.482115
0.200000	0.339761	-2.350272	0.549077	0.547765
0.300000	0.304951	-2.872722	0.725904	0.565523
0.400000	0.286302	-5.362423	0.838321	0.889548
0.500000	0.273285	-7.681798	0.925889	1.141976
0.600000	0.262586	-9.346971	1.004356	1.274416
0.800000	0.245580	-11.760374	1.143156	1.440917
1.000000	0.232263	-15.018677	1.266034	1.627638
1.500000	0.207692	-20.349332	1.534115	1.865108
2.000000	0.189872	-28.057565	1.771956	2.102247

UNLOADING PATH

0.	0.526316	0.	0.
0.000000	0.526315	0.000002	0.044114
0.000003	0.526279	0.000070	0.044134

Table A8. Coordinated failure model, UM - 2.1/0.80 (Fig. 8).

Input variables

ρ_0 = 2.1 Mg/m^3 S_w = 0.80 K = 5.0 GPa

P_T = 100 kPa P_M = 10.4 MPa

Output

Z = 0.1161 ϕ_0 = 0.3048 ϕ_a = 0.0610

e_w = 0.3508 EF = 8.226 kJ EV = 37.99 kJ

LOADING PATH

P	V	DP/DV	MU	DP/DMU
0.	0.476190	0.	0.	0.
0.000001	0.476181	-0.105002	0.000020	0.050000
0.000010	0.461279	-0.000604	0.032326	0.000279
0.000020	0.456927	-0.002298	0.042158	0.001017
0.000030	0.454394	-0.003947	0.047969	0.001721
0.000050	0.451196	-0.006254	0.055396	0.002693
0.000070	0.449073	-0.009420	0.060386	0.004008
0.000100	0.446791	-0.013150	0.065800	0.005541
0.000104	0.446538	-0.015773	0.066406	0.006608
0.000200	0.445980	-0.172121	0.067739	0.071983
0.000400	0.444867	-0.179648	0.070411	0.074849
0.000600	0.443813	-0.189825	0.072952	0.078705
0.001000	0.441861	-0.204852	0.077694	0.084362
0.002000	0.437676	-0.238958	0.087998	0.097046
0.004000	0.431210	-0.309336	0.104311	0.122600
0.006000	0.426218	-0.400621	0.117246	0.154623
0.009000	0.420261	-0.503644	0.133081	0.189450
0.009600	0.419219	-0.575516	0.135899	0.212930
0.010000	0.418545	-0.593924	0.137727	0.218843
0.015000	0.411222	-0.682765	0.157988	0.246780
0.020000	0.405235	-0.835130	0.175097	0.292252
0.024000	0.401036	-0.952483	0.187402	0.325062
0.030000	0.395394	-1.063508	0.204344	0.354138
0.040000	0.387155	-1.213749	0.229974	0.390178
0.060000	0.373236	-1.436864	0.275844	0.436017
0.100000	0.350676	-1.773069	0.357921	0.487343
0.150000	0.326160	-2.039471	0.459991	0.489862
0.200000	0.306465	-2.538763	0.553816	0.532909
0.300000	0.273703	-3.052330	0.739805	0.537665
0.400000	0.256802	-6.368760	0.845687	0.944446
0.500000	0.247808	-9.809891	0.921611	1.317108
0.600000	0.239610	-12.197490	0.987360	1.520930
0.800000	0.226921	-15.761653	1.098490	1.799695
1.000000	0.217282	-20.749450	1.191581	2.148438
1.500000	0.200174	-29.227079	1.378879	2.669538
2.000000	0.188294	-42.086405	1.528974	3.331239

UNLOADING PATH

0.	0.447161	0.064920	0.
0.000001	0.447155	0.064935	0.069013
0.000010	0.447100	0.065065	0.069111
0.000020	0.447039	0.065209	0.069298
0.000030	0.446979	0.065353	0.069495
0.000050	0.446859	0.065640	0.069790
0.000070	0.446739	0.065925	0.070184
0.000100	0.446561	0.066349	0.070674
0.000104	0.446538	0.066406	0.071008

Table A9. Coordinated failure model, UM - 2.1/0.90 (Fig. 8).

Input variables

ρ_0 = 2.1 Mg/m^3 S_w = 0.90 K = 5.0 GPa

P_T = 100 kPa P_M = 10.4 MPa

Output

Z = 0.1380 ϕ_0 = 0.3220 ϕ_a = 0.0322

e_w = 0.4275 EF = 8.551 kJ EV = 39.038 kJ

LOADING PATH

P	V	DP/DV	MU	DP/DMU
0.	0.476190	0.	0.	0.
0.000001	0.476181	-0.105002	0.000020	0.050000
0.000010	0.468390	-0.001155	0.016653	0.000541
0.000020	0.466042	-0.004258	0.021777	0.001952
0.000030	0.464649	-0.007181	0.024839	0.003265
0.000050	0.462854	-0.011142	0.028814	0.005032
0.000070	0.461631	-0.016360	0.031538	0.007341
0.000100	0.460282	-0.022233	0.034562	0.009921
0.000104	0.460129	-0.026201	0.034905	0.011653
0.000200	0.459480	-0.147723	0.036369	0.065586
0.000400	0.458184	-0.154316	0.039301	0.068224
0.000600	0.456958	-0.163248	0.042087	0.071777
0.001000	0.454692	-0.176474	0.047282	0.077001
0.002000	0.449853	-0.206657	0.058547	0.088768
0.004000	0.442436	-0.269662	0.076292	0.112710
0.006000	0.436768	-0.352833	0.090260	0.143182
0.009000	0.430081	-0.448637	0.107212	0.176976
0.009600	0.428920	-0.516684	0.110209	0.200157
0.010000	0.428171	-0.534266	0.112151	0.206049
0.015000	0.420106	-0.619965	0.133501	0.234187
0.020000	0.413614	-0.770209	0.151291	0.281049
0.024000	0.409112	-0.888482	0.163961	0.315722
0.030000	0.403125	-1.002115	0.181248	0.347071
0.040000	0.394490	-1.158088	0.207105	0.386755
0.060000	0.380130	-1.392745	0.252705	0.438590
0.100000	0.357252	-1.748455	0.332925	0.498633
0.150000	0.332194	-1.995318	0.433472	0.497277
0.200000	0.312226	-2.504019	0.525148	0.545402
0.300000	0.279110	-3.019666	0.706106	0.552614
0.400000	0.262898	-6.168479	0.811312	0.950516
0.500000	0.252216	-9.361209	0.888028	1.303500
0.600000	0.243585	-11.586166	0.954927	1.494794
0.800000	0.230149	-14.885425	1.069055	1.752425
1.000000	0.219874	-19.464453	1.165746	2.068443
1.500000	0.201475	-27.175850	1.363522	2.528115
2.000000	0.188567	-38.735521	1.525313	3.090405

UNLOADING PATH

0.	0.460856	0.033275	0.
0.000001	0.460848	0.033291	0.062858
0.000010	0.460785	0.033434	0.062948
0.000020	0.460714	0.033592	0.063120
0.000030	0.460644	0.033750	0.063301
0.000050	0.460503	0.034065	0.063572
0.000070	0.460364	0.034378	0.063933
0.000100	0.460157	0.034844	0.064384
0.000104	0.460129	0.034905	0.064691

Table A10. Coordinated failure model, UM - 2.1/0.95 (Fig. 8).

Input variables

ρ_0 = 2.1 Mg/m^3 S_w = 0.95 K = 5.0 GPa

P_T = 100 kPa P_M = 10.4 MPa

Output

Z = 0.1499 ϕ_0 = 0.3314 ϕ_a = 0.0166

e_w = 0.4709 EF = 8.749 kJ EV = 39.645 kJ

LOADING PATH

P	V	DP/DV	MU	DP/DMU
0.	0.476190	0.	0.	0.
0.000001	0.476181	-0.105002	0.000020	0.050000
0.000010	0.472169	-0.002243	0.008518	0.001059
0.000020	0.470918	-0.007993	0.011197	0.003732
0.000030	0.470157	-0.013150	0.012833	0.006114
0.000050	0.469147	-0.019793	0.015014	0.009168
0.000070	0.468432	-0.028002	0.016562	0.012923
0.000100	0.467613	-0.036608	0.018343	0.016839
0.000104	0.467518	-0.042084	0.018550	0.019321
0.000200	0.466818	-0.137155	0.020077	0.062860
0.000400	0.465423	-0.143330	0.023136	0.065396
0.000600	0.464104	-0.151703	0.026042	0.068814
0.001000	0.461667	-0.164115	0.031459	0.073844
0.002000	0.456472	-0.192511	0.043197	0.085196
0.004000	0.448539	-0.252087	0.061649	0.108389
0.006000	0.442503	-0.331347	0.076130	0.138108
0.009000	0.435419	-0.423493	0.093638	0.171352
0.009600	0.434193	-0.489483	0.096726	0.194333
0.010000	0.433403	-0.506604	0.098724	0.200199
0.015000	0.424935	-0.590442	0.120619	0.228356
0.020000	0.418169	-0.738981	0.138751	0.275757
0.024000	0.413503	-0.857172	0.151602	0.311255
0.030000	0.407327	-0.971625	0.169061	0.343669
0.040000	0.398477	-1.129921	0.195026	0.385136
0.060000	0.383877	-1.369880	0.240476	0.440046
0.100000	0.360827	-1.735360	0.319718	0.504778
0.150000	0.335474	-1.972110	0.419457	0.501312
0.200000	0.315357	-2.485527	0.510003	0.552204
0.300000	0.282048	-3.002201	0.688329	0.560771
0.400000	0.265560	-6.064802	0.793157	0.953942
0.500000	0.254612	-9.134106	0.870260	1.296959
0.600000	0.245746	-11.278876	0.937737	1.482005
0.800000	0.231904	-14.448779	1.053397	1.729196
1.000000	0.221283	-18.830524	1.151956	2.029256
1.500000	0.202182	-26.177152	1.355256	2.459414
2.000000	0.188715	-37.128547	1.523327	2.974931

UNLOADING PATH

0.	0.468300	0.016849	0.
0.000001	0.468292	0.016866	0.060238
0.000010	0.468224	0.017015	0.060325
0.000020	0.468148	0.017180	0.060490
0.000030	0.468072	0.017345	0.060664
0.000050	0.467921	0.017673	0.060924
0.000070	0.467771	0.018000	0.061271
0.000100	0.467547	0.018486	0.061705
0.000104	0.467518	0.018550	0.061999

Table A11. Coordinated failure model, SM - 2.1/1.0 (Fig. 7).

Input variables

ρ_0 = 2.1 Mg/m^3	S_w = 1.0	K = 5.0 GPa
P_T = 10 kPa	P_M = 311 kPa	

Output

Z = 0.1625	ϕ_0 = 0.3413	ϕ_a = 0.
e_w = 0.5182	EF = 8.926 kJ	EV = 40.318 kJ

LOADING PATH

P	V	DP/DV	MU	DP/DMU
0.	0.476190	0.	0.	0.
0.000000	0.476190	-0.105000	0.000002	0.050000
0.000003	0.476165	-0.121502	0.000054	0.057893
0.000010	0.476108	-0.121777	0.000173	0.057976
0.000020	0.476026	-0.122109	0.000345	0.058117
0.000030	0.475945	-0.122503	0.000516	0.058284
0.000050	0.475782	-0.123092	0.000858	0.058535
0.000070	0.475621	-0.123879	0.001198	0.058869
0.000100	0.475380	-0.124862	0.001704	0.059286
0.000200	0.474596	-0.127408	0.003361	0.060365
0.000400	0.473095	-0.133273	0.006543	0.062840
0.000600	0.471678	-0.141124	0.009567	0.066132
0.001000	0.469059	-0.152776	0.015203	0.070982
0.002000	0.463488	-0.179489	0.027406	0.081945
0.004000	0.455006	-0.235798	0.046558	0.104428
0.006000	0.448581	-0.311258	0.061549	0.133413
0.008000	0.441076	-0.399748	0.079611	0.166096
0.009600	0.439782	-0.463615	0.082788	0.188855
0.010000	0.438949	-0.480250	0.084843	0.194687
0.015000	0.430053	-0.562074	0.107282	0.222818
0.020000	0.422996	-0.708533	0.125755	0.270669
0.024000	0.418156	-0.826309	0.138787	0.306928
0.030000	0.411781	-0.941272	0.156416	0.340361
0.040000	0.402703	-1.101526	0.182485	0.383588
0.060000	0.387849	-1.346453	0.227772	0.441630
0.100000	0.364616	-1.721694	0.306005	0.511298
0.150000	0.338950	-1.948095	0.404898	0.505593
0.200000	0.318676	-2.466225	0.494277	0.559419
0.300000	0.285163	-2.983910	0.669888	0.569440
0.400000	0.268381	-5.958647	0.774309	0.957661
0.500000	0.257151	-8.905133	0.851791	1.290625
0.600000	0.248036	-10.970493	0.919844	1.469430
0.800000	0.233764	-14.013109	1.037060	1.706261
1.000000	0.222776	-18.202208	1.137531	1.990622
1.500000	0.202931	-25.195779	1.346559	2.392019
2.000000	0.188873	-35.564769	1.521227	2.862578

UNLOADING PAT'

0.	0.476190	0.000000	0.
0.000000	0.476190	0.000002	0.057867
0.000003	0.476165	0.000054	0.057893

Table A12. Coordinated failure model, UX - 1.7/0.90 (Fig. 8).

Input variables

ρ_0 = 1.7 Mg/m^3	S_w = 0.90	K = 5.0 GPa
P_T = 100 kPa	P_M = 14.7 MPa	

Output

Z = 0.2901	ϕ_0 = 0.5480	ϕ_a = 0.0548
e_w = 1.0913	EF = 5.938 kJ	EV = 31.773 kJ

LOADING PATH

P	V	DP/DV	MU	DP/DMU
0.	0.588235	0.	0.	0.
0.000001	0.588224	-0.085002	0.000020	0.050000
0.000010	0.572764	-0.000582	0.027012	0.000333
0.000020	0.568163	-0.002173	0.035329	0.001202
0.000030	0.565445	-0.003680	0.040304	0.002010
0.000050	0.561953	-0.005727	0.046769	0.003094
0.000070	0.559581	-0.008430	0.051207	0.004506
0.000100	0.556966	-0.011473	0.056142	0.006079
0.000147	0.553972	-0.015700	0.061850	0.008235
0.000200	0.553265	-0.074946	0.063207	0.039050
0.000400	0.550699	-0.077952	0.068160	0.040376
0.000600	0.548283	-0.082755	0.072869	0.042478
0.001000	0.543835	-0.089927	0.081644	0.045584
0.002000	0.534451	-0.106573	0.100634	0.052659
0.004000	0.520426	-0.142600	0.130295	0.067427
0.006000	0.510060	-0.192940	0.153266	0.087067
0.009000	0.498299	-0.255084	0.180486	0.110216
0.009600	0.496313	-0.302120	0.185209	0.127021
0.010000	0.495042	-0.314674	0.188253	0.131434
0.015000	0.481824	-0.378255	0.220852	0.153378
0.020000	0.471826	-0.500113	0.246721	0.193280
0.024000	0.465222	-0.605718	0.264418	0.226028
0.030000	0.456834	-0.715261	0.287636	0.258424
0.040000	0.445448	-0.878275	0.320548	0.303833
0.060000	0.428024	-1.147882	0.374303	0.372059
0.100000	0.402941	-1.594661	0.459856	0.467549
0.150000	0.374113	-1.734453	0.572346	0.444483
0.200000	0.352247	-2.286609	0.669953	0.512260
0.300000	0.316068	-2.810702	0.857575	0.532985
0.400000	0.290915	-5.062453	0.981156	0.809183
0.500000	0.269838	-7.103901	1.079758	1.014183
0.600000	0.251140	-8.593845	1.168992	1.120644
0.800000	0.219677	-10.738134	1.328936	1.250444
1.000000	0.193881	-13.609175	1.472814	1.390061
1.500000	0.148611	-18.268455	1.794316	1.555199
2.000000	0.120463	-24.940076	2.088445	1.699939

UNLOADING PATH

0.	0.555999	0.057980	0.
0.000001	0.555985	0.058007	0.037216
0.000010	0.555858	0.058248	0.037269
0.000020	0.555717	0.058516	0.037370
0.000030	0.555577	0.058782	0.037476
0.000050	0.555298	0.059314	0.037636
0.000070	0.555022	0.059842	0.037848
0.000100	0.554610	0.060629	0.038113
0.000147	0.553972	0.061850	0.038521

Table A13. Coordinated failure model, UX - 2.1/0.90 (Fig. 8).

Input variables

ρ_0 = 2.1 Mg/m^3 | S_w = 0.90 | K = 5.0 GPa

P_T = 100 kPa | P_M = 14.7 kPa

Output

Z = 0.1380 | ϕ_0 = 0.3220 | ϕ_a = 0.0322

e_w = 0.4275 | EF = 8.551 kJ | EV = 39.04 kJ

LOADING PATH

P	V	DP/DV	MU	DP/DMU
0.	0.476190	0.	0.	0.
0.000001	0.476181	-0.105002	0.000020	0.050000
0.000010	0.476018	-0.001239	0.015509	0.000581
0.000020	0.475922	-0.004553	0.020288	0.002093
0.000030	0.475817	-0.007663	0.023149	0.003496
0.000041	0.475751	-0.011862	0.026869	0.005376
0.000070	0.475629	-0.017366	0.029425	0.007823
0.000100	0.475504	-0.023527	0.032271	0.010543
0.000147	0.475356	-0.032021	0.035566	0.014264
0.000300	0.475030	-0.148694	0.036369	0.065976
0.000400	0.474814	-0.154316	0.039301	0.068224
0.000600	0.474658	-0.163248	0.042087	0.071777
0.001000	0.474492	-0.176474	0.047282	0.077001
0.002000	0.449853	-0.206657	0.058547	0.088768
0.004000	0.443436	-0.269662	0.076292	0.112710
0.006000	0.436768	-0.352833	0.090260	0.143182
0.009000	0.430081	-0.448637	0.107212	0.176976
0.009600	0.428920	-0.516684	0.110209	0.200157
0.010000	0.428171	-0.534266	0.112151	0.206049
0.015000	0.420106	-0.619965	0.133501	0.234187
0.020000	0.413614	-0.770209	0.151291	0.281049
0.024000	0.409112	-0.888482	0.163961	0.315722
0.030000	0.403125	-1.002115	0.181248	0.347071
0.040000	0.394490	-1.158088	0.207105	0.386755
0.060000	0.380130	-1.392745	0.252705	0.438590
0.100000	0.357252	-1.748455	0.332925	0.498633
0.150000	0.332194	-1.995318	0.433472	0.497277
0.200000	0.312226	-2.504019	0.525148	0.545402
0.300000	0.279110	-3.019666	0.706106	0.552614
0.400000	0.262898	-6.168479	0.811312	0.950516
0.500000	0.252216	-9.361209	0.888028	1.303500
0.600000	0.243585	-11.586166	0.954927	1.494794
0.800000	0.230149	-14.885425	1.069055	1.752425
1.000000	0.219874	-19.464453	1.165746	2.068443
1.500000	0.201475	-27.175850	1.363522	2.528115
2.000000	0.188567	-38.735521	1.525313	3.090405

UNLOADING PATH

0.	0.460856	0.033275	0.
0.000001	0.460848	0.033291	0.062858
0.000010	0.460785	0.033434	0.062948
0.000020	0.460714	0.033592	0.063120
0.000030	0.460644	0.033750	0.063301
0.000050	0.460503	0.034065	0.063572
0.000070	0.460364	0.034378	0.063933
0.000100	0.460157	0.034844	0.064384
0.000147	0.459836	0.035566	0.065077

Table A14. Coordinated failure model, SX - 1.7/1.0 (Fig. 8).

Input variables

ρ_0 = 1.7 Mg/m^3 S_w = 1.0 K = 5.0 GPa

P_T = 10 kPa P_M = 68.9 MPa

Output

Z = 0.3417 ϕ_0 = 0.5808 ϕ_a = 0.

e_w = 1.386 EF = 6.612 kJ EV = 33.30 kJ

LOADING PATH

P	V	DP/DV	MU	DP/DMU
0.	0.588235	0.	0.	0.
0.000000	0.588234	-0.085000	0.000002	0.050000
0.000007	0.588122	-0.060408	0.000193	0.035527
0.000010	0.588071	-0.060766	0.000280	0.035728
0.000020	0.587906	-0.060900	0.000560	0.035794
0.000030	0.587743	-0.061106	0.000838	0.035894
0.000050	0.587417	-0.061414	0.001393	0.036046
0.000070	0.587094	-0.061826	0.001945	0.036247
0.000100	0.586612	-0.062340	0.002767	0.036498
0.000200	0.585042	-0.063675	0.005459	0.037150
0.000400	0.582046	-0.066758	0.010634	0.038646
0.000600	0.579225	-0.070908	0.015555	0.040640
0.001000	0.574038	-0.077113	0.024732	0.043588
0.002000	0.563115	-0.091550	0.044609	0.050309
0.004000	0.546851	-0.122969	0.075678	0.064374
0.006000	0.534893	-0.167259	0.099724	0.083171
0.008000	0.521413	-0.222552	0.128155	0.105519
0.009600	0.519148	-0.264854	0.133078	0.121879
0.010000	0.517700	-0.276209	0.136248	0.126199
0.015000	0.502735	-0.334118	0.170070	0.147831
0.020000	0.491549	-0.447001	0.196696	0.187786
0.024000	0.484234	-0.546760	0.214776	0.221242
0.030000	0.475031	-0.652023	0.238308	0.254970
0.040000	0.462713	-0.811816	0.271274	0.303348
0.060000	0.444252	-1.083348	0.324102	0.378581
0.100000	0.418421	-1.548510	0.405846	0.489335
0.150000	0.388316	-1.660881	0.514835	0.458761
0.200000	0.365807	-2.221264	0.608050	0.536397
0.300000	0.329394	-2.746310	0.785810	0.562556
0.400000	0.308441	-4.772514	0.907125	0.824297
0.500000	0.293214	-6.567338	1.006164	1.009706
0.600000	0.280559	-7.902338	1.096651	1.105132
0.800000	0.260176	-9.811885	1.260913	1.217569
1.000000	0.243982	-12.350373	1.410976	1.332767
1.500000	0.213573	-16.442434	1.754258	1.456531
2.000000	0.191106	-22.254618	2.078061	1.544150

UNLOADING PATH

0.	0.588235	0.000000	0.
0.000000	0.588234	0.000003	0.035643
0.000007	0.588122	0.000193	0.035678

Table A15. Coordinated failure model, SX - 2.1/1.0 (Fig. 7).

Input variables

ρ_0 = 2.1 Mg/m^3	S_w = 1.0	K = 5.0 GPa
P_T = 10 kPa	P_M = 68.9 MPa	

Output

Z = 0.1625	ϕ_0 = 0.3413	ϕ_a = 0.
e_w = 0.5182	EF = 8.926 kJ	EV = 40.32 kJ

LOADING PATH

P	V	DP/DV	MU	DP/DMU
0.	0.476190	0.	0.	0.
0.000000	0.476190	-0.105000	0.000002	0.050000
0.000007	0.476134	-0.121657	0.000119	0.057925
0.000010	0.476108	-0.121851	0.000173	0.058008
0.000020	0.476026	-0.122109	0.000345	0.058117
0.000030	0.475945	-0.122503	0.000516	0.058284
0.000050	0.475782	-0.123092	0.000858	0.058535
0.000070	0.475621	-0.123879	0.001198	0.058869
0.000100	0.475380	-0.124862	0.001704	0.059286
0.000200	0.474596	-0.127408	0.003361	0.060365
0.000400	0.473095	-0.133273	0.006543	0.062840
0.000600	0.471678	-0.141124	0.009567	0.066132
0.001000	0.469059	-0.152776	0.015203	0.070982
0.002000	0.463488	-0.179489	0.027406	0.081945
0.004000	0.455006	-0.235798	0.046558	0.104428
0.006000	0.448581	-0.311258	0.061549	0.133413
0.009000	0.441076	-0.399748	0.079611	0.166096
0.009600	0.439782	-0.463615	0.082788	0.188855
0.010000	0.438949	-0.480250	0.084843	0.194687
0.015000	0.430053	-0.562074	0.107282	0.222818
0.020000	0.422996	-0.708533	0.125755	0.270669
0.024000	0.418156	-0.826309	0.138787	0.306928
0.030000	0.411781	-0.941272	0.156416	0.340361
0.040000	0.402703	-1.101526	0.182485	0.383588
0.060000	0.387049	-1.346453	0.227772	0.441630
0.100000	0.361616	-1.721694	0.306005	0.511298
0.150000	0.338950	-1.948095	0.404898	0.505593
0.200000	0.318676	-2.466225	0.494277	0.559419
0.300000	0.285163	-2.983910	0.669888	0.569440
0.400000	0.268381	-5.958647	0.774309	0.957661
0.500000	0.257151	-8.905133	0.851791	1.290625
0.600000	0.249036	-10.970493	0.919844	1.469430
0.800000	0.233764	-14.013109	1.037060	1.706261
1.000000	0.222776	-18.202208	1.137531	1.990622
1.500000	0.202931	-25.195779	1.346559	2.392019
2.000000	0.188873	-35.564769	1.521227	2.862578

UNLOADING PATH

0.	0.476190	0.000000	0.
0.000000	0.476190	0.000002	0.057867
0.000007	0.476134	0.000119	0.057925

Table A16. Coordinated failure model, CM - 1.7/0.90 (Fig. 9).

Input variables

ρ_0 = 1.7 Mg/m^3 S_w = 0.90 K = 5.0 GPa

P_T = 5 MPa P_M = 21.5 MPa

Output

Z = 0.2901 ϕ_0 = 0.5480 ϕ_a = 0.0548

e_w = 1.091 EF = 5.939 kJ EV = 31.77 kJ

LOADING PATH

P	V	DP/DV	MU	DP/DMU
0.	0.588235	0.	0.	0.
0.000010	0.588118	-0.085017	0.000200	0.050000
0.000020	0.588000	-0.085051	0.000400	0.050000
0.000030	0.587883	-0.085085	0.000600	0.050000
0.000050	0.587648	-0.085136	0.001000	0.050000
0.000070	0.587451	-0.002440	0.015159	0.001413
0.000100	0.587132	-0.003563	0.030126	0.002004
0.000200	0.586173	-0.006150	0.060318	0.003312
0.000215	0.586067	-0.008796	0.063587	0.004588
0.000400	0.585099	-0.078135	0.068160	0.040456
0.000600	0.584283	-0.082755	0.072869	0.042478
0.001000	0.583835	-0.089927	0.081644	0.045584
0.002000	0.582451	-0.106573	0.100634	0.052659
0.004000	0.580426	-0.142600	0.130295	0.067427
0.006000	0.579060	-0.192940	0.153266	0.087067
0.009000	0.577299	-0.255084	0.180486	0.110216
0.009600	0.576913	-0.302120	0.185209	0.127021
0.010000	0.576642	-0.314674	0.188253	0.131434
0.015000	0.573824	-0.378255	0.220852	0.153378
0.020000	0.571326	-0.500113	0.246721	0.193280
0.024000	0.569222	-0.605718	0.264418	0.226028
0.030000	0.566834	-0.715261	0.287636	0.258424
0.040000	0.563448	-0.878275	0.320548	0.303833
0.060000	0.558024	-1.147882	0.374303	0.372059
0.100000	0.552941	-1.594661	0.459856	0.467549
0.150000	0.544113	-1.734453	0.572346	0.444483
0.200000	0.532247	-2.286609	0.669953	0.512260
0.300000	0.516668	-2.810702	0.857575	0.532985
0.400000	0.496915	-5.062453	0.981156	0.809183
0.500000	0.482838	-7.103901	1.079758	1.014183
0.600000	0.471202	-8.593845	1.168992	1.120644
0.800000	0.452577	-10.738134	1.328936	1.250444
1.000000	0.437881	-13.609175	1.472814	1.390061
1.500000	0.410511	-18.268455	1.794316	1.555199
2.000000	0.390463	-24.940076	2.088445	1.699939

UNLOADING PATH

0.	0.555999		0.057980	0.
0.000010	0.555858		0.058248	0.037264
0.000020	0.555717		0.058516	0.037370
0.000030	0.555577		0.058782	0.037476
0.000050	0.555298		0.059314	0.037636
0.000070	0.555022		0.059842	0.037848
0.000100	0.554610		0.060629	0.038113
0.000200	0.553265		0.063207	0.038799
0.000215	0.553067		0.063587	0.039410

Table A17. Coordinated failure model, CM - 2.1/0.90 (Fig. 9).

Input variables

ρ_0 = 2.1 Mg/m^3 S_w = 0.90 K = 5.0 GPa

P_T = 5 MPa P_M = 21.5 MPa

Output

Z = 0.1380 ϕ_0 = 0.3220 ϕ_a = 0.0322

e_w = 0.4275 EF = 8.552 kJ EV = 39.04 kJ

LOADING PATH

P	V	DP/DV	MU	DP/DMU
0.	0.476190	0.	0.	0.
0.000010	0.476095	-0.105021	0.000200	0.050000
0.000020	0.476000	-0.105063	0.000400	0.050000
0.000030	0.475905	-0.105105	0.000600	0.050000
0.000050	0.475715	-0.105168	0.001000	0.050000
0.000070	0.472059	-0.005471	0.008751	0.002580
0.000100	0.468067	-0.007515	0.017355	0.003487
0.000200	0.460214	-0.012734	0.034714	0.005760
0.000215	0.459380	-0.017971	0.036594	0.007979
0.000400	0.458184	-0.154658	0.039301	0.068360
0.000600	0.456958	-0.163248	0.042087	0.071777
0.001000	0.454692	-0.176474	0.047282	0.077001
0.002000	0.448053	-0.206657	0.058547	0.088768
0.004000	0.442436	-0.269662	0.076292	0.112710
0.006000	0.436768	-0.352833	0.090260	0.143182
0.008000	0.430081	-0.448637	0.107212	0.176976
0.010500	0.420171	-0.534266	0.112151	0.206049
0.015000	0.420106	-0.619965	0.133501	0.234187
0.020000	0.413614	-0.770209	0.151291	0.281049
0.024000	0.409112	-0.888482	0.163961	0.315722
0.030000	0.403125	-1.002115	0.181248	0.347071
0.040000	0.394490	-1.153088	0.207105	0.386755
0.060000	0.380150	-1.392745	0.252705	0.438590
0.100000	0.357252	-1.748455	0.332925	0.498633
0.150000	0.332194	-1.995318	0.433472	0.497277
0.200000	0.312026	-2.504019	0.525148	0.545402
0.300000	0.279110	-3.019666	0.706106	0.552614
0.400000	0.262898	-6.168479	0.811312	0.950516
0.500000	0.252216	-9.361209	0.888028	1.303500
0.600000	0.245585	-11.586166	0.954927	1.494794
0.800000	0.230149	-14.885425	1.069055	1.752425
1.000000	0.219874	-19.464453	1.165746	2.068443
1.500000	0.201475	-27.175850	1.363522	2.528115
2.000000	0.188567	-38.735521	1.525313	3.090405

UNLOADING PATH

0.	0.460856	.033275	0.
0.000010	0.460785	0.033434	0.062939
0.000020	0.460714	0.033592	0.063120
0.000030	0.460644	0.033750	0.063301
0.000050	0.460503	0.034065	0.063572
0.000070	0.460364	0.034378	0.063933
0.000100	0.460157	0.034844	0.064384
0.000200	0.459400	0.036369	0.065550
0.000215	0.459380	0.036594	0.066587

Table A18. Coordinated failure model, CX - 1.7/0.90 (Fig. 9).

Input variables

ρ_0 = 1.7 Mg/m^3	S_w = 0.90	K = 5.0 GPa
P_T = 5 MPa	P_M = 25.1 MPa	

Output

Z = 0.2901	ϕ_0 = 0.5480	ϕ_a = 0.0548
e_w = 1.091	EF = 5.939 kJ	EV = 31.77 kJ

LOADING PATH

P	V	DP/DV	MU	DP/DMU
0.	0.588235	0.	0.	0.
0.000010	0.588118	-0.085017	0.000200	0.050000
0.000020	0.588000	-0.085051	0.000400	0.050000
0.000030	0.587883	-0.085085	0.000600	0.050000
0.000050	0.587648	-0.085136	0.001000	0.050000
0.000070	0.580186	-0.002680	0.013873	0.001554
0.000100	0.572505	-0.003906	0.027476	0.002205
0.000200	0.557567	-0.006694	0.055004	0.003633
0.000251	0.552596	-0.010260	0.064495	0.005374
0.000400	0.550699	-0.078574	0.068160	0.040649
0.000600	0.548283	-0.082755	0.072869	0.042478
0.001000	0.543835	-0.089927	0.081644	0.045584
0.001999	0.534451	-0.106573	0.100634	0.052659
0.002850	0.526426	-0.142600	0.130295	0.067427
0.003800	0.518000	-0.192940	0.153266	0.087067
0.004900	0.508299	-0.255084	0.180486	0.110216
0.005900	0.499513	-0.302120	0.185209	0.127021
0.010000	0.470042	-0.314674	0.188253	0.131434
0.015000	0.431024	-0.378255	0.220852	0.153378
0.020000	0.471026	-0.500113	0.246721	0.193280
0.024000	0.465222	-0.605718	0.264418	0.226028
0.030000	0.456834	-0.715261	0.287636	0.258424
0.040000	0.445448	-0.878275	0.320548	0.303833
0.060000	0.423024	-1.147882	0.374303	0.372059
0.100000	0.382041	-1.594661	0.459856	0.467549
0.150000	0.374113	-1.734453	0.572346	0.444483
0.200000	0.352247	-2.286609	0.669953	0.512260
0.300000	0.316668	-2.810702	0.857575	0.532985
0.400000	0.296915	-5.062453	0.981156	0.809183
0.500000	0.282838	-7.103901	1.079758	1.014183
0.600000	0.271202	-8.593845	1.168992	1.120644
0.800000	0.252577	-10.738134	1.328936	1.250444
1.000000	0.237881	-13.609175	1.472814	1.390061
1.500000	0.210511	-18.268455	1.794316	1.555199
2.000000	0.190463	-24.940076	2.088445	1.699939

UNLOADING PATH

0.	0.555999	0.057980	0.
0.000010	0.555858	0.058248	0.037264
0.000020	0.555717	0.058516	0.037370
0.000030	0.555577	0.058782	0.037476
0.000050	0.555298	0.059314	0.037636
0.000070	0.555022	0.059842	0.037848
0.000100	0.554610	0.060629	0.038113
0.000200	0.553265	0.063207	0.038799
0.000251	0.552596	0.064495	0.039599

Table A19. Coordinated failure model, CX - 2.1/0.90 (Fig. 9).

Input variables

ρ_0 = 2.1 Mg/m^3 S_w = 0.90 K = 5.0 GPa

P_T = 5 MPa P_M = 25.1 MPa

Output

Z = 0.1380 ϕ_0 = 0.3220 ϕ_a = 0.0322

e_w = 0.4275 EF = 8.552 kJ EV = 39.04 kJ

LOADING PATH

P	V	DP/DV	MU	DP/DMU
0.	0.476190	0.	0.	0.
0.000010	0.476095	-0.105021	0.000200	0.050000
0.000020	0.476000	-0.105063	0.000400	0.050000
0.000030	0.475905	-0.105105	0.000600	0.050000
0.000050	0.475715	-0.105168	0.001000	0.050000
0.000070	0.472485	-0.006042	0.008014	0.002851
0.000100	0.468767	-0.008248	0.015835	0.003836
0.000200	0.461572	-0.013898	0.031671	0.006315
0.000251	0.459142	-0.020986	0.037131	0.009340
0.000400	0.458184	-0.155476	0.039301	0.068686
0.000600	0.456958	-0.163248	0.042087	0.071777
0.001000	0.454692	-0.176474	0.047282	0.077001
0.002000	0.449853	-0.206657	0.058547	0.088768
0.004000	0.442436	-0.269662	0.076292	0.112710
0.006000	0.436768	-0.352833	0.090260	0.143182
0.008060	0.430081	-0.448637	0.107212	0.176976
0.009600	0.428920	-0.516684	0.110209	0.200157
0.010000	0.428171	-0.534266	0.112151	0.206049
0.015000	0.420106	-0.619965	0.133501	0.234187
0.020000	0.413614	-0.770209	0.151291	0.281049
0.024000	0.409112	-0.888482	0.163961	0.315722
0.030000	0.403125	-1.002115	0.181248	0.347071
0.040000	0.394490	-1.158088	0.207105	0.386755
0.060000	0.380130	-1.392745	0.252705	0.438590
0.100000	0.357252	-1.748455	0.332925	0.498633
0.150000	0.332194	-1.995318	0.433472	0.497277
0.200000	0.312226	-2.504019	0.525148	0.545402
0.300000	0.279110	-3.019666	0.706106	0.552614
0.400000	0.262890	-6.168479	0.811312	0.950516
0.500000	0.252216	-9.361209	0.888028	1.303500
0.600000	0.243585	-11.586166	0.954927	1.494794
[illegible]	[illegible]	-14.885425	1.069055	1.752425
[illegible]	[illegible]	-19.464453	1.165746	2.068443
[illegible]	[illegible]	-27.175850	1.363522	2.528115
[illegible]	[illegible]	-38.735521	1.525313	3.090405

[illegible]LOADING PATH

0.	[illegible]	0.033275	0.
0.000010	[illegible]	0.033434	0.062939
0.000020	[illegible]	0.033592	0.063120
0.000030	[illegible]	0.033750	0.063301
0.000050	[illegible]	0.034065	0.063572
0.000070	[illegible]	0.034378	0.063933
0.000100	[illegible]	0.034844	0.064384
0.000200	[illegible]	0.036369	0.065550
0.000251	0.459142	0.037131	0.066908

Table A20. Coordinated failure model, RM - 1.7/0.90 (Fig. 10).

Input variables

ρ_0 = 1.7 Mg/m^3	S_w = 0.90	K = 5.0 GPa
P_T = 8 MPa	P_M = 34.5 MPa	

Output

Z = 0.2901	ϕ_0 = 0.5480	ϕ_a = 0.0548
e_w = 1.0913	EF = 5.940 kJ	EV = 31.77 kJ

LOADING PATH

P	V	DP/DV	MU	DP/DMU
0.	0.588235	0.	0.	0.
0.000010	0.588118	-0.085017	0.000200	0.050000
0.000020	0.588000	-0.085051	0.000400	0.050000
0.000030	0.587883	-0.085085	0.000600	0.050000
0.000050	0.587648	-0.085136	0.001000	0.050000
0.000070	0.587413	-0.085204	0.001400	0.050000
0.000080	0.587296	-0.085255	0.001600	0.050000
0.000100	0.587617	-0.003522	0.011379	0.002045
0.000200	0.564812	-0.005951	0.041470	0.003323
0.000345	0.551389	-0.010802	0.066824	0.005719
0.000400	0.550699	-0.079712	0.068160	0.041148
0.000600	0.548283	-0.082755	0.072869	0.042478
0.001000	0.543835	-0.089927	0.081644	0.045584
0.002000	0.534451	-0.106573	0.100634	0.052659
0.004000	0.520426	-0.142600	0.130295	0.067427
0.006000	0.510060	-0.192940	0.153266	0.087067
0.008000	0.498299	-0.255084	0.180486	0.110216
0.009600	0.496313	-0.302120	0.185209	0.127021
0.010000	0.495042	-0.314674	0.188253	0.131434
0.015000	0.481824	-0.378255	0.220852	0.153378
0.020000	0.471826	-0.500113	0.246721	0.193280
0.024000	0.465222	-0.605718	0.264418	0.226028
0.030000	0.456834	-0.715261	0.287636	0.258424
0.040000	0.445448	-0.878275	0.320548	0.303833
0.060000	0.428024	-1.147882	0.374303	0.372059
0.100000	0.402941	-1.594661	0.459856	0.467549
0.150000	0.374113	-1.734453	0.572346	0.444483
0.200000	0.353247	-2.286609	0.669953	0.512260
0.300000	0.316668	-2.810702	0.857575	0.532985
0.400000	0.296915	-5.062453	0.981156	0.809183
0.500000	0.282038	-7.103901	1.079758	1.014183
0.600000	0.271202	-8.593845	1.168992	1.120644
0.800000	0.252577	-10.738134	1.328936	1.250444
1.000000	0.237881	-13.609175	1.472814	1.390061
1.500000	0.210511	-18.268455	1.794316	1.555199
2.000000	0.190463	-24.940076	2.088445	1.699939

UNLOADING PATH

0.	0.588235	0.057980	0.
0.000010	0.588358	0.058248	0.037264
0.000020	0.588717	0.058516	0.037370
0.000030	0.588577	0.058782	0.037476
0.000050	0.588298	0.059314	0.037636
0.000070	0.588022	0.059842	0.037848
0.000080	0.587884	0.060105	0.038007
0.000100	0.587610	0.060629	0.038166
0.000200	0.586265	0.063207	0.038799
0.000345	0.581389	0.066824	0.040091

Table A21. Coordinated failure model, RM - 2.1/0.90 (Fig. 10).

Input variables

ρ_0 = 2.1 Mg/m^3 S_w = 0.90 K = 5.0 GPa

P_T = 8 MPa P_M = 34.5 MPa

Output

Z = 0.1380 ϕ_0 = 0.3220 ϕ_a = 0.0322

e_w = 0.4275 EF = 8.552 kJ EV = 39.04 kJ

LOADING PATH

P	V	DP/DV	MU	DP/DMU
0.	0.476190	0.	0.	0.
0.000010	0.476095	-0.105021	0.000200	0.050000
0.000020	0.476000	-0.105063	0.000400	0.050000
0.000030	0.475905	-0.105105	0.000600	0.050000
0.000050	0.475715	-0.105168	0.001000	0.050000
0.000070	0.475525	-0.105252	0.001400	0.050000
0.000080	0.475430	-0.105315	0.001600	0.050000
0.000110	0.475065	-0.008458	0.006606	0.003995
0.000260	0.475067	-0.012502	0.023919	0.005776
0.000345	0.458533	-0.022191	0.038510	0.009938
0.000400	0.458184	-0.157598	0.039301	0.069531
0.000600	0.456958	-0.163248	0.042087	0.071777
0.001000	0.454692	-0.176474	0.047282	0.077001
0.002000	0.449853	-0.206657	0.058547	0.088768
0.004000	0.442436	-0.269662	0.076292	0.112710
0.006000	0.436768	-0.352833	0.090260	0.143182
0.008000	0.430681	-0.448637	0.107212	0.176976
0.009600	0.428920	-0.516684	0.110209	0.200157
0.010000	0.428171	-0.534266	0.112151	0.206049
0.015000	0.420106	-0.619965	0.133501	0.234187
0.020000	0.413614	-0.770209	0.151291	0.281049
0.024000	0.409112	-0.888482	0.163961	0.315722
0.030000	0.403125	-1.062115	0.181248	0.347071
0.040000	0.394490	-1.158088	0.207105	0.386755
0.060000	0.380130	-1.392745	0.252705	0.438590
0.100000	0.357352	-1.748455	0.332925	0.498633
0.150000	0.332194	-1.995318	0.433472	0.497277
0.200000	0.312220	-2.504019	0.525148	0.545402
0.300000	0.279110	-3.019666	0.706106	0.552614
0.400000	0.252898	-6.168479	0.811312	0.950516
0.500000	0.232216	-9.361209	0.888028	1.303500
0.600000	0.243585	-11.586166	0.954927	1.494794
0.800000	0.230149	-14.885425	1.069055	1.752425
1.000000	0.219074	-19.464453	1.165746	2.068443
1.500000	0.201475	-27.175850	1.363522	2.528115
2.000000	0.188567	-38.735521	1.525313	3.090405

UNLOADING PATH

0.	0.460856	0.033275	0.
0.000010	0.460785	0.033434	0.062939
0.000020	0.460714	0.033592	0.063120
0.000030	0.460644	0.033750	0.063301
0.000050	0.460503	0.034065	0.063572
0.000070	0.460364	0.034378	0.063933
0.000080	0.460295	0.034533	0.064204
0.000100	0.460157	0.034844	0.064474
0.000200	0.459480	0.036369	0.065550
[illegible]	[illegible]	0.038510	0.067741

Table A22. Coordinated failure model, RX - 1.7/0.90 (Fig. 10).

Input variables

ρ_0 = 1.7 Mg/m^3 S_w = 0.90 K = 5.0 GPa

P_T = 8 MPa P_M = 60 MPa

Output

Z = 0.2901 ϕ_0 = 0.5480 ϕ_a = 0.0548

e_w = 1.091 EF = 5.941 kJ EV = 31.78 kJ

LOADING PATH

P	V	DP/DV	MU	DP/DMU
0.	0.588235	0.	0.	0.
0.000010	0.588118	-0.085017	0.000200	0.050000
0.000020	0.588000	-0.085051	0.000400	0.050000
0.000030	0.587883	-0.085085	0.000600	0.050000
0.000041	0.587765	-0.085136	0.001000	0.050000
0.000051	0.587647	-0.085204	0.001400	0.050000
0.000061	0.587530	-0.085255	0.001600	0.050000
0.000100	0.587060	-0.084680	0.008942	0.002724
0.000200	0.585906	-0.087864	0.031438	0.004445
0.000350	0.584140	-0.014852	0.056381	0.008018
0.000500	0.582383	-0.023371	0.072869	0.012130
0.001000	0.576835	-0.089927	0.081644	0.045584
0.002000	0.566451	-0.106573	0.100634	0.052659
0.004000	0.546426	-0.142600	0.130295	0.067427
0.006000	0.527060	-0.192940	0.153266	0.087067
0.008000	0.508299	-0.255084	0.180486	0.110216
0.009600	0.496313	-0.302120	0.185209	0.127021
0.010000	0.493042	-0.314674	0.188253	0.131434
0.015000	0.481824	-0.378255	0.220852	0.153378
0.020000	0.471826	-0.500113	0.246721	0.193280
0.024000	0.465222	-0.605718	0.264418	0.226028
0.030000	0.456834	-0.715261	0.287636	0.258424
0.040000	0.445448	-0.878275	0.320548	0.303833
0.060000	0.428024	-1.147882	0.374303	0.372059
0.100000	0.402941	-1.594661	0.459856	0.467549
0.150000	0.374113	-1.734453	0.572346	0.444483
0.200000	0.352247	-2.286609	0.669953	0.512260
0.300000	0.316668	-2.810702	0.857575	0.532985
0.400000	0.290915	-5.062453	0.981156	0.809183
0.500000	0.282838	-7.103901	1.079758	1.014183
0.600000	0.271202	-8.593845	1.168992	1.120644
0.800000	0.252577	-10.738134	1.328936	1.250444
1.000000	0.237881	-13.609175	1.472814	1.390061
1.500000	0.210511	-18.268455	1.794316	1.555199
2.000000	0.190463	-24.940076	2.088445	1.699939

UNLOADING PATH

0.	0.555999	0.057980	0.
0.000010	0.555858	0.058248	0.037264
0.000020	0.555717	0.058516	0.037370
0.000030	0.555577	0.058782	0.037476
0.000050	0.555298	0.059314	0.037636
0.000070	0.555022	0.059842	0.037848
0.000080	0.554884	0.060105	0.038007
0.000100	0.554610	0.060629	0.038166
0.000200	0.553265	0.063207	0.038799
0.000400	0.550699	0.068160	0.040376
0.000600	0.548283	0.072869	0.042478

Table A23. Coordinated failure model, RX - 2.1/0.90 (Fig. 10).

Input variables

ρ_0 = 2.1 Mg/m^3 S_w = 0.90 K = 5.0 GPa

P_T = 8 MPa P_M = 60 MPa

Output

Z = 0.1380 ϕ_0 = 0.3220 ϕ_a = 0.0322

e_w = 0.4275 EF = 8.553 kJ EV = 39.04 kJ

LOADING PATH

P	V	DP/DV	MU	DP/DMU
0.	0.476190	0.	0.	0.
0.000010	0.476095	-0.105021	0.000200	0.050000
0.000020	0.476000	-0.105063	0.000400	0.050000
0.000030	0.475905	-0.105105	0.000600	0.050000
0.000050	0.475715	-0.105168	0.001000	0.050000
0.000070	0.475525	-0.105252	0.001400	0.050000
0.000080	0.475430	-0.105315	0.001600	0.050000
0.000100	0.473723	-0.011717	0.005209	0.005542
0.000200	0.467692	-0.016580	0.018172	0.007714
0.000400	0.461172	-0.030677	0.032566	0.013895
0.000600	0.456958	-0.047464	0.042087	0.021005
0.001000	0.454692	-0.176474	0.047282	0.077001
0.002000	0.449853	-0.206657	0.058547	0.088768
0.004000	0.442436	-0.269662	0.076292	0.112710
0.006000	0.436768	-0.352833	0.090260	0.143182
0.008000	0.430081	-0.448637	0.107212	0.176976
0.008500	0.428420	-0.516684	0.110209	0.200157
0.010000	0.423171	-0.534266	0.112151	0.206049
0.012000	0.420186	-0.619565	0.133501	0.234187
0.020000	0.413614	-0.770209	0.151291	0.281049
0.024000	0.409112	-0.888482	0.163961	0.315722
0.030000	0.403125	-1.002115	0.181248	0.347071
0.040000	0.394490	-1.158088	0.207105	0.386755
0.060000	0.380130	-1.392745	0.252705	0.438590
0.100000	0.357252	-1.748455	0.332925	0.498633
0.150000	0.332194	-1.995318	0.433472	0.497277
0.200000	0.312226	-2.504019	0.525148	0.545402
0.300000	0.279110	-3.019666	0.706106	0.552614
0.400000	0.252898	-6.168479	0.811312	0.950516
0.500000	0.252216	-9.361209	0.888028	1.303500
0.600000	0.243585	-11.586166	0.954927	1.494794
0.800000	0.230149	-14.885425	1.069055	1.752425
1.000000	0.219874	-19.464453	1.165746	2.068443
1.500000	0.201475	-27.175850	1.363522	2.528115
2.000000	0.188567	-38.735521	1.525313	3.090405

UNLOADING PATH

0.	0.460856	0.033275	0.
0.000010	0.460785	0.033434	0.062939
0.000020	0.460714	0.033592	0.063120
0.000030	0.460644	0.033750	0.063301
0.000050	0.460503	0.034065	0.063572
0.000070	0.460364	0.034378	0.063933
0.000080	0.460295	0.034533	0.064204
0.000100	0.460157	0.034844	0.064474
0.000200	0.459480	0.036369	0.065550
0.000400	0.458184	0.039301	0.068224
0.000600	0.456958	0.042087	0.071777

Table A24. Coordinated failure model, CX - 1.7/0.90 (2.5)(Fig. 9).

Input variables

ρ_0 = 1.7 Mg/m^3 S_w = 0.90 K = 2.5 GPa

P_T = 5 MPa P_M = 25.1 MPa

Output

Z = 0.2901 ϕ_0 = 0.5480 ϕ_a = 0.0548

e_w = 1.091 EF = 5.939 kJ EV = 31.77 kJ

LOADING PATH

P	V	DP/DV	MU	DP/DMU
0.	0.588235	0.	0.	0.
0.000010	0.588000	-0.042517	0.000400	0.025000
0.000020	0.587765	-0.042551	0.000800	0.025000
0.000030	0.587530	-0.042585	0.001200	0.025000
0.000050	0.587061	-0.042656	0.002000	0.025000
0.000670	0.586186	-0.002909	0.013873	0.001684
0.000100	0.572595	-0.003906	0.027476	0.002205
0.000200	0.557567	-0.006694	0.055004	0.003633
0.000251	0.552596	-0.010260	0.064495	0.005374
0.000300	0.550699	-0.078574	0.068160	0.040649
0.000600	0.548283	-0.082755	0.072869	0.042470
0.001000	0.543835	-0.089927	0.081644	0.045584
0.002000	0.534451	-0.106573	0.100634	0.052659
0.004000	0.520426	-0.142600	0.130295	0.067427
0.006000	0.510060	-0.192940	0.153266	0.087067
0.009000	0.498299	-0.255084	0.180486	0.110216
0.009600	0.496313	-0.302120	0.185209	0.127021
0.010000	0.495042	-0.314674	0.188253	0.131434
0.015000	0.481824	-0.378255	0.220852	0.153378
0.020000	0.471826	-0.500113	0.246721	0.193280
0.024000	0.465322	-0.605718	0.264418	0.226028
0.030000	0.456834	-0.715261	0.287636	0.258424
0.040000	0.445448	-0.878275	0.320548	0.303833
0.060000	0.428024	-1.147882	0.374303	0.372059
0.100000	0.402941	-1.594661	0.459856	0.467549
0.150000	0.374113	-1.734453	0.572346	0.444483
0.200000	0.352247	-2.286609	0.669953	0.512260
0.300000	0.316668	-2.810702	0.857575	0.532985
0.400000	0.290915	-5.062453	0.981156	0.809183
0.500000	0.282838	-7.103901	1.079758	1.014183
0.600000	0.271202	-8.593845	1.168992	1.120644
0.800000	0.252577	-10.738134	1.328936	1.250444
1.000000	0.237881	-13.609175	1.472814	1.390061
1.500000	0.210511	-18.268455	1.794316	1.555199
2.000000	0.190463	-24.940076	2.088445	1.699939

UNLOADING PATH

0.	[illegible]		0.057980	0.
[illegible]	[illegible]		0.050248	0.037264
[illegible]	[illegible]		0.058516	0.037370
[illegible]	[illegible]		0.058782	0.037476
0.000650	[illegible]		0.059314	0.037636
0.000770	[illegible]		0.059842	0.037848
0.000100	[illegible]		0.060629	0.038113
0.000200	[illegible]		0.063207	0.038799
0.000251	[illegible]		0.064495	0.039599

Table A25. Coordinated failure model, CX - 1.7/0.90 (7.5)(Fig. 9).

Input variables

ρ_0 = 1.7 Mg/m^3 S_w = 0.90 K = 7.5 GPa

P_T = 5 MPa P_M = 25.1 MPa

Output

Z = 0.2901 ϕ_0 = 0.5480 ϕ_a = 0.0548

e_w = 1.091 EF = 5.939 kJ EV = 31.77 kJ

LOADING PATH

P	V	DP/DV	MU	DP/DMU
0.	0.588285	0.	0.	0.
0.000010	0.588157	-0.127517	0.000133	0.075000
0.000020	0.588078	-0.127551	0.000267	0.075000
0.000030	0.588000	-0.127585	0.000400	0.075000
0.000050	0.587843	-0.127636	0.000667	0.075000
0.000070	0.586186	-0.002612	0.013873	0.001514
0.000100	0.572505	-0.003906	0.027476	0.002205
0.000200	0.557567	-0.006694	0.055004	0.003633
0.000251	0.552596	-0.010260	0.064495	0.005374
0.000400	0.550699	-0.078574	0.068160	0.040649
0.000600	0.548283	-0.082755	0.072869	0.042478
0.001000	0.543835	-0.089927	0.081644	0.045584
0.002000	0.534451	-0.106573	0.100634	0.052659
0.004000	0.520426	-0.142600	0.130295	0.067427
0.006000	0.510060	-0.192940	0.153266	0.087067
0.009000	0.498209	-0.255084	0.180486	0.110216
0.009600	0.496313	-0.302120	0.185209	0.127021
0.010000	0.495042	-0.314674	0.188253	0.131434
0.015000	0.481824	-0.378255	0.220852	0.153378
0.020000	0.471026	-0.500113	0.246721	0.193280
0.024000	0.465222	-0.605718	0.264418	0.226028
0.030000	0.456834	-0.715261	0.287636	0.258424
0.040000	0.445448	-0.878275	0.320548	0.303833
0.060000	0.428024	-1.147882	0.374303	0.372059
0.100000	0.402941	-1.594661	0.459856	0.467549
0.150000	0.374113	-1.734453	0.572346	0.444483
0.200000	0.352247	-2.286609	0.669953	0.512260
0.300000	0.316068	-2.810702	0.857575	0.532985
0.400000	0.288915	-5.062453	0.981156	0.809183
0.500000	0.282838	-7.103901	1.079758	1.014183
0.600000	0.271202	-8.593845	1.168992	1.120644
0.800000	0.252577	-10.738134	1.328936	1.250444
1.000000	0.237881	-13.609175	1.472814	1.390061
1.500000	0.210511	-18.268455	1.794316	1.555199
2.000000	0.190463	-24.940076	2.088445	1.699939

UNLOADING PATH

0.	0.555999		0.057980	0.
0.000010	0.555858		0.058248	0.037264
0.000020	0.555717		0.058516	0.037370
0.000030	0.555577		0.058782	0.037476
0.000050	0.555298		0.059314	0.037636
0.000070	0.555022		0.059842	0.037848
0.000100	0.554610		0.060629	0.038113
0.000	0.553265		0.063207	0.038799
0.000251	0.552596		0.064495	0.039599

DISTRIBUTION

LLL Internal Distribution

Roger E. Batzel, L-1
J. M. Thomsen, L-200 (10)
J. B. Bryan, L-200 (10)
C. M. Snell, L-200 (10)
L. S. Germain, L-203
D. E. Burton, L-200
J. L. Cortez, L-200
M. E. Cunningham, L-200
M. Heusinkveld, L-205
J. Toman, L-222
B. K. Germain, L-209
L. L. Schwartz, L-212
R. W. Terhune, L-200
J. T. Rambo, L-200
A. E. Lewis, L-207
L. W. Woodruff, L-96
R. N. Schock, L-203
TID File, L-3 (24)
Vault Reference, L-9 (6)

External Distribution

Asst. to the Secretary of Defense
Atomic Energy
ATTN: D. R. Cotter
Washington, D.C. 20301

Director
Defense Advanced Research Projects Agency
ATTN: Technical Library
Architect Building
1400 Wilson Blvd.
Arlington, VA 22209

Director
Defense Civil Preparedness Agency
ATTN: RE(ADM)
Washington, D.C. 20301

Defense Docum. Center (2)
ATTN: TC/M. B. Kahn
Cameron Station
Alexandria, VA 22314

Director
Defense Intelligence Agency
ATTN: DT-2, Weapons & Systems Division
Washington, D.C. 20301

Director
Defense Intelligence Agency
ATTN: DI-7D, Phys. Vul. Div., Edward O'Farrell
Washington, D.C. 20301

Director
Defense Intelligence Agency
ATTN: Technical Library
Washington, D.C. 20301

Director
Defense Nuclear Agency
ATTN: STSI (Archives)
Washington, D.C. 20305

Director (2)
Defense Nuclear Agency
ATTN: STTL (Technical Library)
Washington, D.C. 20305

Director (2)
Defense Nuclear Agency
ATTN: SPSS/E. Sevin
Washington, D.C. 20305

Director
Defense Nuclear Agency
ATTN: DDST
Washington, D.C. 20305

Director
Defense Nuclear Agency
ATTN: SPSS/T. Kennedy
Washington, D.C. 20305

Director of Defense
Research & Engineering
ATTN: Dep Dir, Tactical Warfare
Washington, D.C. 20301

Director of Defense
Research & Engineering
ATTN: Dep Dir, Strategic
Systems
Washington, D.C. 20301

Chairman
Department of Defense Explosive
Safety Board
ATTN: T. Zaker
Room 6A145
Forrestal Building
Washington, D.C. 20314

Interservice Nuclear Weapons
School
ATTN: Technical Library
Kirtland AFB, NM 87115

Director
Joint Strategic Target
Planning Staff, JCS
ATTN: Science and Technology
Info Library
Offutt AFB, Nebraska 68113

Commander
Field Command
DNA
ATTN: FCTA-D
Lawrence Livermore Laboratory
P. O. Box 808
Livermore, CA 94550

Director, Weapons Systems
Evaluation Group
ATTN: Technical Director
400 Army-Navy Drive
Arlington, VA 22202

Commander, U.S. Army
Ballistic Missile Defense
Systems Command
ATTN: BMDSC-TEN (N. J. Hurst)
P. O. Box 1500
Huntsville, Alabama 35807

Commander, U.S. Army
Ballistic Missile Defense
Systems Command
ATTN: BMDSC-HS
P. O. Box 1500
Huntsville, Alabama 35807

Office, Chief of Engineers
Department of the Army
ATTN: DAEN-MCD-D
Washington, D.C. 20314

Office, Chief of Engineers
Department of the Army
ATTN: DAEN-RDL
Washington, D.C. 20314

Engineer Studies Group
ATTN: DAEN-FES/G. H. Orrell
6500 Brooks Lane
Washington, D.C. 20315

Commander
Harry Diamond Lab.
ATTN: AMXDO-NP
2800 Powder Mill Road
Adelphi, MD 20783

Commander
Harry Diamond Laboratories
ATTN: AMXDO-TI, Tech. Library
2800 Powder Mill Road
Adelphi, MD 20783

Office, Chief of Research,
Development, and
Acquisition
Department of the Army
ATTN: DAMA-CSM/LTC E. V. DeBoesser, Jr.
Washington, D.C. 20310

Commanding Officer
Picatinny Arsenal
ATTN: SMUPA-ND-S/E. Zimpo
Dover, NJ 07801

Commanding Officer
Picatinny Arsenal
ATTN: Technical Library
Dover, NJ 07801

Commanding Officer
Picatinny Arsenal
ATTN: P. Angelloti
Dover, NJ 07801

Director, U.S. Army
Ballistic Research Lab.
ATTN: J. H. Keefer
Aberdeen Proving Ground, MD 21005

Director, U. S. Army
Ballistic Research Laboratories,
ATTN: AMXBR-X, J. J. Meszaros
Aberdeen Proving Grounds, MD 21005

Director, U. S. Army
Ballistic Research Laboratories
ATTN: W. J. Taylor
Aberdeen Proving Ground, MD 21005

Director, U. S. Army (2)
Ballistic Research Laboratories
ATTN: Technical Library/Edward Baicy
Aberdeen Proving Ground, MD 21005

Commander, U.S. Army (2)
Aberdeen Research & Development
Center
ATTN: Technical Library
Aberdeen Proving Ground, MD 21005

Commander, U. S. Army
Engineer School
ATTN: ATSEN-SY-L
Fort Belvoir, Virginia 22060

Division Engineer, U.S. Army
Engineer Division, Huntsville
ATTN: HNDED-CS/Michael M. Dembo
P. O. Box 1600
Huntsville, Alabama 35807

Division Engineer, U.S. Army
Engineer Division, Ohio River
ATTN: ORDAS-L/Technical Library
P.O. Box 1159
Cincinnati, Ohio 45201

Director, U.S. Army Engineer (5)
Waterways Experiment Station
ATTN: Library
P.O. Box 631
Vicksburg, Mississippi 39180

Director, U.S. Army Engineer
Waterways Experiment Station
ATTN: L. F. Ingram
P.O. Box 631
Vicksburg, Mississippi 39180

Director, U.S. Army Engineer
Waterways Experiment Station
ATTN: William J. Flathau
P.O. Box 631
Vicksburg, Mississippi 39180

Director, U.S. Army Engineer
Waterways Experiment Station
ATTN: John Strange
P.O. Box 631
Vicksburg, Mississippi 39180

Director, U.S. Army Engineer (21)
Waterways Experiment Station
ATTN: MAJ L. C. Webster
P.O. Box 631
Vicksburg, Mississippi 39180

Director, U. S. Army Engineer
Waterways Experiment Station
ATTN: J. Zelasko
P.O. Box 631
Vicksburg, Mississippi 39180

Director, U.S. Army Engineer
Waterways Experiment Station
ATTN: J. Ehrgott
P.O. Box 631
Vicksburg, Mississippi 39180

Commander, U.S. Army Materials
and Mechanics Research Center
ATTN: Technical Library
Watertown, Mass. 02172

Commander, U.S. Army Materiel (2)
Development and Readiness
Command (DARCOM),
ATTN: AMCRD-BN
5001 Eisenhower Ave.,
Alexandria, Virginia 22333

Commander, U.S. Army Materiel
Development and Readiness
Command (DARCOM),
ATTN: Technical Library
5001 Eisenhower Ave.,
Alexandria, Virginia 22333

Commander, U.S. Army Materiel (2)
Development and Readiness
Command (DARCOM),
ATTN: AMCRD-WN
5001 Eisenhower Ave.,
Alexandria, Virginia 22333

Commander, U.S. Army
Missile Command
ATTN: Technical Library
Redstone Arsenal, Alabama 35809

Commander, U.S. Army
Missile Command
ATTN: W. Jann/AMCPM-PE
Redstone Arsenal, Alabama 35809

Commander, U.S. Army
Missile Command
ATTN: W. Fowler/AMSMI-YDR
Redstone Arsenal, Alabama 35809

Commander, U.S. Army Mobility
Equipment Research & Development
Center
ATTN: Technical Library
Fort Belvoir, Virginia 22060

Commander, U.S. Army
Nuclear Agency
ATTN: CDINS-E
Fort Bliss, TX 79916

Commander, U.S. Army
Nuclear Agency
ATTN: Technical Library
Fort Bliss, TX 79916

Commander, U.S. Army Strategic
Communications Command
ATTN: Technical Library
Fort Huachuca, Arizona 85613

Commander, U.S. Army Strategic
Communications Command
Safeguard Communications Agency
ATTN: Klaus Donat
Fort Huachuca, Arizona 85613

Commander, U.S. Army Armament
Command, Rock Island Arsenal
ATTN: Technical Library
Rock Island, Illinois 61201

Chief of Naval Operations,
Department of the Navy
ATTN: OP-985F
Washington, D.C. 20350

Chief of Naval Research
Department of the Navy
ATTN: Technical Library
Arlington, Virginia 22217

Officer in Charge
Civil Engineering Laboratory
Naval Construction Battalion Center
ATTN: Technical Library
Port Hueneme, California 93043

Officer in Charge,
Civil Engineering Laboratory
Naval Construction Battalion Center
ATTN: Mr. R. J. Odello
Port Hueneme, California 93043

Commander, Naval Electronics
Systems Command, Headquarters
ATTN: PME-117-21A
Washington, D.C. 20360

Commander, Naval Facilities
Engineering Command
ATTN: Technical Library, Code 0911C
Hoffman Building
200 Stovall Street,
Alexandria, Virginia 22332

Superintendent,
U.S. Naval Postgraduate School
ATTN: Library, Code 2124
Monterey, California 93940

Director,
Naval Research Laboratory
ATTN: Library, Code 2029
Washington, D.C. 20375

Commander, Naval Ship Research
and Development Center
Underwater Explosive Research Division
ATTN: Technical Librarian
Portsmouth, Virginia 23709

Commander, Naval Surface Weapons
Center, Dahlgren Laboratory
ATTN: Technical Library
Dahlgren, Virginia 22448

Commander, Naval Surface Weapons
Center, White Oak,
ATTN: Technical Library, Code 730
Silver Spring, Maryland 20910

Commander, Naval Surface Weapons
Center, White Oak,
ATTN: Code 1224 Navy Nuc Prgms Off
Silver Spring, Maryland 20910

Commander,
Naval Weapons Center
ATTN: Code 533, Technical Library
China Lake, California 93555

Commander, Naval Weapons
Evaluation Facility
ATTN: Technical Library
Kirtland AFB
Albuquerque, New Mexico 87117

Commander, Weapons
Evaluation Facility,
ATTN: R. Hughes
Kirtland AFB
Albuquerque, New Mexico 87117

Director, Strategic Systems
Project Office
ATTN: NSP-43, Technical Library
Navy Department
Washington, D.C. 20376

Air Force Armament and Testing
Laboratory, AFSC
ATTN: Technical Library
Eglin AFB, Florida 32542

Air Force Cambridge Research
Laboratories, AFSC
ATTN: LWW, Ker P. Thompson
Hanscom Field,
Bedford, Massachusetts 01730

Air Force Cambridge Research
Laboratories, AFSC
ATTN: SUOL AFCRL, Research Library
L. G. Hanscom Field
Bedford, Massachusetts 01730

Air Force Institute of Technology
ATTN: Technical Library
AFIT Building 640, Area B
Wright-Patterson AFB, Ohio 45433

Commander, Air Force Weapons
Laboratory, AFSC
ATTN: SUL, Technical Library
Kirtland AFB, New Mexico 87117

Commander, Air Force Weapons
Laboratory, AFSC
ATTN: DEV-S/Dr. M. A. Plamondon
Kirtland AFB, New Mexico 87117

Commander, Air Force Weapons
Laboratory, AFSC
ATTN: DEV-F/Mr. J. L. Bratton
Kirtland AFB, New Mexico 87117

Commander, Air Force Weapons
Laboratory, AFSC
ATTN: DEV-G/Mr. R. W. Henny
Kirtland AFB, New Mexico 87117

Commander, Air Force Weapons
Laboratory, AFSC
ATTN: DEV, Mr. R. J. Port
Kirtland AFB, New Mexico 87117

Headquarters,
Air Force Systems Command
ATTN: Technical Library
Andrews AFB,
Washington, D.C. 20331

Commander,
Armament Development & Test Center
ATTN: Technical Library
Eglin AFB, Florida 32542

Commander,
Foreign Technology Division, AFSC
ATTN: TD-BTA Library
Wright-Patterson AFB, Ohio 45433

Commander
Rome Air Development Center, AFSC
ATTN: EMTLD, Documents Library
Griffiss AFB, New York 13440

Space and Missile Systems
Organization
ATTN: MMH/Hard Rock Silo Department
Norton AFB, California 92409

Space and Missile Systems
Organization,
ATTN: MMH/Engineering Division
Norton AFB, California 92409

Commander,
Strategic Air Command
ATTN: NRI-STINFO Library
Offutt AFB, Nebraska 68113

Los Alamos Scientific Laboratory
ATTN: Document Control for Reports
Library
P.O. Box 1663
Los Alamos, New Mexico 87544

Sandia Laboratories,
Livermore Laboratory
ATTN: Document Control for Technical
Library
P.O. Box 969
Livermore, California 94550

Sandia Laboratories
ATTN: Document Control for
Mr. L. J. Vortman
P.O. Box 5800
Albuquerque, New Mexico 87115

Sandia Laboratories
ATTN: Document Control for
3141 Sandia Rpt Coll
P.O. Box 5800
Albuquerque, New Mexico 87115

U.S. Energy Research &
Development Administration
Albuquerque Operations Office
ATTN: Document Control for
Technical Library
P.O. Box 5400
Albuquerque, New Mexico 87115

U. S. Energy Research &
Development Administration
Nevada Operations Office
ATTN: Document Control for
Technical Library
P.O. Box 14100
Las Vegas, Nevada 89114

U. S. Energy Research &
Development Administration
Division of Headquarters Services
Library Branch G-043
ATTN: Doc Control for Class. Tech Lib
Washington, D.C. 20545

Aerospace Corporation
ATTN: Dr. Prem N. Mathur
P.O. Box 92957
Los Angeles, California 90009

Aerospace Corporation
ATTN: Technical Information Services
P.O. Box 92957
Los Angeles, California 90009

Agbabian Associates
ATTN: Dr. M. S. Agbabian
250 North Nash Street
El Segundo, California 90245

Applied Theory, Incorporated
ATTN: Dr. John G. Trulio
1010 Westwood Boulevard
Los Angeles, California 90024

Bell Telephone Laboratories, Inc.
ATTN: Technical Report Center
Mountain Avenue
Murray Hill, New Jersey 07974

Boeing Company Aerospace Group
Missile and Information Systems
Division
ATTN: Mr. R. H. Carlson
P.O. Box 3707
Seattle, Washington 98124

Braddock, Dunn, & McDonald, Inc.
ATTN: A. Lavagnino
1920 Aline Ave.
Vienna, Virginia 22180

Braddock, Dunn, & McDonald, Inc.
ATTN: Mr. Richard Hensley
P.O. Box 9274
Albuquerque International
Albuquerque, New Mexico 87119

California Research & Technology, Inc.
ATTN: Technical Library
6269 Variel Ave.,
Woodland Hills, California 91364

California Research & Technology, Inc.
ATTN: Dr. K. N. Kreyenhagen
6269 Variel Ave.
Woodland Hills, California 91364

General American Transportation Corp.
General American Research Division
ATTN: Dr. G. L. Neidhardt
7449 N. Natchez Ave.
Niles, Illinois 60648

General Electric Company
TEMPO-Center for Advanced Studies
ATTN: DASIAC
816 State Street
Santa Barbara, California 93102

IIT Research Institute
ATTN: Technical Library
10 West 35th Street
Chicago, Illinois 60616

Institute for Defense Analyses
ATTN: IDA Librarian Ruth S. Smith
400 Army-Navy Drive
Arlington, Virginia 22202

Consulting & Special Engineering
Services, Inc.
ATTN: Dr. J. L. Merritt
P.O. Box 1206
Redlands, California 92373

Consulting & Special Engineering
Services, Inc.
ATTN: Technical Library
P.O. Box 1206
Redlands, California 92373

Kaman Avidyne
Division of Kaman Sciences Corp.
ATTN: Technical Library
83 Second Avenue,
Northwest Industrial Park
Burlington, Massachusetts 01803

Kaman Avidyne
Division of Kaman Sciences Corp.
ATTN: E. S. Crisicone
83 Second Avenue
Northwest Industrial Park
Burlington, Massachusetts 01803

Kaman Avidyne
Division of Kaman Sciences Corp.
ATTN: N. P. Hobbs
83 Second Avenue,
Northwest Industrial Park
Burlington, Massachusetts 01803

Kaman Sciences Corporation
ATTN: Gunning Butler, Jr.
P.O. Box 7463
Colorado Springs, Colorado 80933

Kaman Sciences Corporation
ATTN: Technical Library
P.O. Box 7463
Colorado Springs, Colorado 80933

Lockheed Missiles and Space
Company, Inc.
ATTN: Technical Library
P.O. Box 504
Sunnyvale, California 94088

Martin Marietta Aerospace,
Orlando Division
ATTN: Gerbert E. McQuaig - MP 81
P.O. Box 5837
Orlando, Florida 32805

University of Illinois
ATTN: Dr. Nathan M. Newmark
1211 Civil Engineering Building
Urbana, Illinois 61801

Physics International Company
ATTN: Technical Library
2700 Merced Street
San Leandro, California 94577

Physics International Company
ATTN: Doc Control for
Mr. Fred M. Sauer
2700 Merced Street
San Leandro, California 94577

Physics International Company
ATTN: Doc Control for
Mr. Dennis L. Orphal
2700 Merced Street
San Leandro, California 94577

Physics International Company
ATTN: Doc Control for
Dr. Charles Godfrey
2700 Merced Street
San Leandro, California 94577

Physics International Company
ATTN: Doc Control for
Dr. Robert Swift
2700 Merced Street
San Leandro, California 94577

Physics International Company
ATTN: Doc Control for
Mr. Larry Behrman
2700 Merced Street
San Leandro, California 94577

R&D Associates
ATTN: Technical Library
P.O. Box 9695
Marina Del Ray, California 90291

R&D Associates
ATTN: Dr. H. F. Cooper, Jr.
P.O. Box 9695
Marina Del Ray, California 90291

R&D Associates
ATTN: Dr. Harold L. Brode
P.O. Box 9695
Marina Del Ray, California 90291

R&D Associates
ATTN: Mr. William B. Wright
P.O. Box 9695
Marina Del Ray, California 90291

R&D Associates
ATTN: Dr. C. P. Knowles
P.O. Box 9695
Marina Del Ray, California 90291

R&D Associates
ATTN: Mr. J. G. Lewis
P.O. Box 9695
Marina Del Ray, California 90291

Science Applications, Inc.
ATTN: Dr. W. M. Layson
1911 North Fort Myer Drive
Suite 808,
Arlington, Virginia 22209

Science Applications, Inc.
ATTN: Technical Library
P.O. Box 2351
La Jolla, California 92037

Science Applications, Inc.
ATTN: R. A. Shunk
P.O. Box 3507
Albuquerque, New Mexico 87110

Southwest Research Institute
ATTN: Mr. A. B. Wenzel
P.O. Drawer 28510
San Antonio, Texas 78284

Stanford Research Institute
ATTN: SRI Library Room G021
333 Ravenswood Ave.
Menlo Park, California 94025

Stanford Research Institute
ATTN: Dr. G. Abrahamson
333 Ravenswood Ave.,
Menlo Park, California 94025

Science Applications, Inc.
ATTN: Dr. D. Hall
P.O. Box 34
Pleasanton, CA 94566

Science Applications, Inc.
ATTN: Mr. J. Dishon
P.O. Box 34
Pleasanton, CA 94566

Systems, Science and Software
ATTN: Dr. Donald R. Grine
P.O. Box 1620
La Jolla, California 92037

Systems, Science and Software
ATTN: Dr. T. D. Riney
P.O. Box 1620
La Jolla, California 92037

Systems, Science and Software
ATTN: Technical Library
P.O. Box 1620
La Jolla, California 92037

Systems, Science and Software
ATTN: Dr. T. Blake
P.O. Box 1620
La Jolla, California 92037

Systems, Science and Software
Washington Research Center
ATTN: Jack Cane
111 South Fairfax St.
Alexandria, Virginia 22314

Teledyne Brown Engineering Company, Inc.
ATTN: Dr. M. C. Patel
Cummings Research Park,
Huntsville, Alabama 35807

Terra Tek, Inc.
ATTN: Mr. S. J. Green
University Research Park,
420 Wakara Way
Salt Lake City, Utah 84108

TRW Systems Group
ATTN: Greg Hulcher
San Bernardino Operations
P.O. Box 1310
San Bernardino, California 92402

TRW Defense and Space Systems Group
ATTN: Technical Information Center/
S-1930
One Space Park
Building R1/2170
Redondo Beach, California 90278

TRW Defense and Space Systems Group
ATTN: Dr. J. J. Ferrell
One Space Park
Building R./2170
Redondo Beach, California 90278

Weidlinger Associates
Consulting Engineers
ATTN: Dr. Melvin L. Baron
110 East 59th Street
New York, New York 10022

Weidlinger Associates,
Consulting Engineers
ATTN: Dr. J. Isenberg
2710 Sand Hill Road, Suite 230
Menlo Park, California 99025

Distribution Category UC-11 (206)

WC/nus/mla

Technical Information Department
LAWRENCE LIVERMORE LABORATORY
University of California | Livermore, California | 94550